RS2

2D finite element program for stress analysis and support design
around excavations in soil and rock

Slope Stability Verification Manual

Part I

TABLE OF CONTENTS

Introduction

This document contains a series of slope stability verification problems that have been analyzed using the shear strength reduction (SSR) technique in RS2 version 8.0. Results are compared to both Slide22 version 5.0 limit-equilibrium results and referee values from published sources. These verification tests come from published examples found in reference material such as journal and conference proceedings.

For all examples, a short statement of the problem is given first, followed by a presentation of the analysis results, using the SSR finite element method, and various limit equilibrium analysis methods. Full references cited in the verification tests are found at the end of this document.

The RS2 slope stability verification files can be downloaded from the RS2 Online help page for Verification Manuals.

1 Simple slope stability assessment

Introduction

In 1988 a set of 5 basic slope stability problems, together with 5 variants, was distributed both in the Australian Geomechanics profession and overseas as part of a survey sponsored by ACADS (Giam & Donald, 1989). This is the ACADS 1(a) problem.

Problem Description

Verification problem #01 for Slide2 - This problem as shown in Figure 1 is the simple case of a total stress analysis without considering pore water pressures. It represents a homogenous slope with soil properties given in Table 1. The factor of safety and its corresponding critical circular failure is required.

Geometry and Properties

Table 1: Material Properties

c´ (kN/m^2)	ϕ´ (deg.)	γ (kN/m^3)
3.0	19.6	20.0

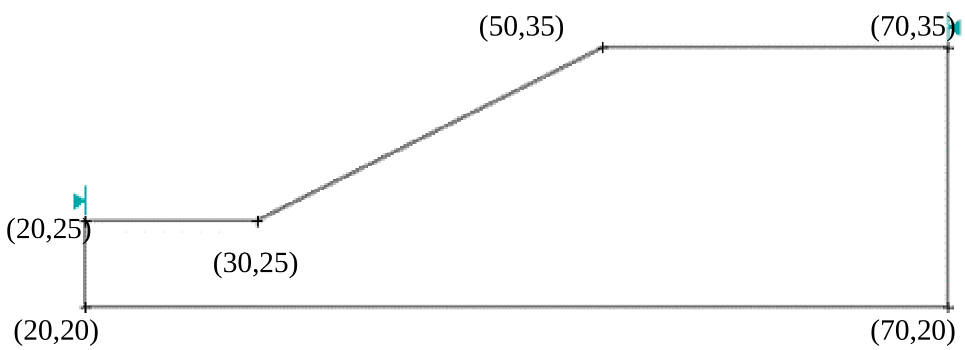

Figure 1

Results (Slide2 limit-equilibrium results are for a circular slip surface)

Method	Factor of Safety
SSR (RS2)	0.99
Bishop (Slide2)	0.987
Spencer (Slide2)	0.986
GLE (Slide2)	0.986
Janbu Corrected (Slide2)	0.990

Note: Referee Factor of Safety = 1.00 [Giam]
Mean Bishop FOS (18 samples) = 0.993
Mean FOS (33 samples) = 0.991

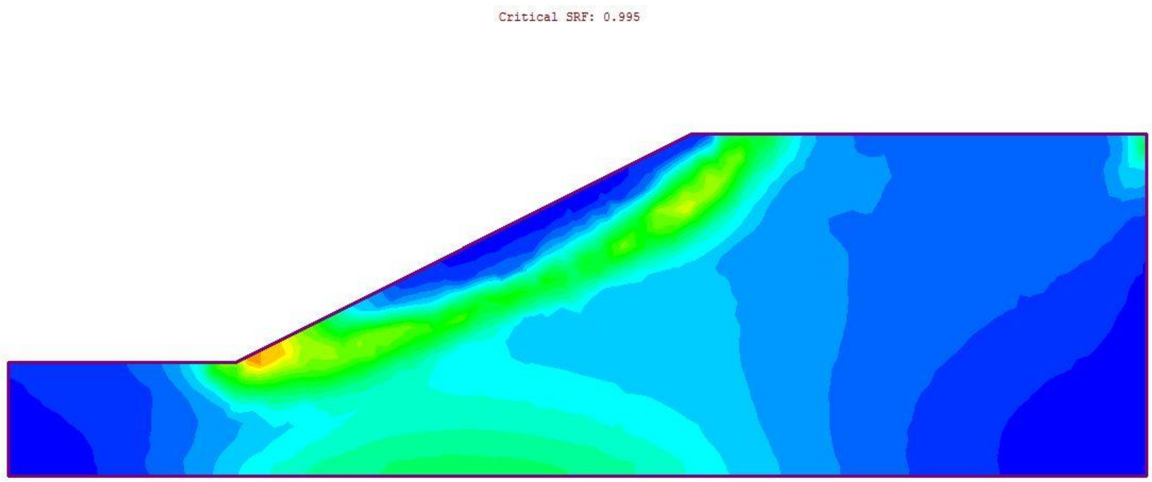

Figure 2 – Solution Using SSR

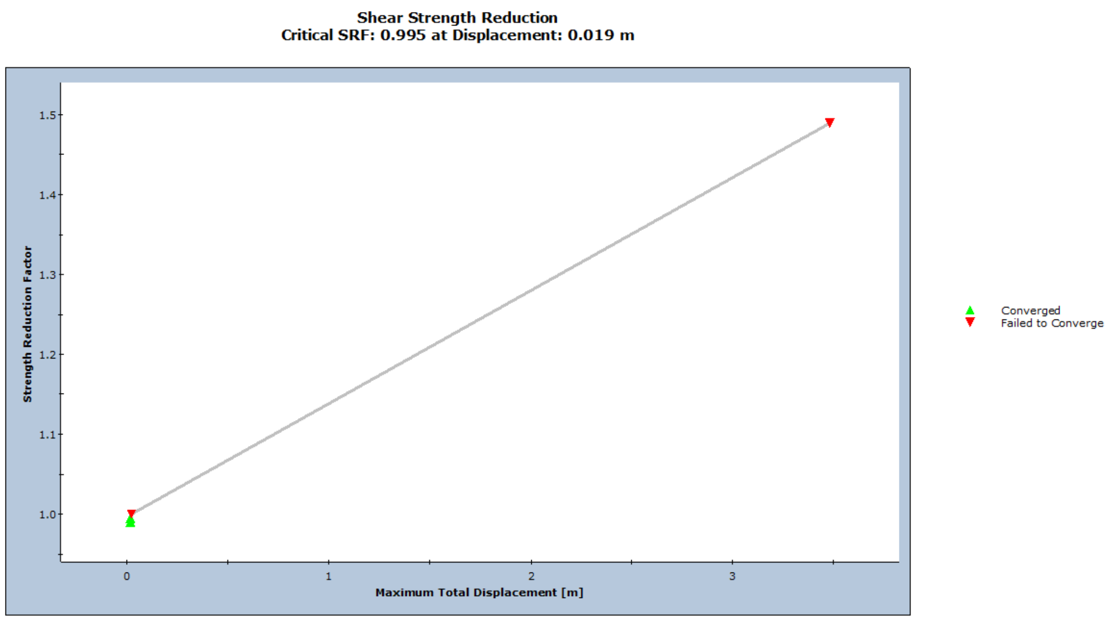

Figure 3 – SSR Convergence Graph

2 Non-Homogeneous Slope

Introduction

In 1988 a set of 5 basic slope stability problems, together with 5 variants, was distributed both in the Australian Geomechanics profession and overseas as part of a survey sponsored by ACADS (Giam & Donald, 1989). This is the ACADS 1(c) problem.

Problem description

Verification problem #03 for Slide2 - This problem models a non-homogeneous, three layer slope with material properties given in Table 1. The factor of safety and its corresponding critical circular failure surface is required.

Geometry and Properties

Table 1: Material Properties

	c′ (kN/m^2)	φ′ (deg.)	γ (kN/m^3)
Soil #1	0.0	38.0	19.5
Soil #2	5.3	23.0	19.5
Soil #3	7.2	20.0	19.5

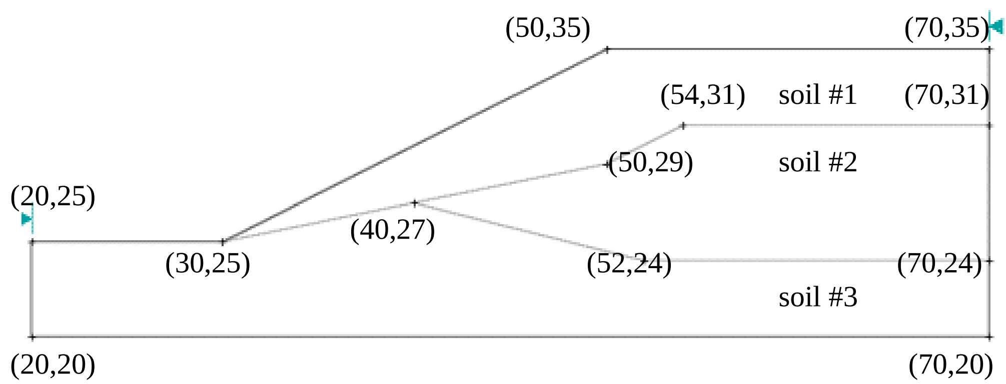

Figure 1

Results (Slide2 limit-equilibrium results are for a circular slip surface)

Method	Factor of Safety
SSR (RS2)	1.36
Bishop (Slide2)	1.405
Spencer (Slide2)	1.375
GLE (Slide2)	1.374
Janbu Corrected (Slide2)	1.357

Note : Referee Factor of Safety = 1.39 [Giam]
Mean Bishop FOS (16 samples) = 1.406
Mean FOS (31 samples) = 1.381

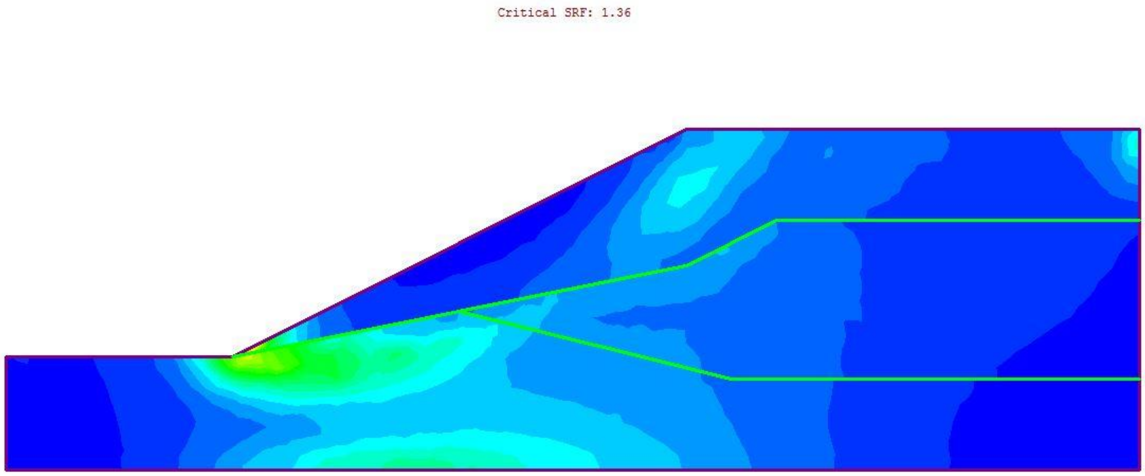

Figure 2 – Solution Using SSR

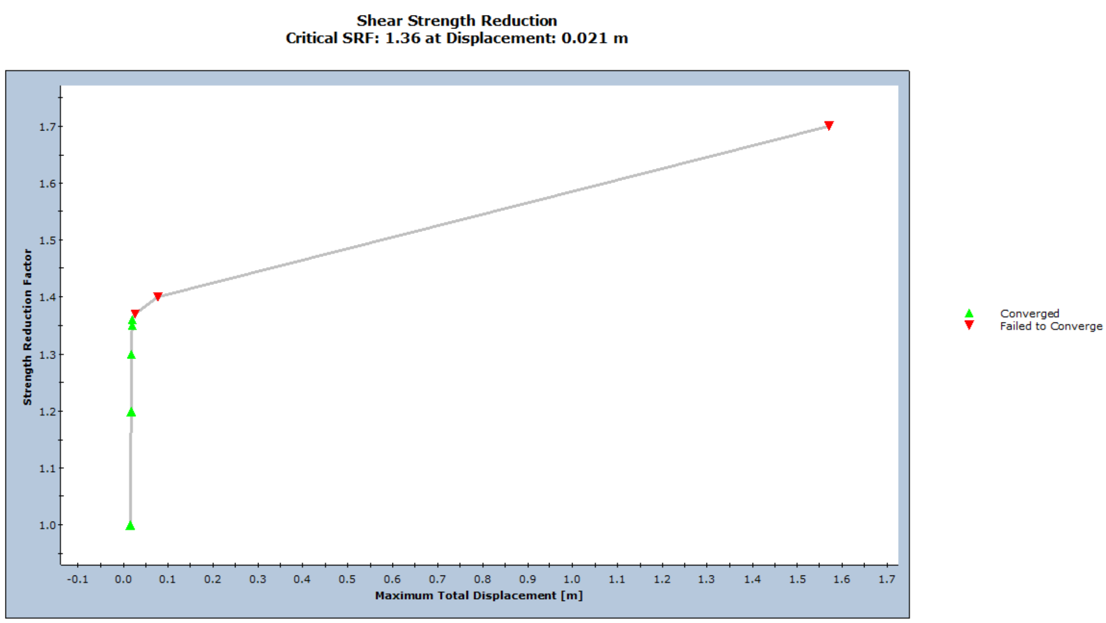

Figure 3 – SSR Convergence Graph

3 Non-Homogeneous Slope with Seismic Load

Introduction

In 1988 a set of 5 basic slope stability problems, together with 5 variants, was distributed both in the Australian Geomechanics profession and overseas as part of a survey sponsored by ACADS (Giam & Donald, 1989). This is the ACADS 1(d) problem.

Problem description

Verification problem #04 for Slide2 - This problem models a non-homogeneous, three layer slope with material properties given in Table 1 and geometry as shown in Figure 1. A horizontal seismically induced acceleration of 0.15g is included in the analysis. The factor of safety and its corresponding critical circular failure surface is required.

Geometry and Properties

Table 1: Material Properties

	c´ (kN/m²)	ϕ´ (deg.)	γ (kN/m³)
Soil #1	0.0	38.0	19.5
Soil #2	5.3	23.0	19.5
Soil #3	7.2	20.0	19.5

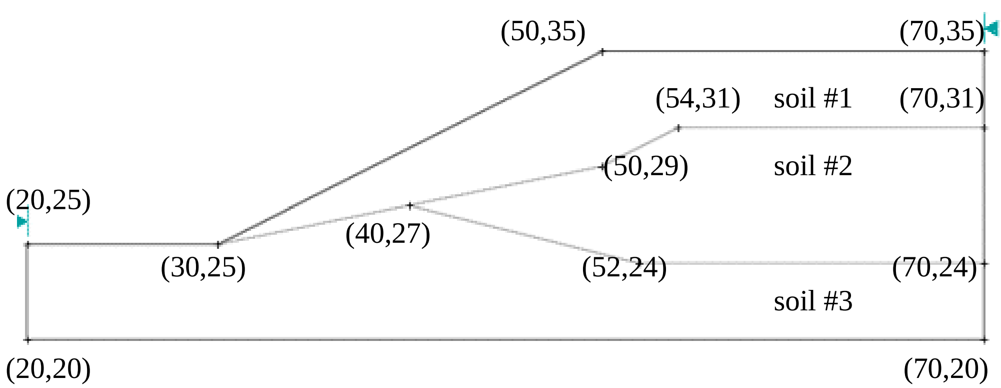

Figure 1

Results (Slide2 limit-equilibrium results are for a circular slip surface)

Method	Factor of Safety
SSR (RS2)	0.97
Bishop (Slide2)	1.015
Spencer (Slide2)	0.991
GLE (Slide2)	0.989
Janbu Corrected (Slide2)	0.965

Note : Referee Factor of Safety = 1.00 [Giam]
Mean FOS (15 samples) = 0.973

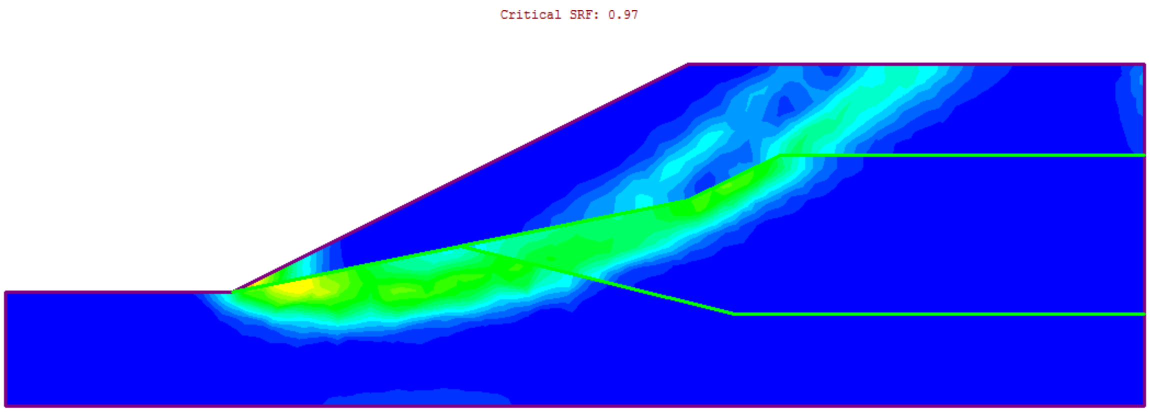

Figure 2 – Solution Using SSR

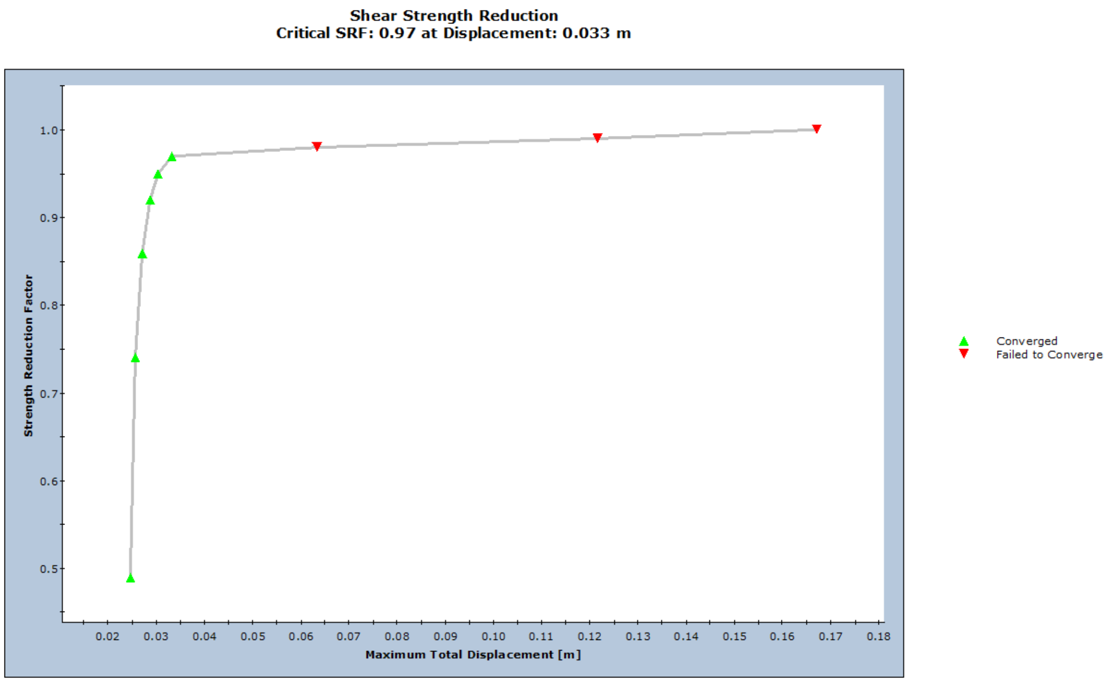

Figure 3 – SSR Convergence Graph

4 Dry slope stability assessment of Talbingo Dam

Introduction

In 1988 a set of 5 basic slope stability problems, together with 5 variants, was distributed both in the Australian Geomechanics profession and overseas as part of a survey sponsored by ACADS (Giam & Donald, 1989). This is the ACADS 2(a) problem.

Problem description

Verification problem #05 for Slide2 - Talbingo Dam is shown in Figure 1. The material properties for the end of construction stage are given in Table 1 while the geometrical data are given in Table 2.

Geometry and Properties

Table 1: Material Properties

	c´ (kN/m^2)	φ´ (deg.)	γ (kN/m^3)
Rockfill	0	45	20.4
Transitions	0	45	20.4
Filter	0	45	20.4
Core	85	23	18.1

Table 2: Geometry Data

Pt.#	Xc (m)	Yc (m)	Pt.#	Xc (m)	Yc (m)	Pt.#	Xc (m)	Yc (m)
1	0	0	10	515	65.3	19	307.1	0
2	315.5	162	11	521.1	65.3	20	331.3	130.6
3	319.5	162	12	577.9	31.4	21	328.8	146.1
4	321.6	162	13	585.1	31.4	22	310.7	0
5	327.6	162	14	648	0	23	333.7	130.6
6	386.9	130.6	15	168.1	0	24	331.3	146.1
7	394.1	130.6	16	302.2	130.6	25	372.4	0
8	453.4	97.9	17	200.7	0	26	347	130.6
9	460.6	97.9	18	311.9	130.6	-	-	-

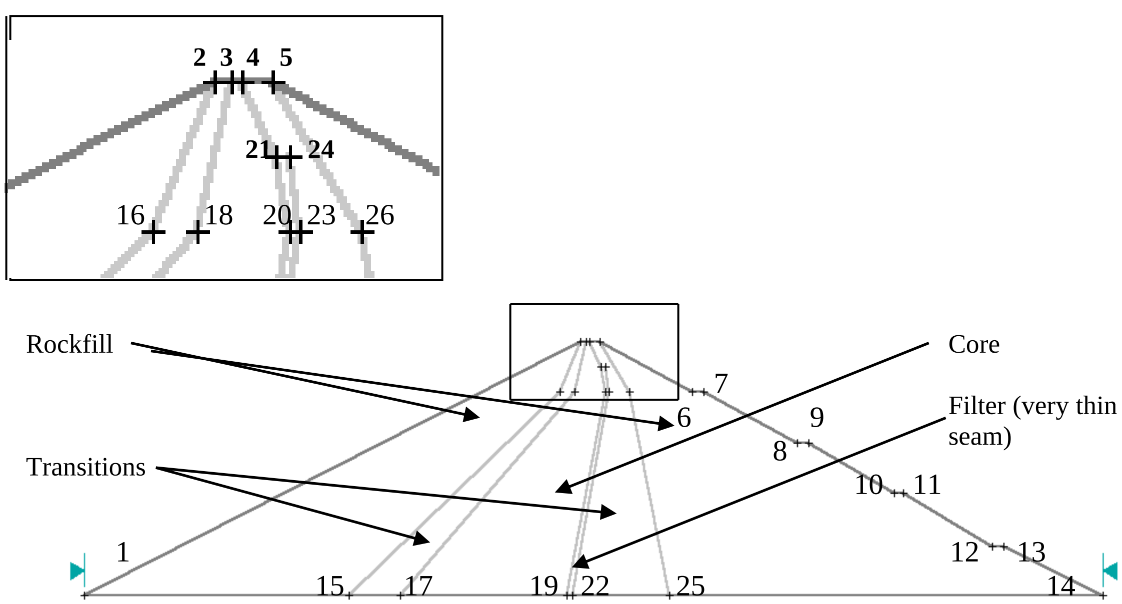

Figure 1

Results (Slide2 limit-equilibrium results are for a circular slip surface)

Method	Factor of Safety
SSR (RS2)	1.88
Bishop (Slide2)	1.948
Spencer (Slide2)	1.948
GLE (Slide2)	1.948
Janbu Corrected (Slide2)	1.949

Note :
Referee Factor of Safety = 1.95 [Giam]
Mean FOS (24 samples) = 2.0

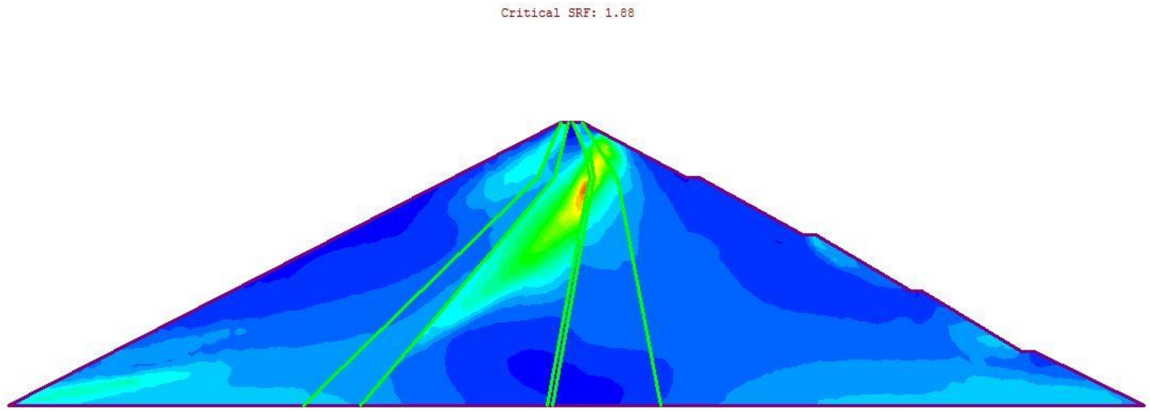

Figure 2 Solution Using SSR

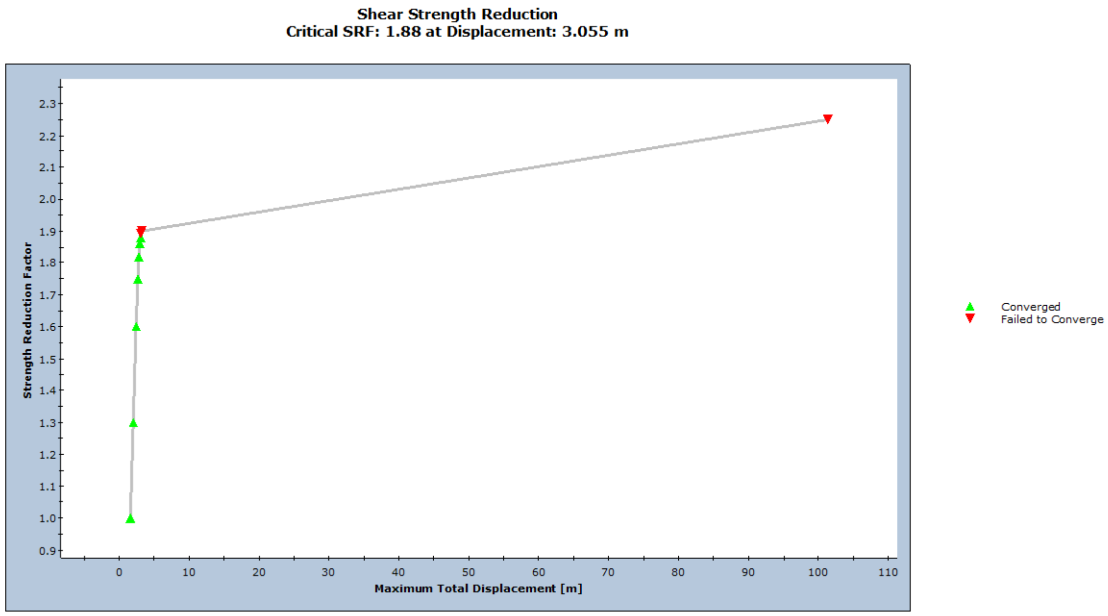

Figure 3 –SSR Convergence Graph

5 Water Table with Weak Seam

Introduction

In 1988 a set of 5 basic slope stability problems, together with 5 variants, was distributed both in the Australian Geomechanics profession and overseas as part of a survey sponsored by ACADS (Giam & Donald, 1989). This is the ACADS 3(a) problem.

Problem description

Verification problem #07 for Slide2 - This problem has material properties given in Table 1, and is shown in Figure 1. The water table is assumed to coincide with the base of the weak layer. The effect of negative pore water pressure above the water table is to be ignored. (i.e. u=0 above water table).

Geometry and Properties

Table 1: Material Properties

	c′ (kN/m^2)	ϕ' (deg.)	γ (kN/m^3)
Soil #1	28.5	20.0	18.84
Soil #2	0	10.0	18.84

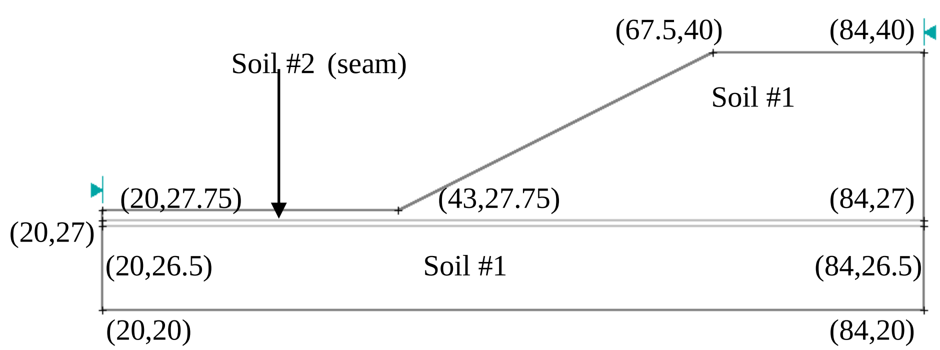

Figure 1

Results

Method	Factor of Safety
SSR (RS2)	1.26
Spencer	1.258
GLE	1.246
Janbu Corrected	1.275

Note : Referee Factor of Safety = 1.24 – 1.27 [Giam]
Mean Non-circular FOS (19 samples) = 1.293

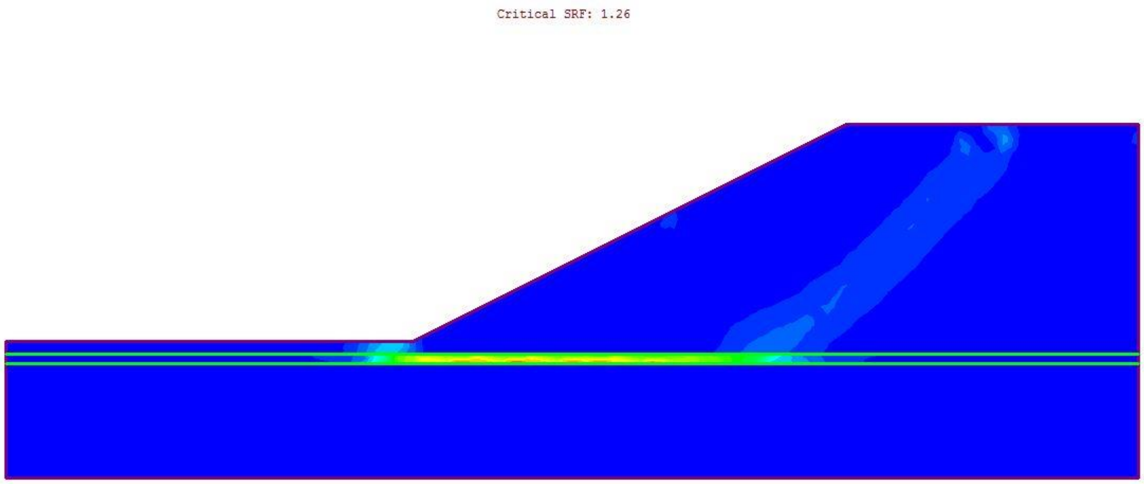

Figure 2 Solution Using SSR

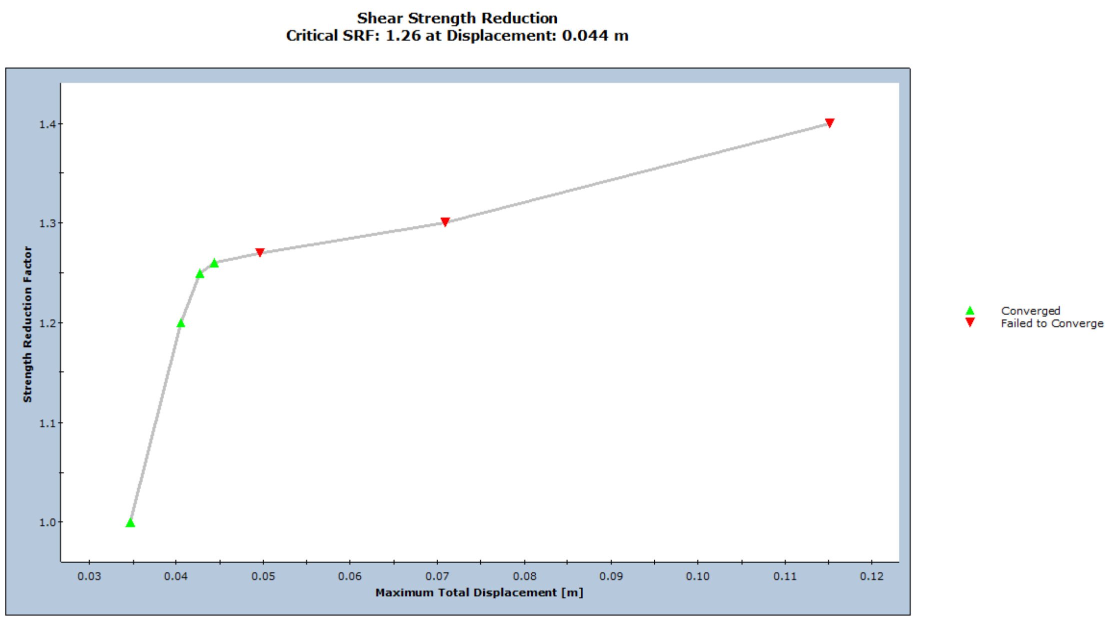

Figure 3 –SSR Convergence Graph

6 Slope with Load and Pore Pressure Defined by Water Table

Introduction

In 1988 a set of 5 basic slope stability problems, together with 5 variants, was distributed both in the Australian Geomechanics profession and overseas as part of a survey sponsored by ACADS (Giam & Donald, 1989). This is the ACADS 4 problem.

Problem description

Verification problem #09 for Slide2 - The geometry is shown in Figure 1. The soil parameters, external loadings and piezometric surface are shown in Table 1, Table 2 and Table 3 respectively. The effect of a tension crack is to be ignored.

Geometry and Properties

Table 1: Material Properties

	c′ (kN/m^2)	φ′ (deg.)	γ (kN/m^3)
Soil #1	28.5	20.0	18.84
Soil #2	0	10.0	18.84

Table 2: External Loadings

Xc (m)	Yc (m)	Normal Stress (kN/m^2)
23.00	27.75	20.00
43.00	27.75	20.00
70.00	40.00	20.00
80.00	40.00	40.00

Table 3: Data for Piezometric surface

Pt.#	Xc (m)	Yc (m)
1	20.0	27.75
2	43.0	27.75
3	49.0	29.8
4	60.0	34.0
5	66.0	35.8
6	74.0	37.6
7	80.0	38.4
8	84.0	38.4

Pt.# : Refer to Figure 1

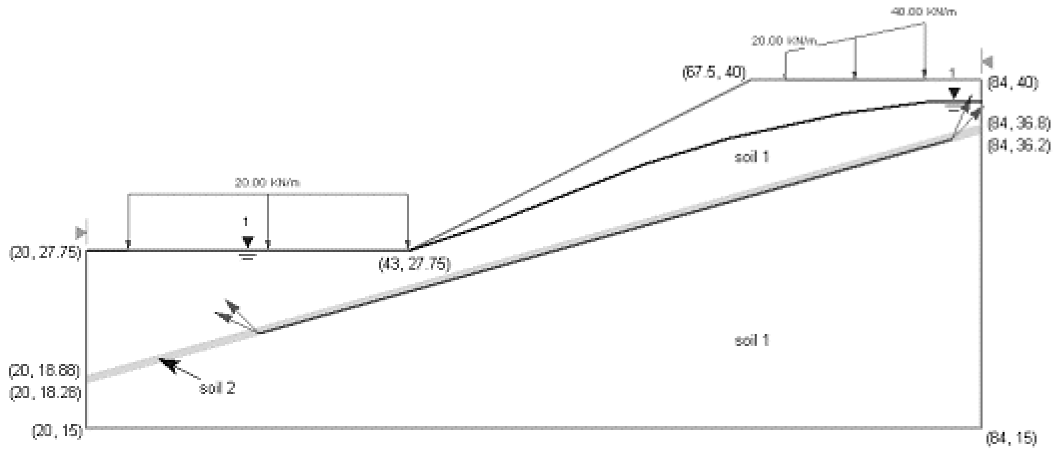

Figure 1 - Geometry

Results – (Side results use Monte-Carlo optimization)

Method	Factor of Safety
SSR	0.69
Spencer	0.707
GLE	0.683
Janbu Corrected	0.700

Note: Referee Factor of Safety = 0.78 [Giam]
Mean Non-circular FOS (20 samples) = 0.808
Referee GLE Factor of Safety = 0.6878 [Slope 2000]

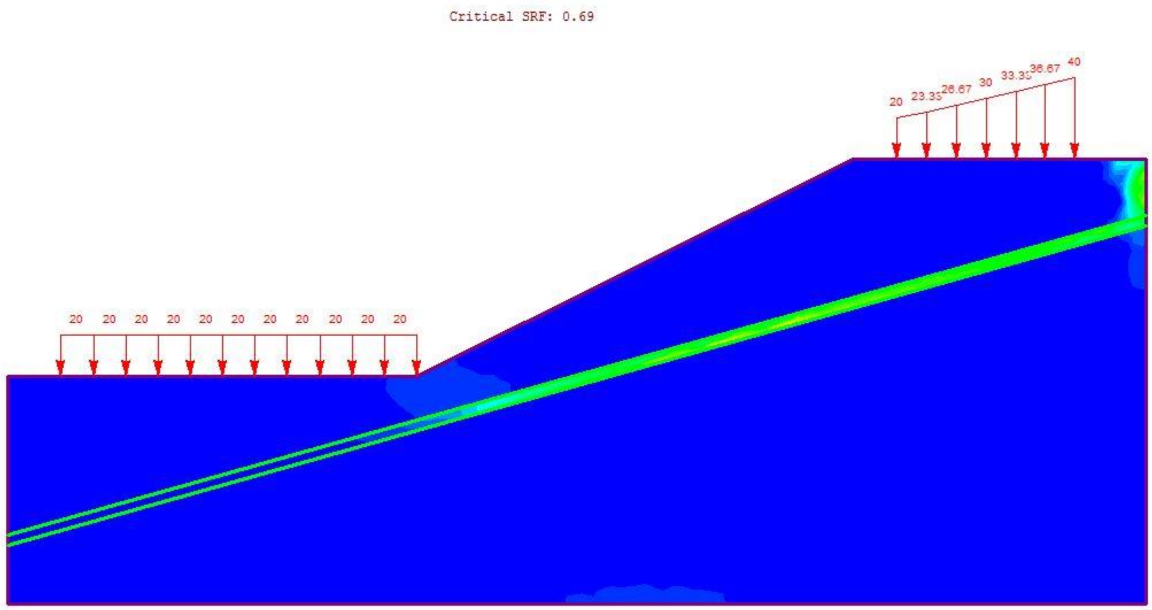

Figure 2 Solution Using SSR

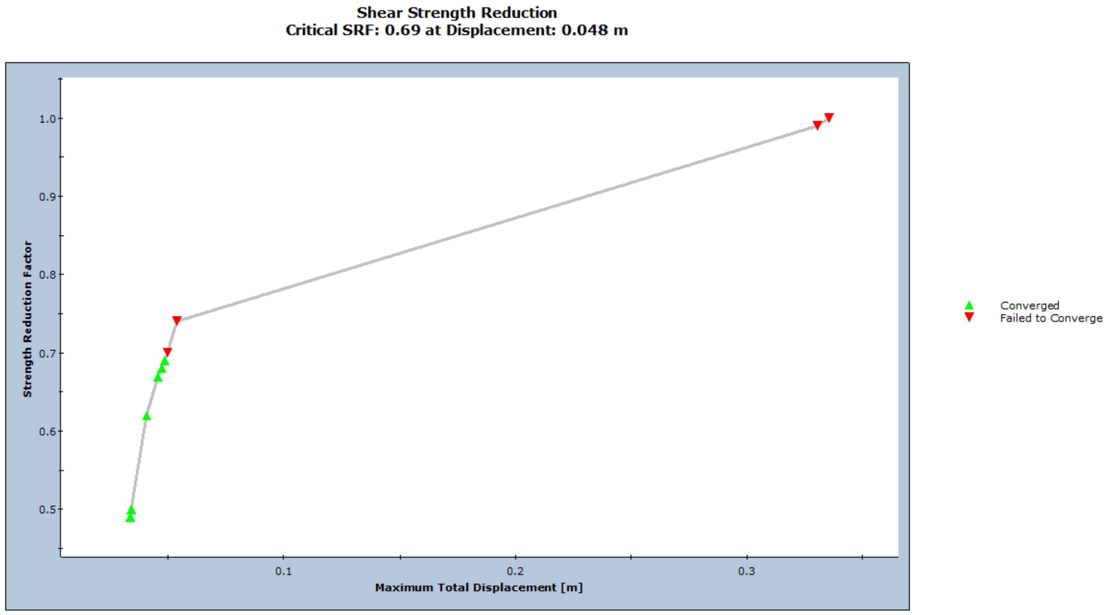

Figure 3 –SSR Convergence Graph

7 Slope with Pore Pressure Defined by Digitized Total Head Grid

Introduction

In 1988 a set of 5 basic slope stability problems, together with 5 variants, was distributed both in the Australian Geomechanics profession and overseas as part of a survey sponsored by ACADS (Giam & Donald, 1989). This is the ACADS 5 problem.

Problem description

Verification problem #10 for Slide2 - Geometry is shown in Figure 1. The soil properties are given in Table 1. This slope has been excavated at a slope of 1:2 (β=26.56˚) below an initially horizontal ground surface. The position of the critical slip surface and the corresponding factor of safety are required for the long term condition, i.e. after the ground water conditions have stabilized. Pore water pressures may be derived from the given boundary conditions or from the approximate flow net provided in Figure 2.

Geometry and Properties

Table 1: Material Properties

c′ (kN/m^2)	ϕ′ (deg.)	γ (kN/m^3)
11.0	28.0	20.00

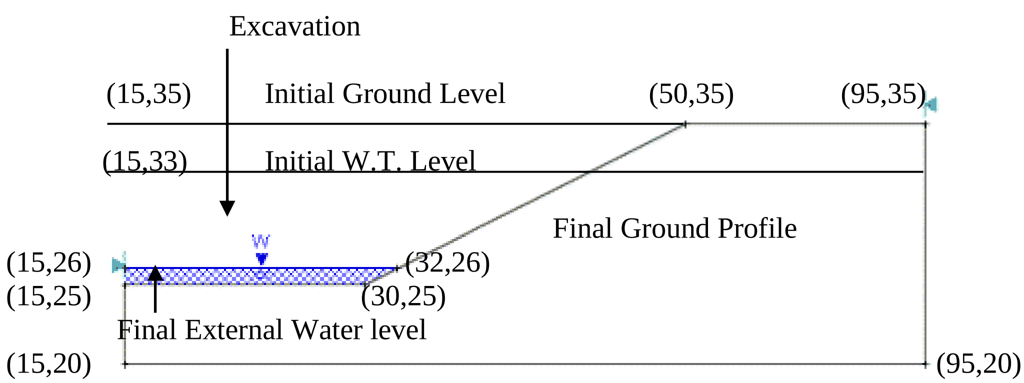

Figure 1

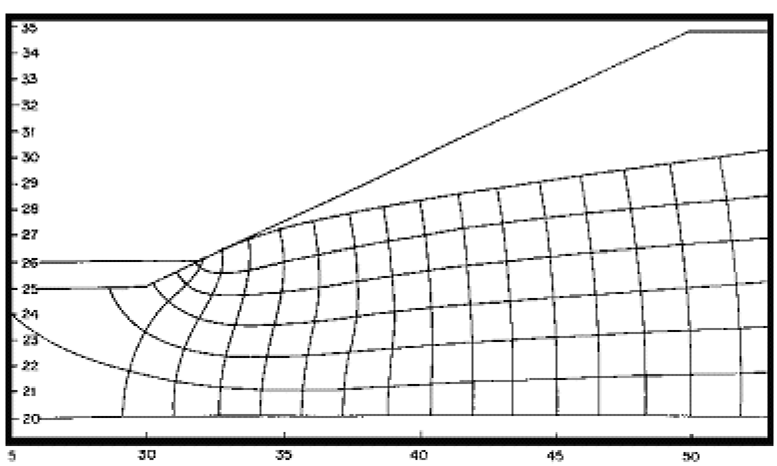

Figure 2

Results

Method	Factor of Safety
SSR	1.48
Bishop	1.498
Spencer	1.501
GLE	1.500
Janbu Corrected	1.457

Note:
Referee Factor of Safety = 1.53 [Giam]
Mean FOS (23 samples) = 1.464

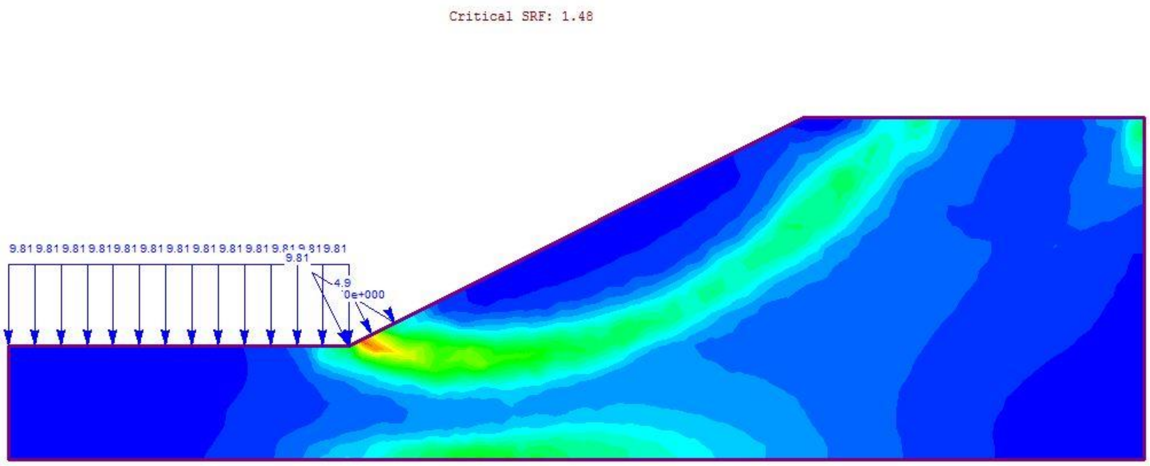

Figure 3 Solution Using SSR

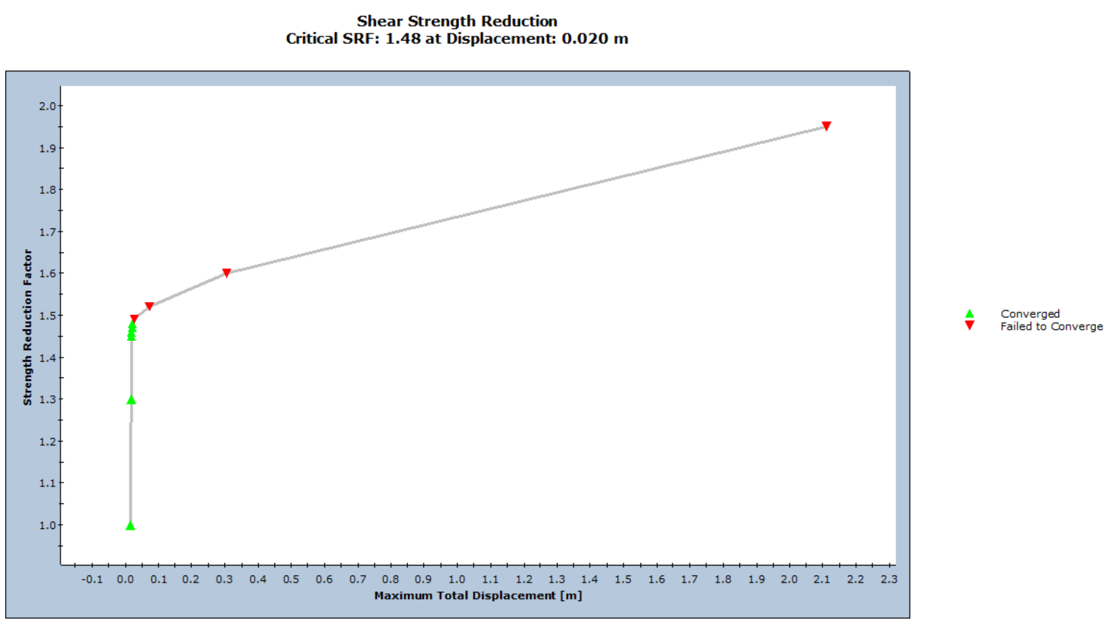

Figure 4 –SSR Convergence Graph

Introduction

This problem is an analysis of the Saint-Alban embankment (in Quebec) which was built and induced to failure for testing and research purposes in 1972 (Pilot et. al, 1982).

Problem description

Verification problem #11 for Slide2 - Geometry is shown in Figure 1. The material properties are given in Table 1. The position of the critical slip surface and the corresponding factor of safety are required. Pore water pressures were derived from the given equal pore pressure lines on Figure 1. using the Thin-Plate Spline interpolation method.

Geometry and Properties

Table 1: Material Properties

	c´ (kN/m^2)	ϕ´ (deg.)	γ (kN/m^3)
Embankment	0	44.0	18.8
Clay Foundation	2	28.0	16.68

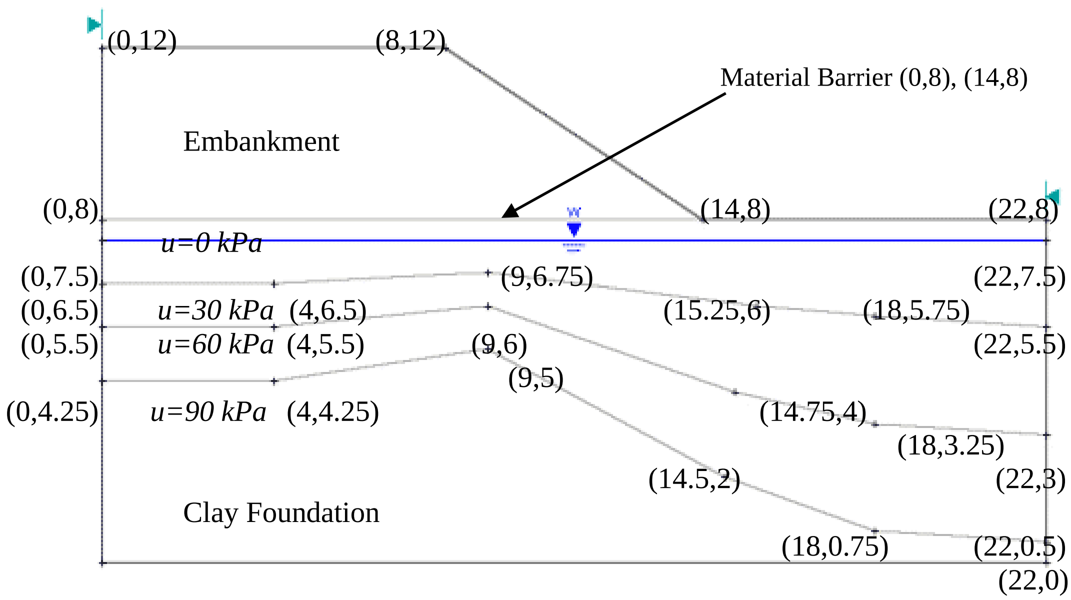

Figure 1

Results

Method	Factor of Safety
SSR	0.96
Bishop	1.037
Spencer	1.065
GLE	1.059
Janbu Corrected	1.077

Note: Referee Factor of Safety = 1.04 [Pilot]

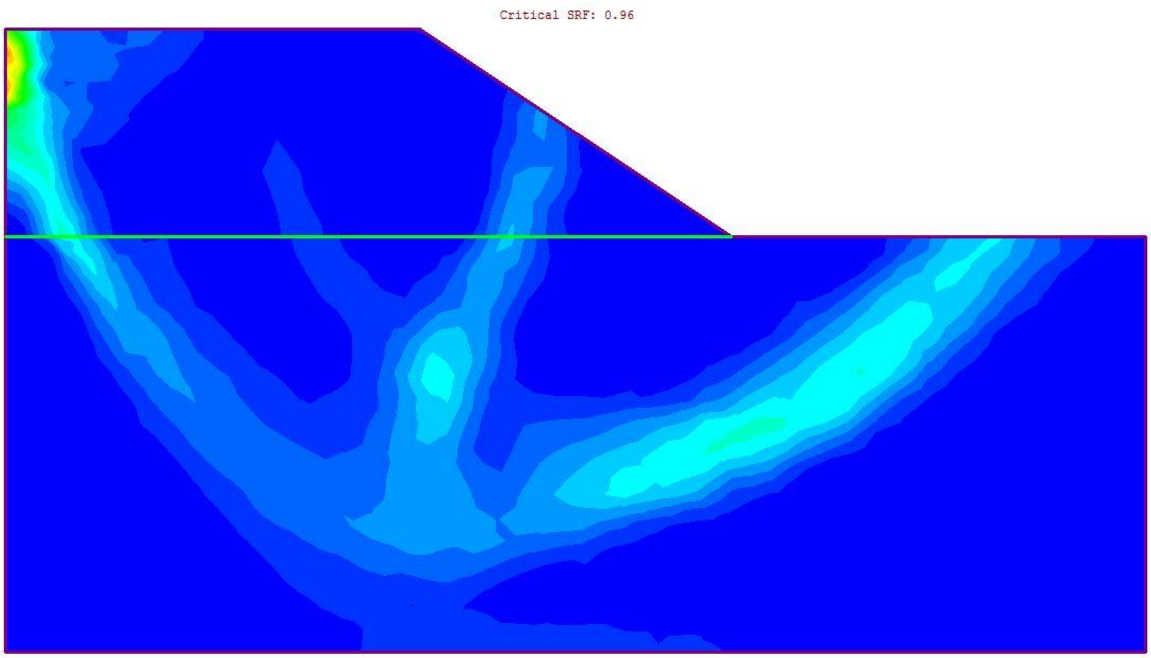

Figure 2 Solution Using SSR

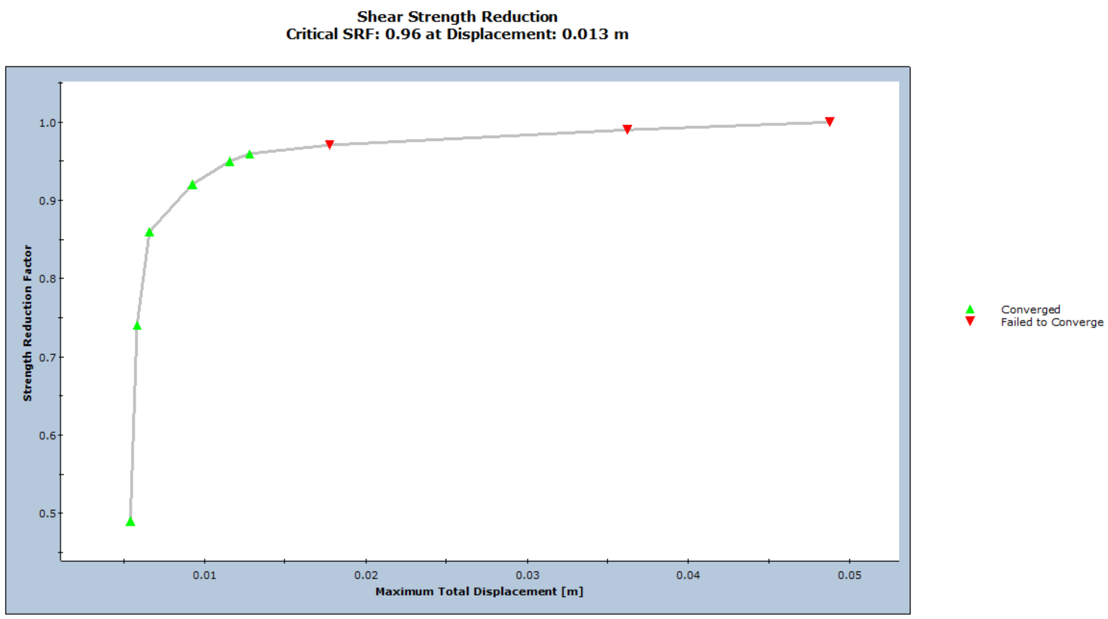

Figure 3 –SSR Convergence Graph

9 Pore Pressure Grid with Two Limit Sets

Introduction

This problem is an analysis of the Cubzac-les-Ponts embankment (in France) which was built and induced to failure for testing and research purposes in 1974 (Pilot et.al, 1982).

Problem description

Verification problem #13 for Slide2 - Geometry is shown in Figure 1. The material properties are given in Table 1. Pore water pressure was derived from the data in Table 2 using the Thin Plate Spline interpolation method. Verification is for a deep failure so support of the face is required since the factor of safety against embankment face failure is 1.11. This is accomplished by using a thin layer of elastic (infinite strength) material on the face of the embankment.

Geometry and Properties

Table 1: Material Properties

	c' (kN/m^2)	ϕ' (deg.)	γ (kN/m^3)
Embankment	0	35	21.2
Upper Clay	10	24	15.5
Lower Clay	10	28.4	15.5

Table 2: Water Pressure Points

Pt.#	Xc (m)	Yc (m)	u (kPa)	Pt.#	Xc (m)	Yc (m)	u (kPa)	Pt.#	Xc (m)	Yc (m)	u (kPa)
1	11.5	4.5	125	16	16	7.2	25	31	24.5	7.2	25
2	11.5	5.3	100	17	18	2.3	125	32	27	3.1	100
3	11.5	6.8	50	18	18	5.3	100	33	27	6.1	50
4	11.5	7.2	25	19	18	6.8	50	34	27	7.2	25
5	12.75	3.35	125	20	18	7.2	25	35	29.75	1.55	100
6	12.75	5.2	100	21	20	1.15	125	36	29.75	5.55	50
7	12.75	6.8	50	22	20	4.85	100	37	29.75	7.2	25
8	12.75	7.2	25	23	20	6.8	50	38	32.5	0	100
9	14	2.3	125	24	20	7.2	25	39	32.5	5	50
10	14	5.1	100	25	22	0	125	40	32.5	7.2	25
11	14	6.8	50	26	22	4.4	100	41	37.25	4.7	50
12	14	7.2	25	27	22	6.8	50	42	37.25	6.85	25
13	16	2.3	125	28	22	7.2	25	43	42	4.4	50
14	16	5.2	100	29	24.5	3.75	100	44	42	6.5	25
15	16	6.8	50	30	24.5	6.45	50	45	-	-	-

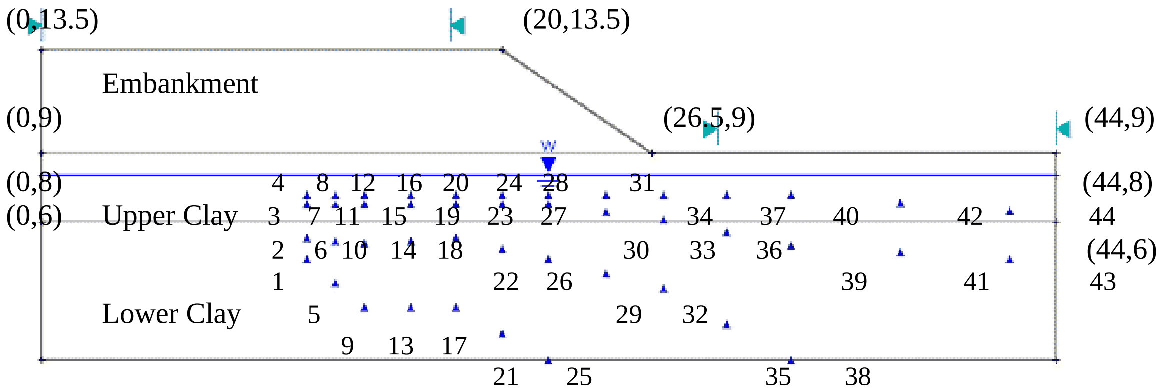

Figure 1

Results

Method	Factor of Safety
SSR	1.31
Bishop	1.314
Spencer	1.334
GLE	1.336
Janbu Corrected	1.306

Note: Author's Factor of Safety (by Bishop method) = 1.24 [Pilot]

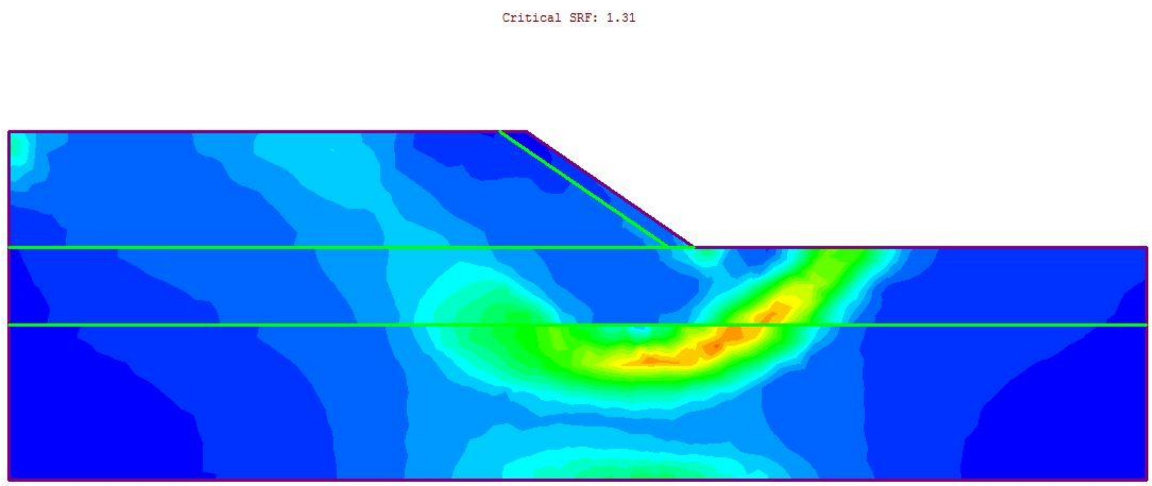

Figure 2 Solution Using SSR

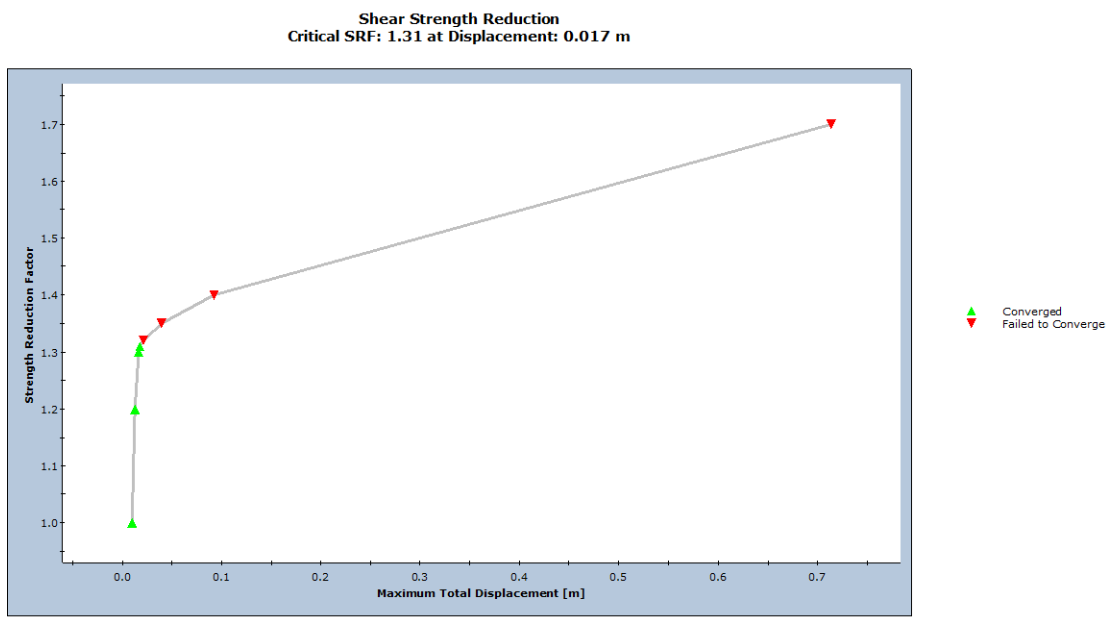

Figure 3 –SSR Convergence Graph

Introduction

This model is taken from Arai and Tagyo (1985) example#1 and consists of a simple slope of homogeneous soil with zero pore pressure.

Problem description

Verification problem #14 for Slide2 - Geometry is shown in Figure 1. The material properties are given in Table 1. There are no pore pressures in this problem.

Geometry and Properties

Table 1: Material Properties

	c′ (kN/m^2)	ϕ′ (deg.)	γ (kN/m^3)
soil	41.65	15	18.82

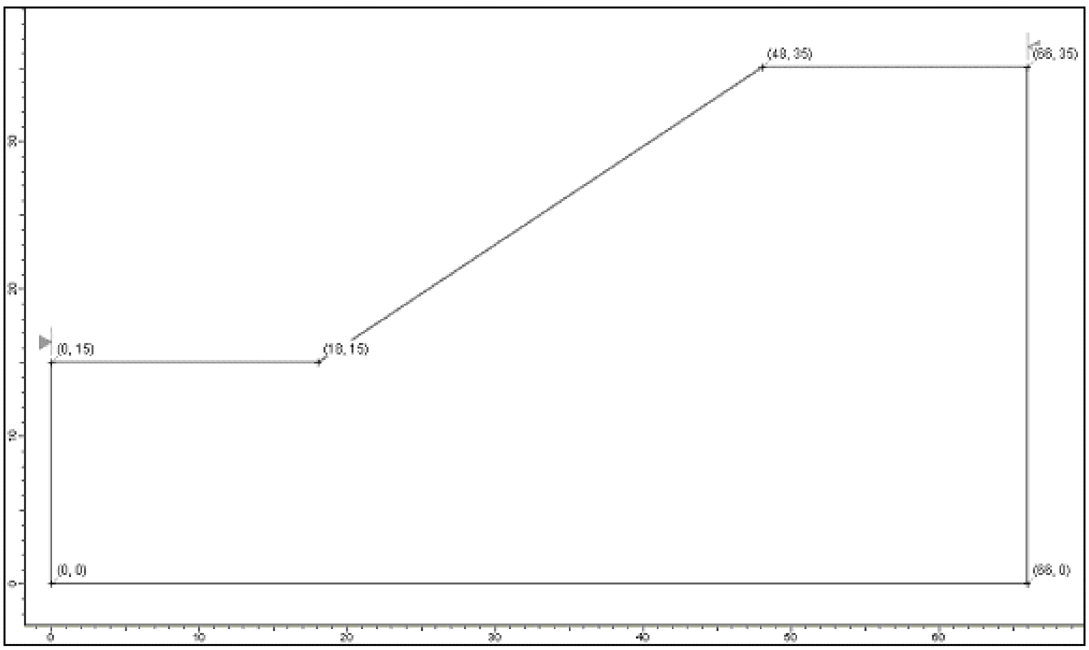

Figure 1 - Geometry

Results

Method	Factor of Safety (circular surface)	Factor of Safety (non-circular surface)
SSR	1.40	
Bishop	1.409	--
Janbu Simplified	1.319	1.253
Janbu Corrected	1.414	1.346
Spencer	1.406	1.388

Arai and Tagyo (1985) Bishops Simplified Factor of Safety = 1.451
Arai and Tagyo (1985) Janbu Simplified Factor of Safety = 1.265
Arai and Tagyo (1985) Janbu Corrected Factor of Safety = 1.357

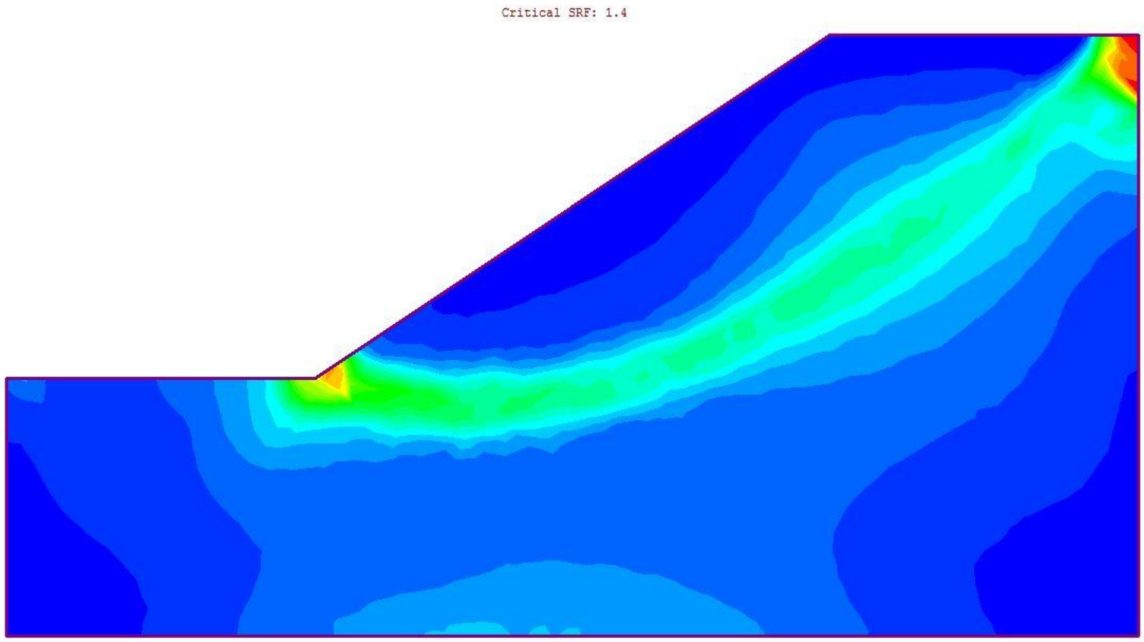

Figure 2 Solution Using SSR

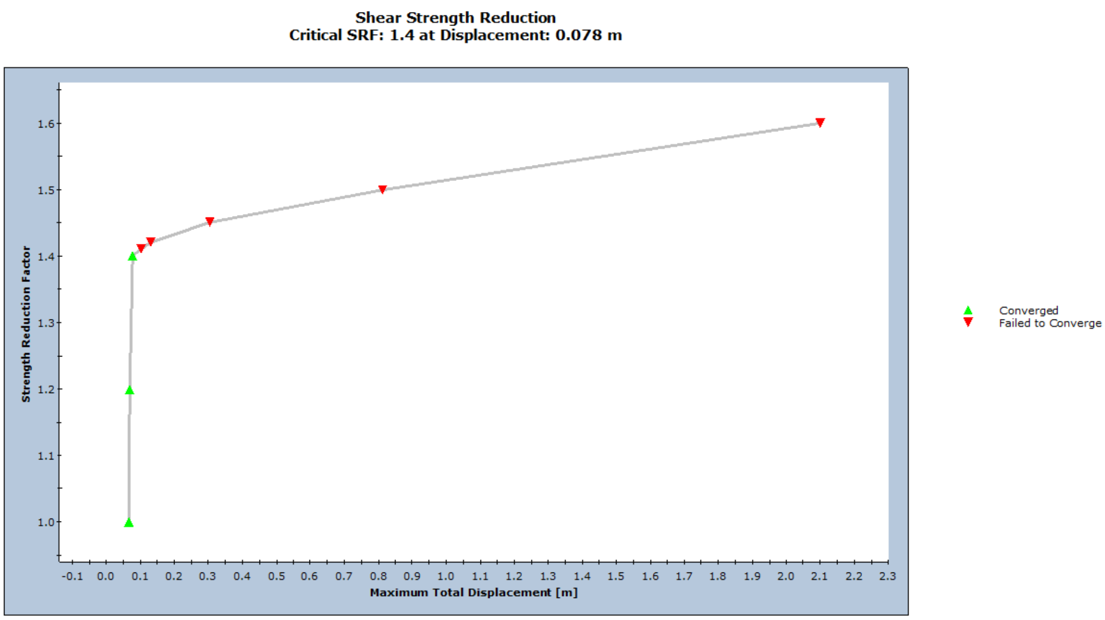

Figure 3 –SSR Convergence Graph

Introduction

This model is taken from Arai and Tagyo (1985) example#2 and consists of a layered slope where a layer of low resistance is interposed between two layers of higher strength. A number of other authors have also analyzed this problem, notably Kim et al. (2002), Malkawi et al. (2001), and Greco (1996).

Problem description

Verification problem #15 for Slide2 - Problem geometry is shown in Figure 1. The material properties are given in Table 1. The factor of safety calculated using SSR and compared to limit equilibrium results of both circular and noncircular slip surfaces. There are no pore pressures in this problem.

Geometry and Properties

Table 1: Material Properties

	c′ (kN/m^2)	ϕ′ (deg.)	γ (kN/m^3)
Upper Layer	29.4	12	18.82
Middle Layer	9.8	5	18.82
Lower Layer	294	40	18.82

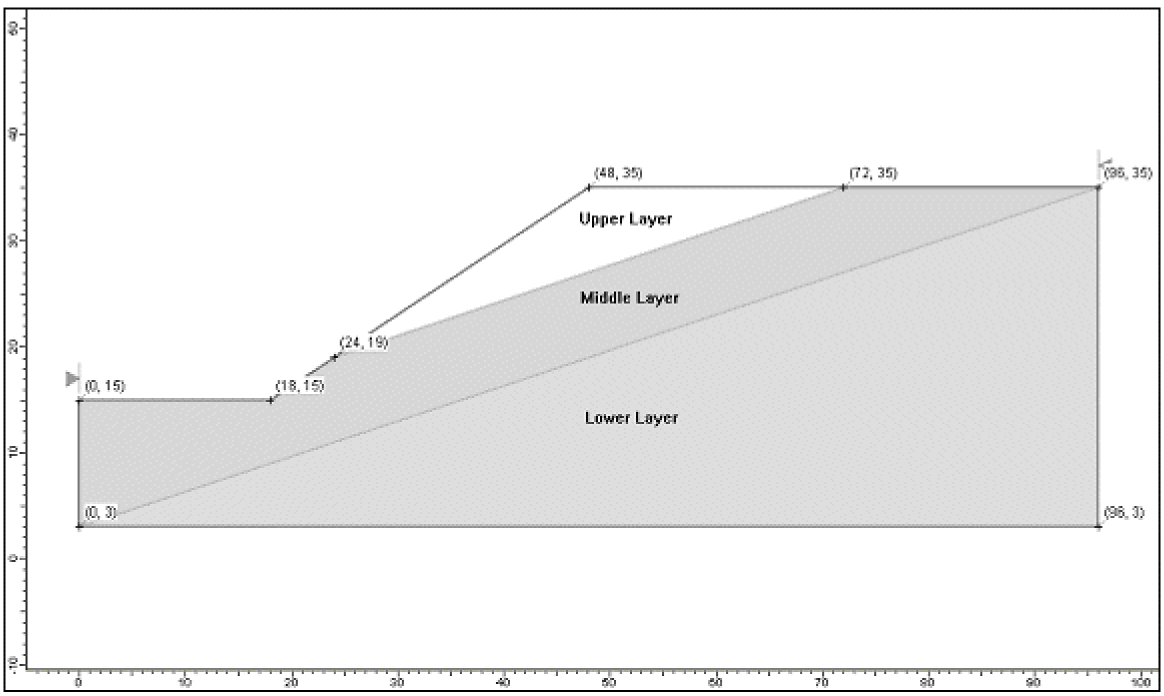

Figure 1 – Geometry

Results

Method	Factor of Safety (circular surface)	Factor of Safety (non-circular surface)
SSR	0.39	
Bishop	0.421	--
Janbu Simplified	0.410	0.394
Janbu Corrected	0.437	0.419
Spencer	0.424	0.412

Arai and Tagyo (1985) Bishops Simplified Factor of Safety = 0.417
Kim et al. (2002) Bishops Simplified Factor of Safety = 0.43
Greco (1996) Spencers method using monte carlo searching = 0.39
Kim et al. (2002) Spencers method using random search = 0.44
Kim et al. (2002) Spencers method using pattern search = 0.39
Arai and Tagyo (1985) Janbu Simplified Factor of Safety = 0.405
Arai and Tagyo (1985) Janbu Corrected Factor of Safety = 0.430

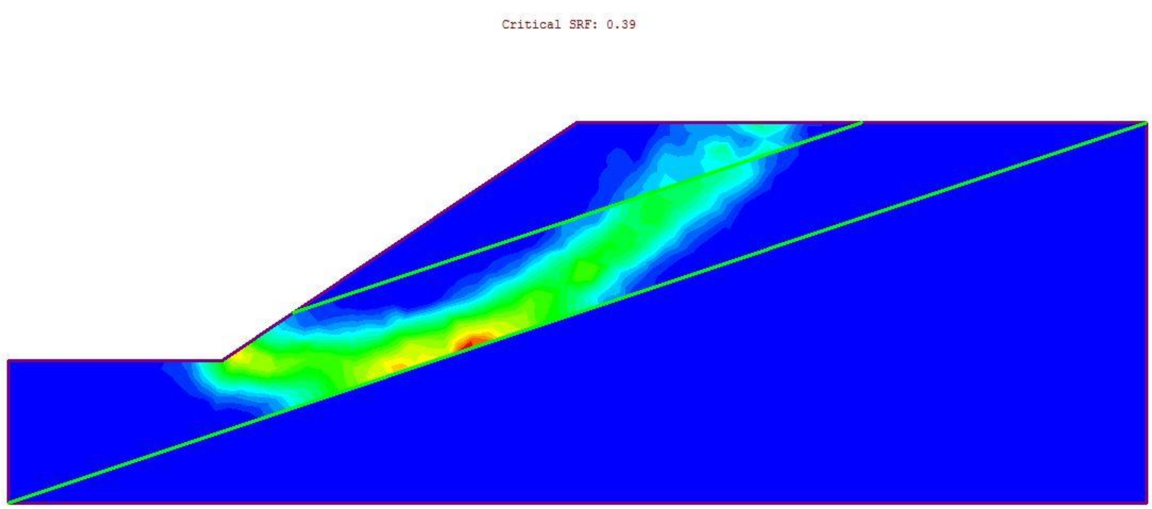

Figure 2 Solution Using SSR

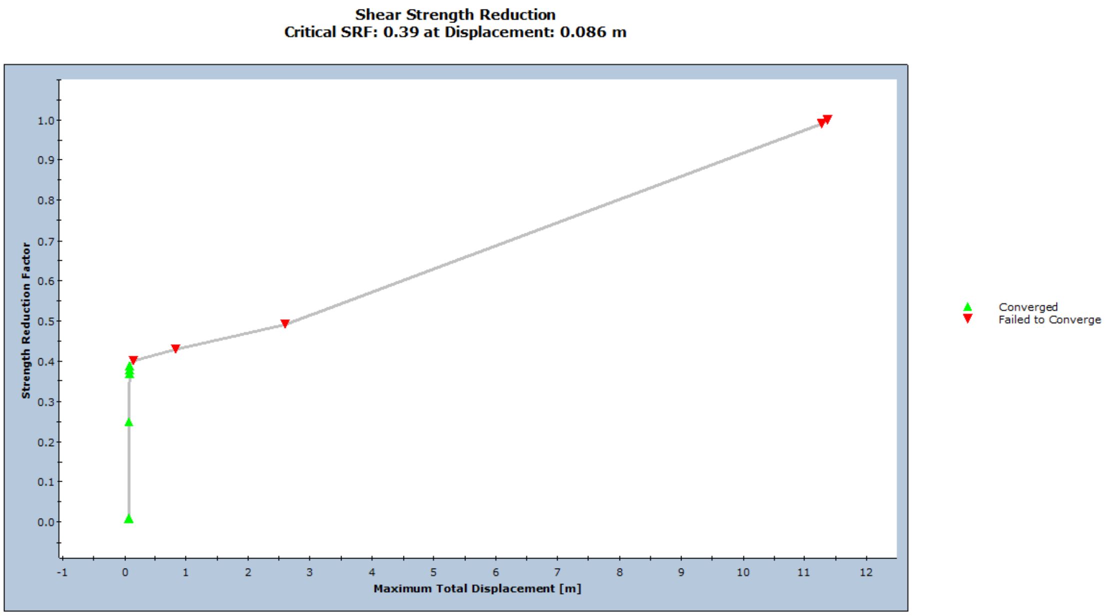

Figure 3 –SSR Convergence Graph

12 Simple Slope with Water Table

Introduction

This model is taken from Arai and Tagyo (1985) example#3 and consists of a simple slope of homogeneous soil with pore pressure.

Problem description

Verification problem #16 for Slide2 - Geometry is shown in Figure 1. The material properties are given in Table 1. The location for the water table is shown in Figure 1. The factor of safety calculated using SSR and compared to limit equilibrium results of both circular and noncircular slip surfaces. Pore pressures are calculated assuming hydrostatic conditions. The pore pressure at any point below the water table is calculated by measuring the vertical distance to the water table and multiplying by the unit weight of water. There is zero pore pressure above the water table.

Geometry and Properties

Table 1: Material Properties

	c´ (kN/m^2)	ϕ´ (deg.)	γ (kN/m^3)
soil	41.65	15	18.82

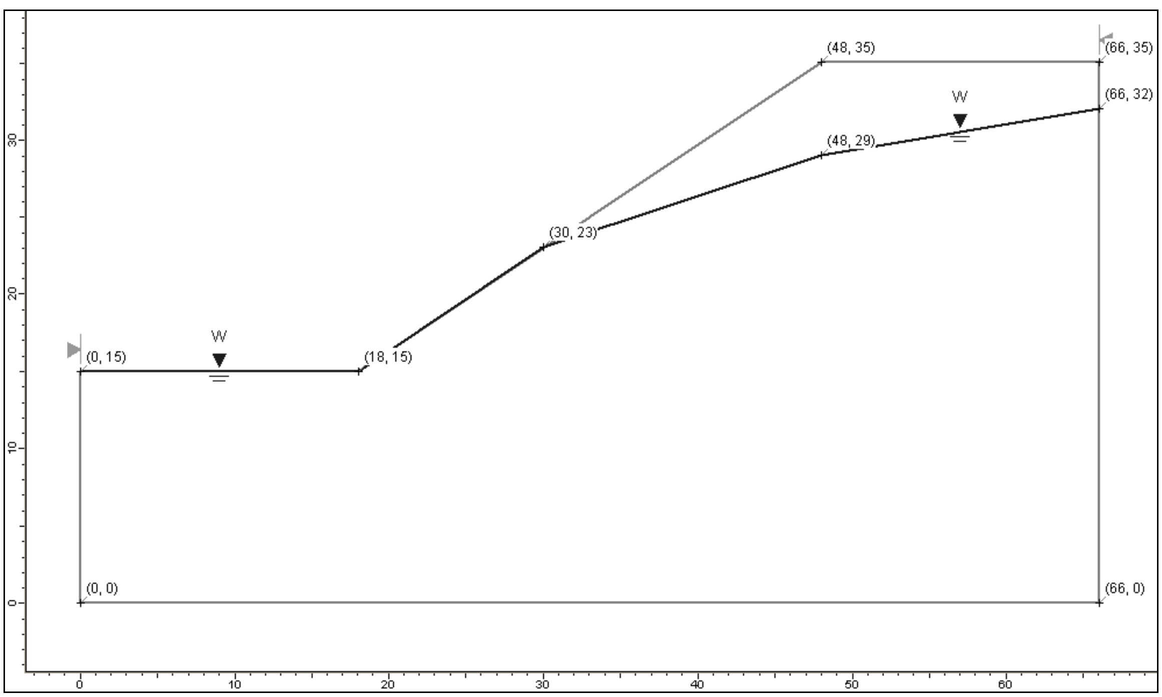

Figure 1 - Geometry

Results

Method	Factor of Safety (circular surface)	Factor of Safety (non-circular surface)
SSR	1.09	
Bishop	1.117	--
Janbu Simplified	1.046	0.968
Janbu Corrected	1.131	1.050
Spencer	1.118	1.094

Arai and Tagyo (1985) Bishops Simplified Factor of Safety = 1.138
Arai and Tagyo (1985) Janbu Simplified Factor of Safety = 0.995
Arai and Tagyo (1985) Janbu Corrected Factor of Safety = 1.071

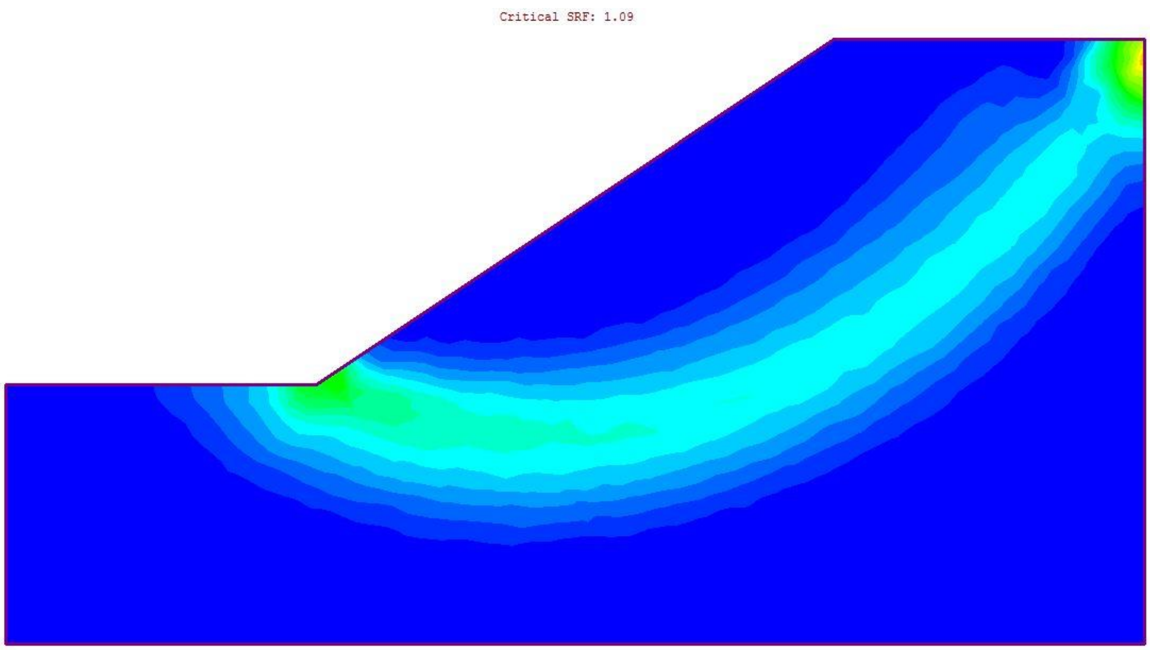

Figure 2 Solution Using SSR

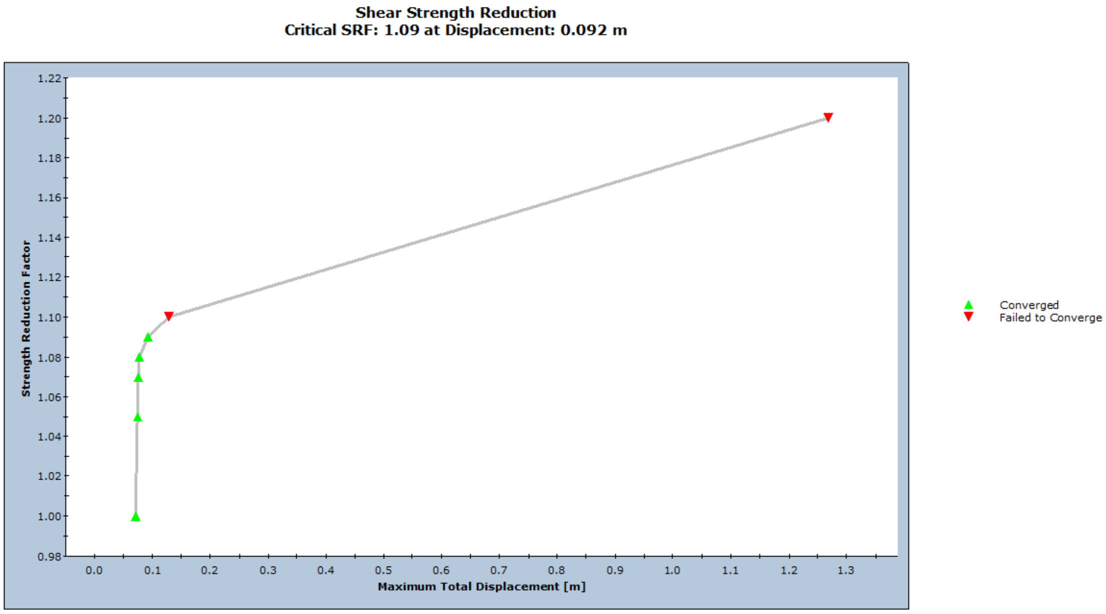

Figure 3 –SSR Convergence Graph

Introduction

This model is taken from Yamagami and Ueta (1988) and consists of a simple slope of homogeneous soil with zero pore pressure. Greco (1996) has also analyzed this slope.

Problem description

Verification problem #17 for Slide2 - Geometry is shown in Figure 1. The material properties are given in Table 1. The factor of safety calculated using SSR and compared to limit equilibrium results of both circular and noncircular slip surfaces. There are no pore pressures in this problem.

Geometry and Properties

Table 1: Material Properties

	c´ (kN/m^2)	ϕ´ (deg.)	γ (kN/m^3)
soil	9.8	10	17.64

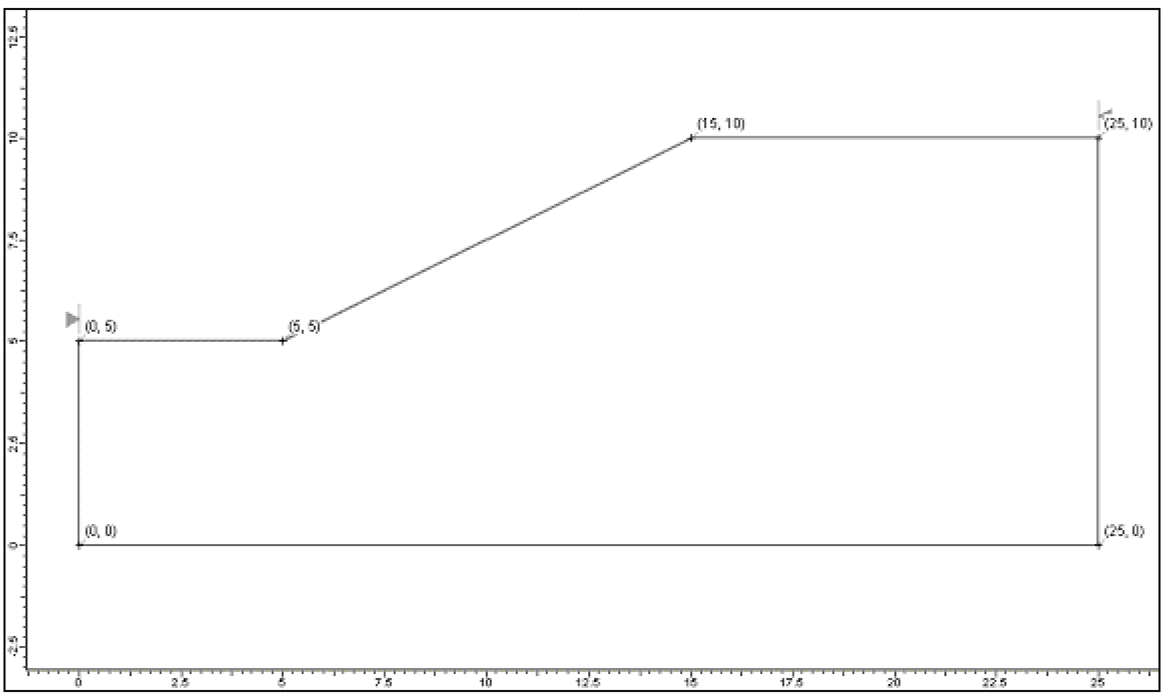

Figure 1 - Geometry

Results

Method	Factor of Safety (circular surface)	Factor of Safety (non-circular surface)
SSR	1.33	
Bishop	1.344	--
Ordinary	1.278	--
Janbu Simplified	--	1.178
Spencer	--	1.324

Yamagami and Ueta (1988) Bishops Simplified Factor of Safety = 1.348
Yamagami and Ueta (1988) Fellenius/Ordinary Factor of Safety = 1.282
Yamagami and Ueta (1988) Janbu Simplified Factor of Safety = 1.185
Yamagami and Ueta (1988) Spencer Factor of Safety = 1.339
Greco (1996) Spencer Factor of Safety = 1.33

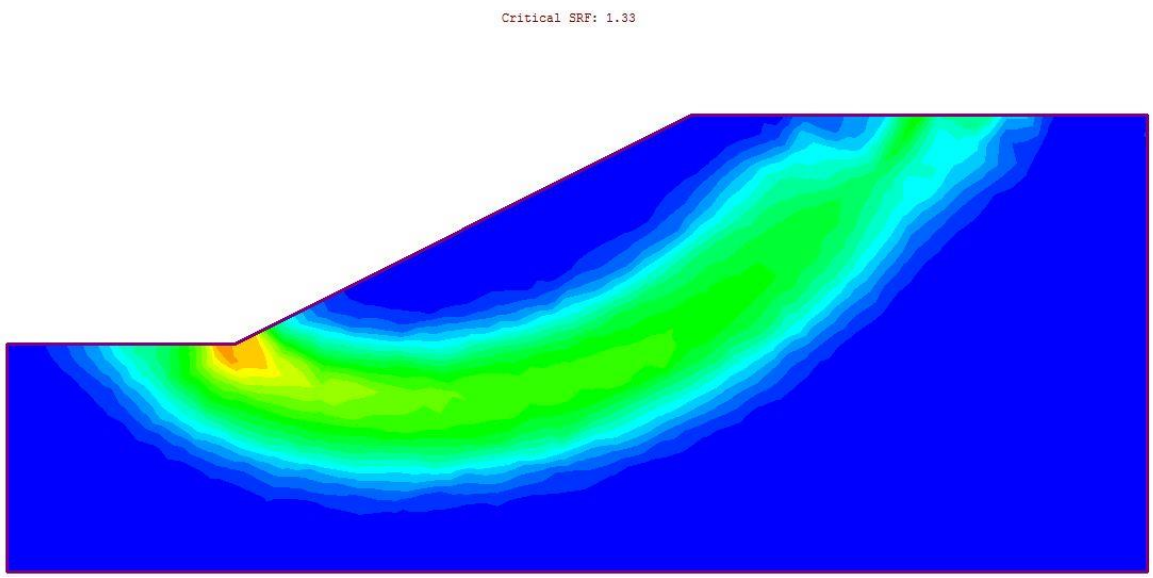

Figure 2 Solution Using SSR

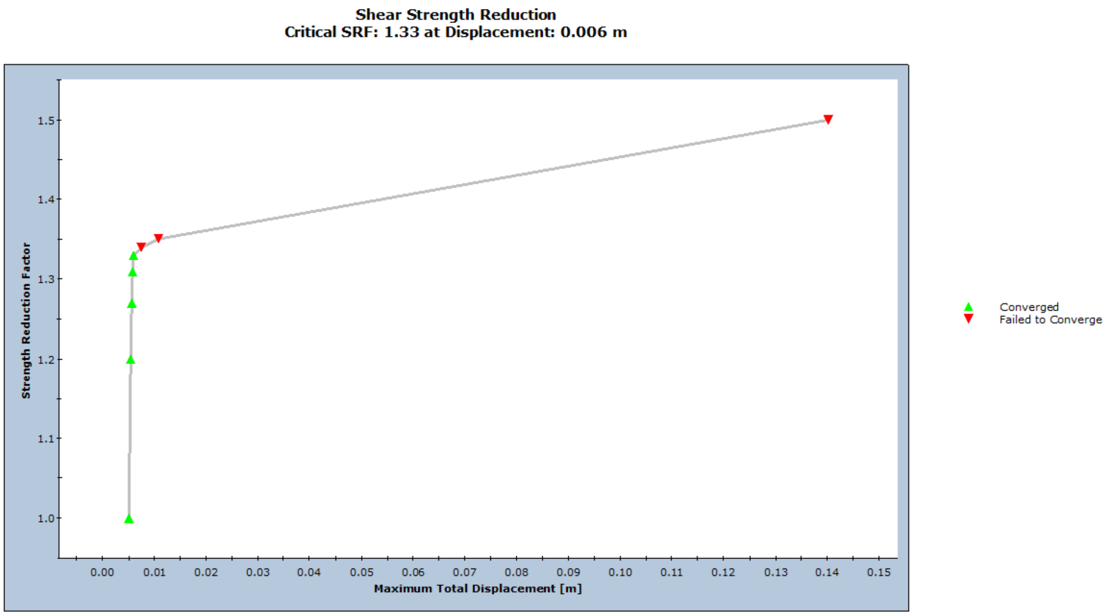

Figure 3 –SSR Convergence Graph

14 Simple Slope with Pore Pressure Defined by R_u Value

Introduction

This model is taken from Baker (1980) and was originally published by Spencer (1969). It consists of a simple slope of homogeneous soil with pore pressure.

Problem description

Verification problem #18 for Slide2 - Geometry is shown in Figure 1. The material properties are given in Table 1. The position of the critical slip surface and the corresponding factor of safety are calculated for a noncircular slip surface. The pore pressure within the slope is modeled using an Ru value of 0.5.

Geometry and Properties

Table 1: Material Properties

	c′ (kN/m^2)	ϕ′ (deg.)	γ (kN/m^3)	Ru
soil	10.8	40	18	0.5

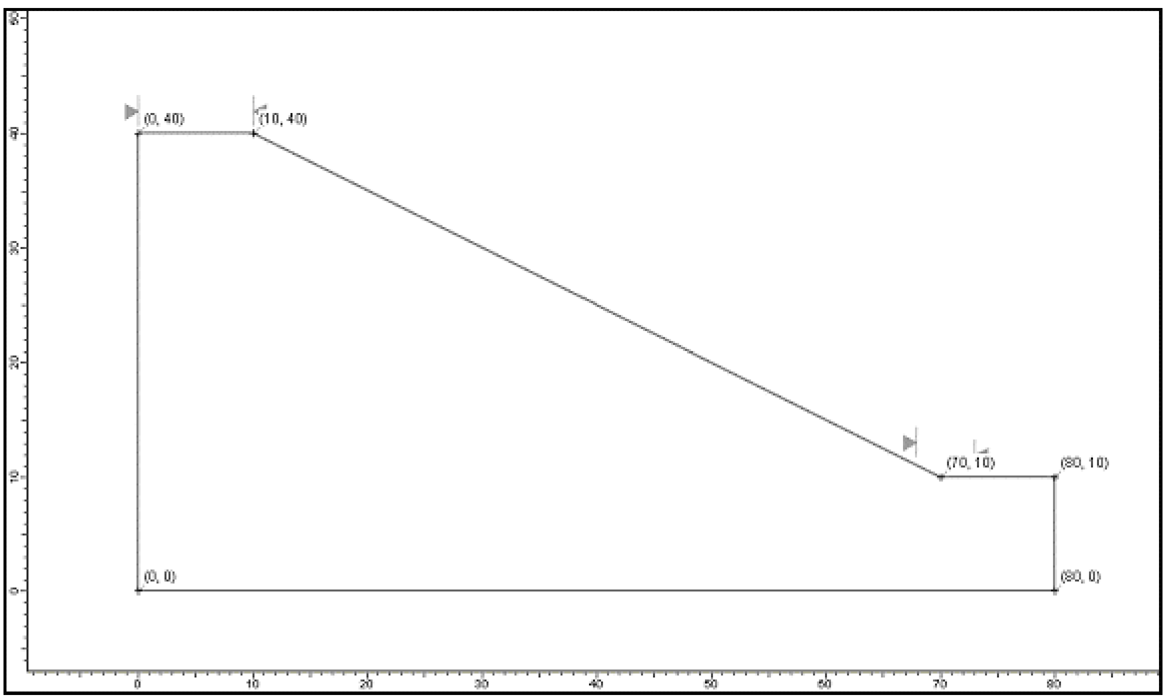

Figure 1 - Geometry

Results – Slide2 result using Random search with Monte-Carlo optimization

Method	Factor of Safety
SSR (RS2)	0.98
Spencer (Slide2)	1.01

Baker (1980) Spencer Factor of Safety = 1.02
Spencer (1969) Spencer Factor of Safety = 1.08

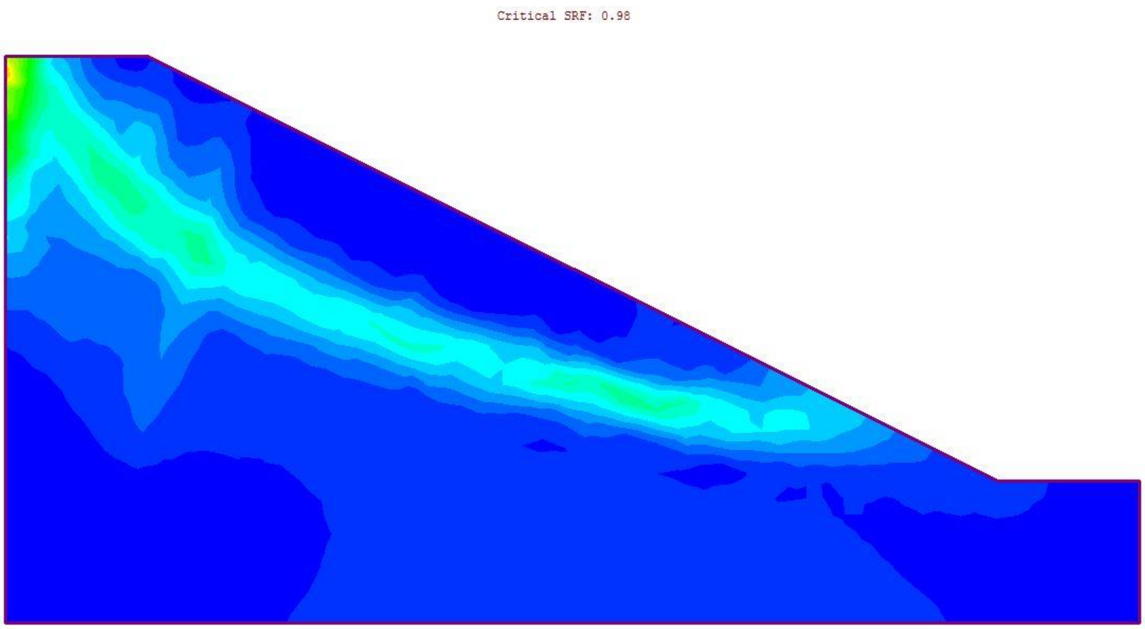

Figure 2 Solution Using SSR

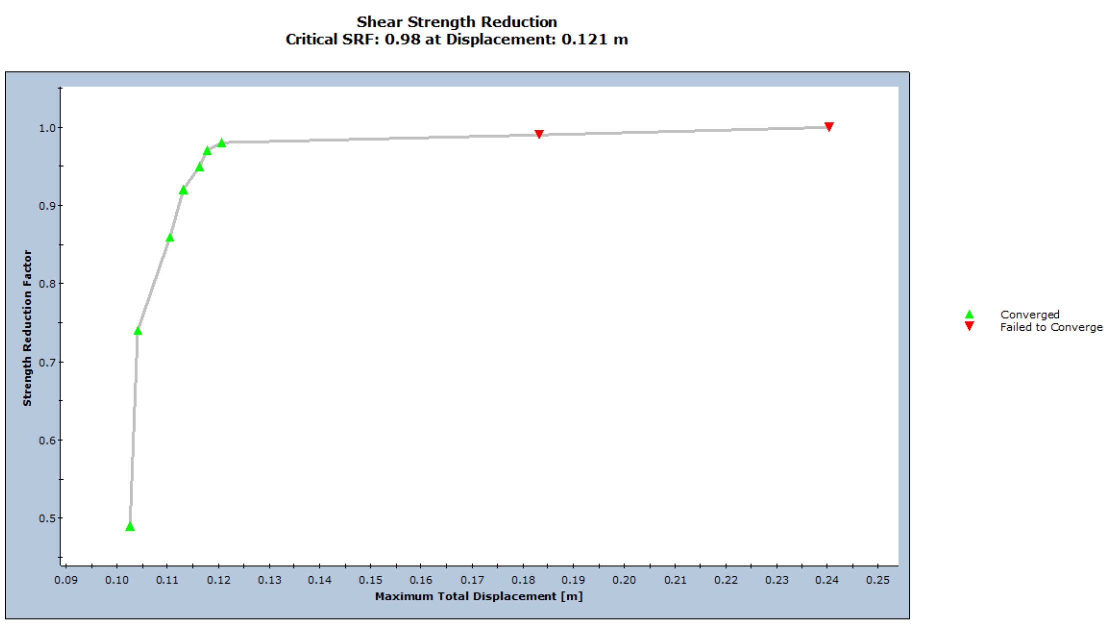

Figure 3 –SSR Convergence Graph

Introduction

This model is taken from Greco (1996) example #4 and was originally published by Yamagami and Ueta (1988). It consists of a layered slope without pore pressure.

Problem description

Verification problem #19 for Slide2 - Geometry is shown in Figure 1. The material properties are given in Table 1.

Geometry and Properties

Table 1: Material Properties

	c´ (kN/m^2)	ϕ´ (deg.)	γ (kN/m^3)
Upper Layer	49	29	20.38
Layer 2	0	30	17.64
Layer 3	7.84	20	20.38
Bottom Layer	0	30	17.64

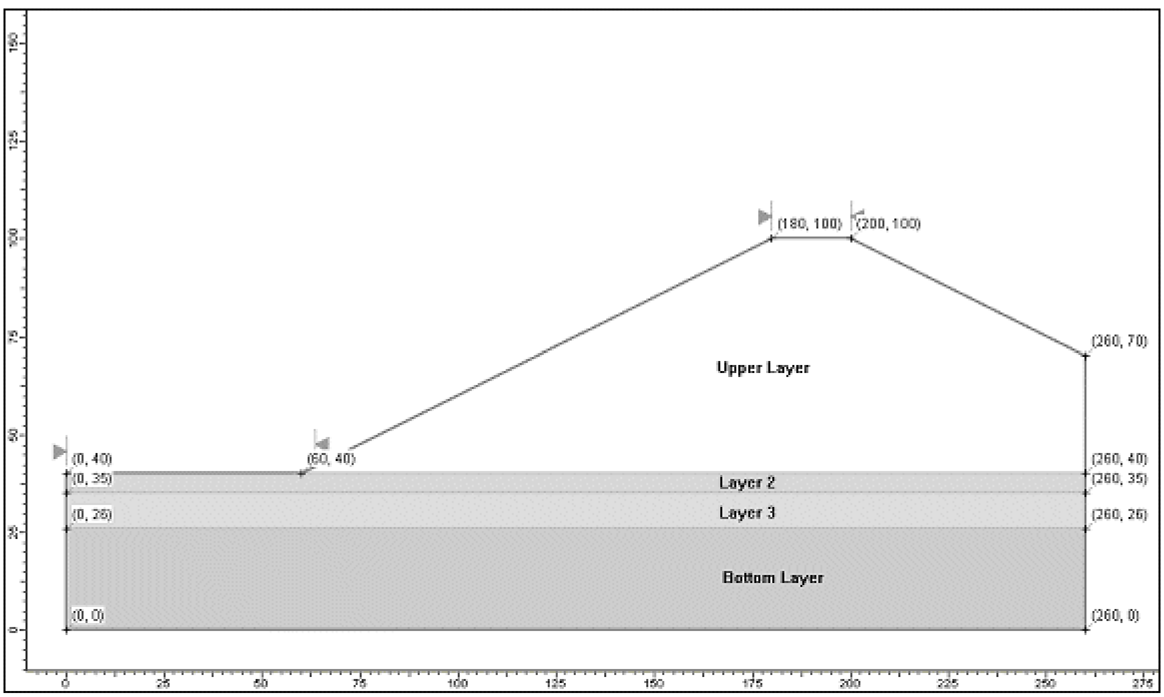

Figure 1 - Geometry

Results

Method	Factor of Safety
SSR (RS2)	1.39
Spencer (Slide2)	1. 398

Greco (1996) Spencer Factor of Safety = 1.40 - 1.42
Spencer (1969) Spencer Factor of Safety = 1.40 - 1.42

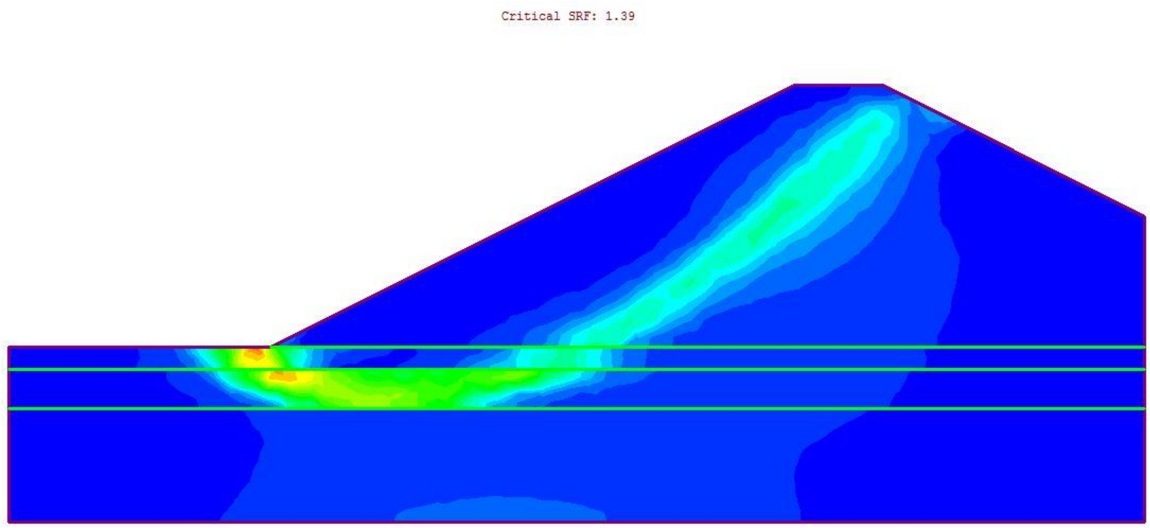

Figure 2 - Solution Using SSR

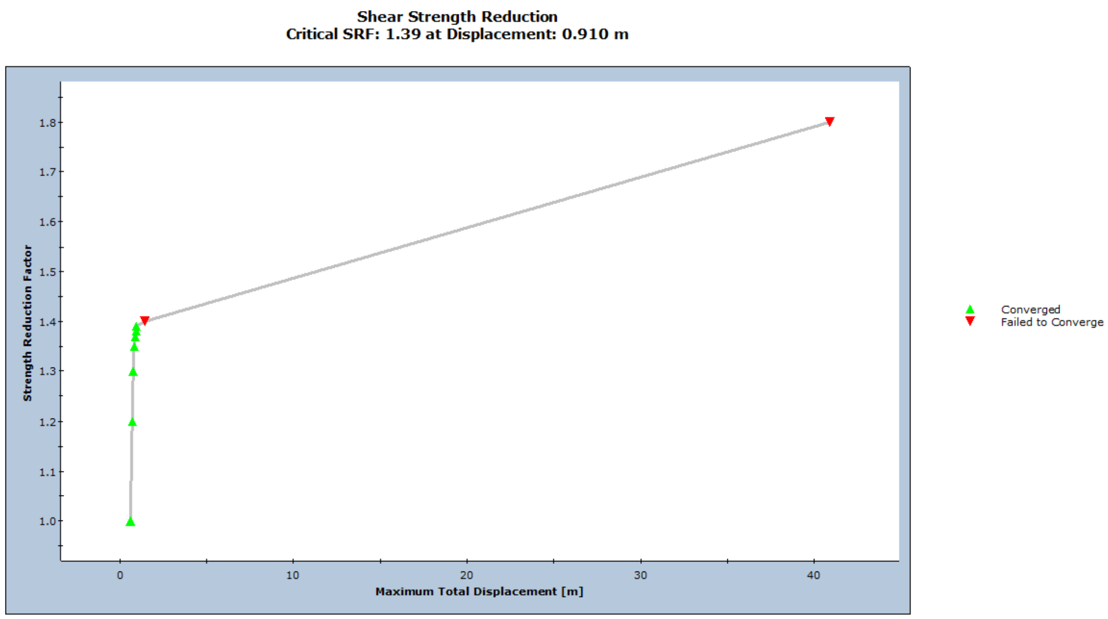

Figure 3 - SSR Convergence Graph

16 Layered Slope and a Water Table with Weak Seam

Introduction

This model is taken from Greco (1996) example #5 and was originally published by Chen and Shao (1988). It consists of a layered slope with pore pressure and a weak seam.

Problem description

Verification problem #20 for Slide2 - Geometry is shown in Figure 1. The material properties are given in Table 1. The factor of safety calculated using SSR and compared to limit equilibrium results of both circular and noncircular slip surfaces. The weak seam is modeled as a 0.5m thick material layer at the base of the model.

Geometry and Properties

Table 1: Material Properties

	c′ (kN/m^2)	ϕ′ (deg.)	γ (kN/m^3)
Layer 1	9.8	35	20
Layer 2	58.8	25	19
Layer 3	19.8	30	21.5
Layer 4	9.8	16	21.5

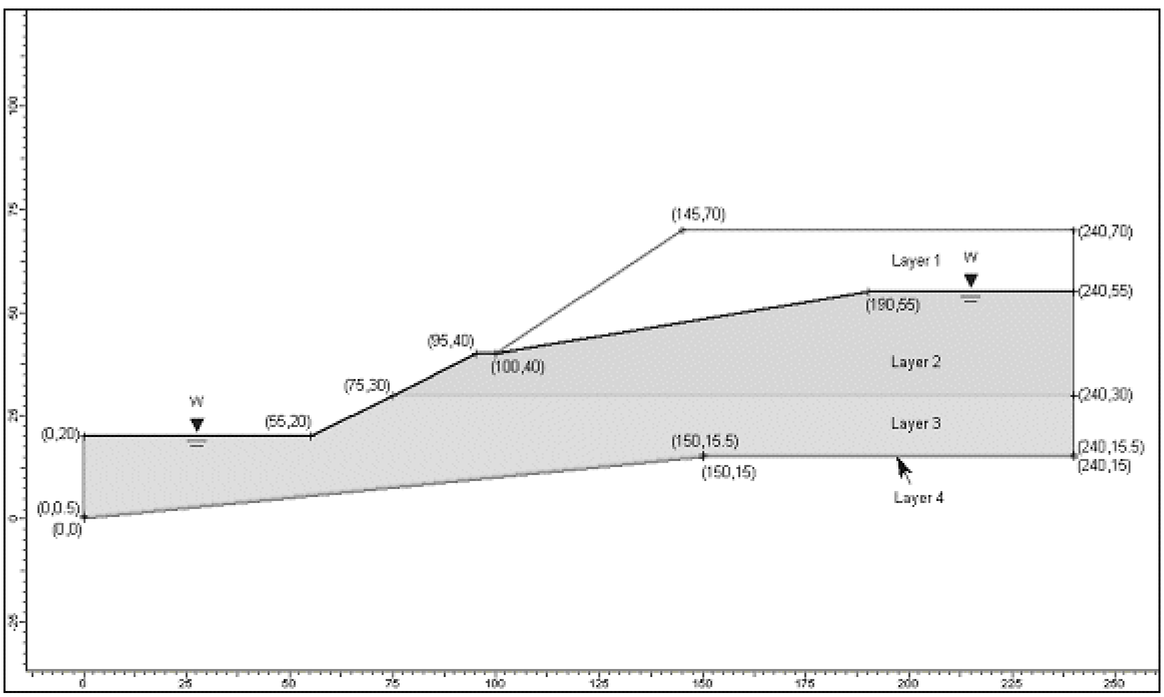

Figure 1 - Geometry

Results

Method	Factor of Safety (circular surface)	Factor of Safety (non-circular surface)
SSR (RS2)	1.02	
Bishop (Slide22)	1.087	--
Spencer (Slide22)	1.093	1.007

Greco (1996) Spencer factor of safety for nearly circular local critical surface = 1.08
Chen and Shao (1988) Spencer Factor of Safety = 1.01 - 1.03
Greco (1996) Spencer Factor of Safety = 0.973 - 1.1

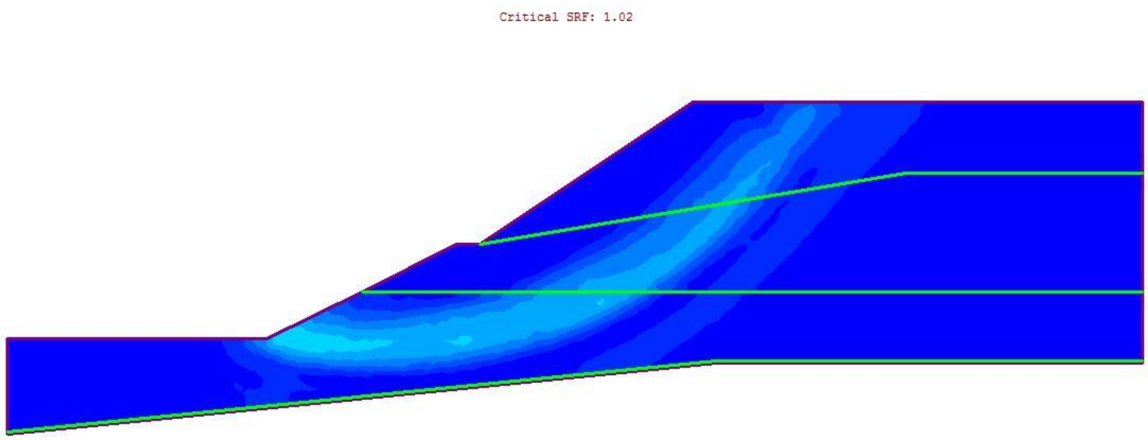

Figure 2 Solution Using SSR

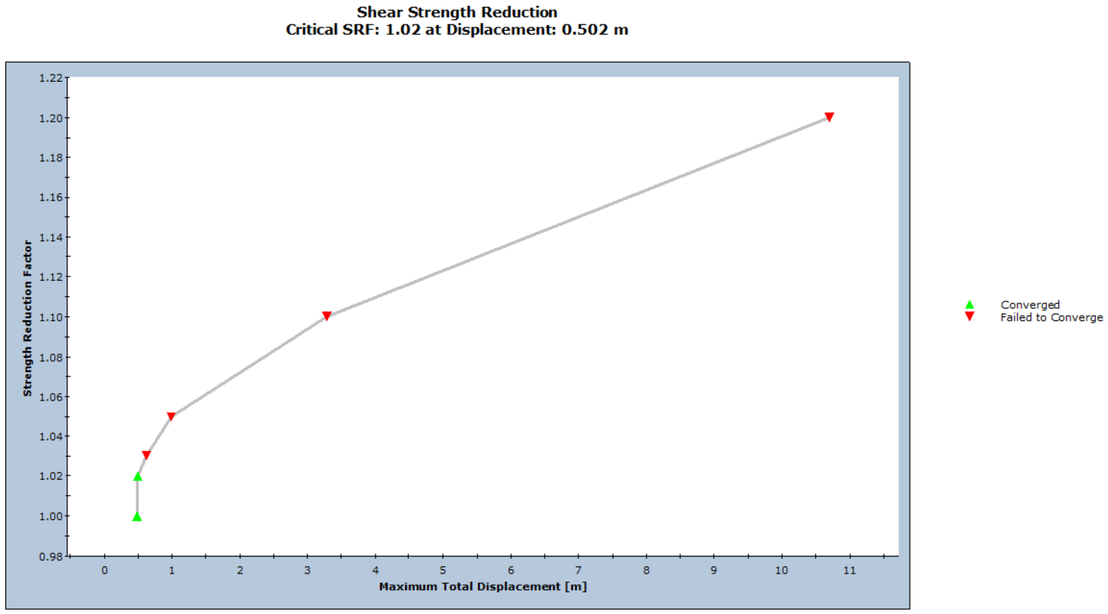

Figure 3 –SSR Convergence Graph

17 Slope with Three Different Pore Pressure Conditions

Introduction

This model is taken from Fredlund and Krahn (1977). It consists of a homogeneous slope with three separate water conditions, 1) dry, 2) Ru defined pore pressure, 3) pore pressures defined using a water table. The model is done in imperial units to be consistent with the original paper. Quite a few other authors, such as Baker (1980), Greco (1996), and Malkawi (2001) have also analyzed this slope.

Problem description

Verification problem #21 for Slide22 - Geometry is shown in Figure 1. The material properties are given in Table 1. The position of the circular slip surface is given in Fredlund and Krahn as being xc=120,yc=90,radius=80. The GLE/Discrete Morgenstern and Price method was run with the half sine interslice force function.

Table 15.1: Material Properties

	c´ (psf)	φ´ (deg.)	γ (pcf)	Ru (case2)
soil	600	20	120	0.25

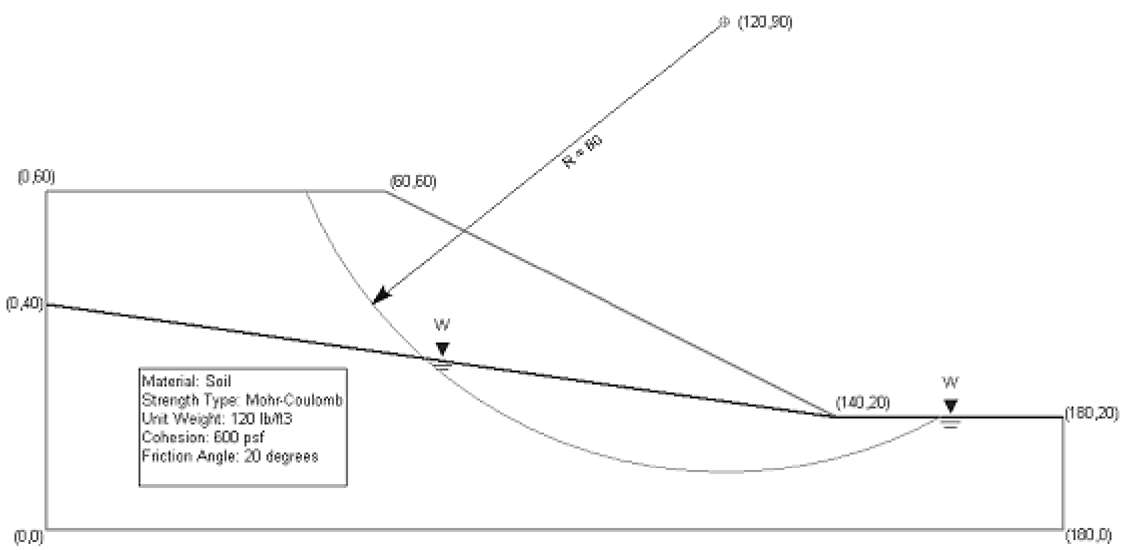

Figure 1 - Geometry

Results

Case	Ordinary (F&K)	Ordinary (Slide22)	Bishop (F&K)	Bishop (Slide22)	Spencer (F&K)	Spencer (Slide22)	M-P (F&K)	M-P (Slide22)	SSR (RS2)
1-Dry	1.928	1.931	2.080	2.079	2.073	2.075	2.076	2.075	2.0
2-Ru	1.607	1.609	1.766	1.763	1.761	1.760	1.764	1.760	1.68
3-WT	1.693	1.697	1.834	1.833	1.830	1.831	1.832	1.831	1.78

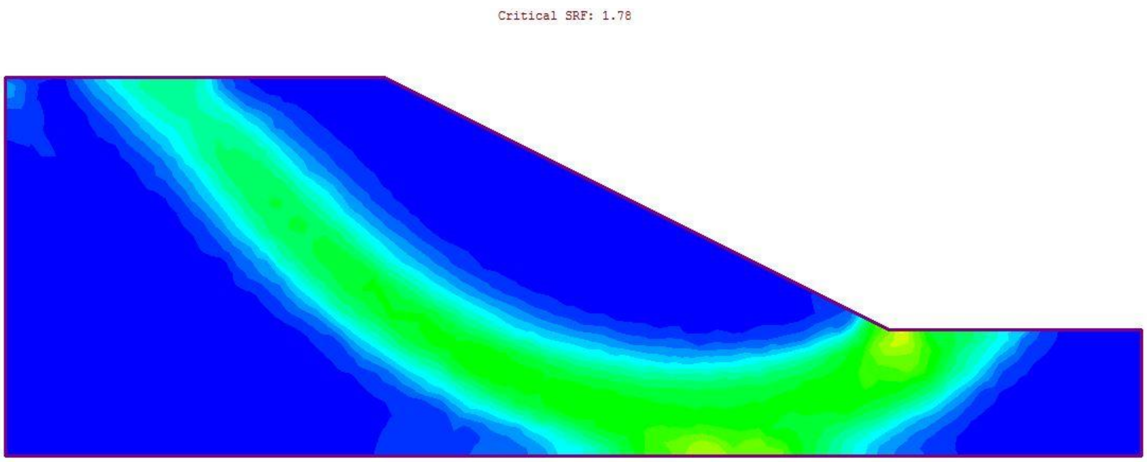

Figure 2 Solution Using SSR – Case 3 with water table

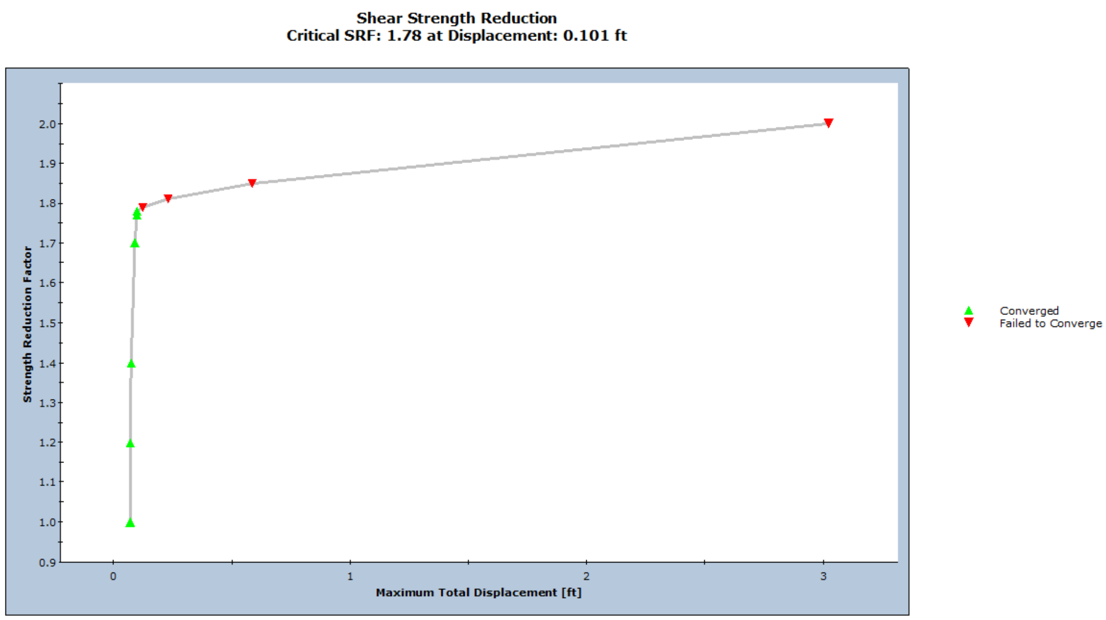

Figure 3 –SSR Convergence Graph – Case 3 with water table

18 Slope with 3 Different Pore Pressure Conditions and a Weak Seam

Introduction

This model is taken from Fredlund and Krahn (1977). It consists of a slope with a weak layer and three separate water conditions, 1) dry, 2) Ru defined pore pressure, 3) pore pressures defined using a water table. The model is done in imperial units to be consistent with the original paper. Quite a few other authors, such as Kim and Salgado (2002), Baker (1980), and Zhu, Lee, and Jiang (2003) have also analyzed this slope. Unfortunately, the location of the weak layer is slightly different in all the above references. Since the results are quite sensitive to this location, results routinely vary in the second decimal place.

Problem description

Verification problem #22 for Slide22 - Geometry is shown in Figure 1. The material properties are given in Table 1. The position of the composite circular slip surface is given in Fredlund and Krahn as being xc=120,yc=90,radius=80. The GLE/Discrete Morgenstern and Price method was run with the half sine interslice force function.

Table 16.1: Material Properties

	c′ (psf)	ϕ′ (deg.)	γ (pcf)	Ru (case2)
Upper soil	600	20	120	0.25
Weak layer	0	10	120	0.25

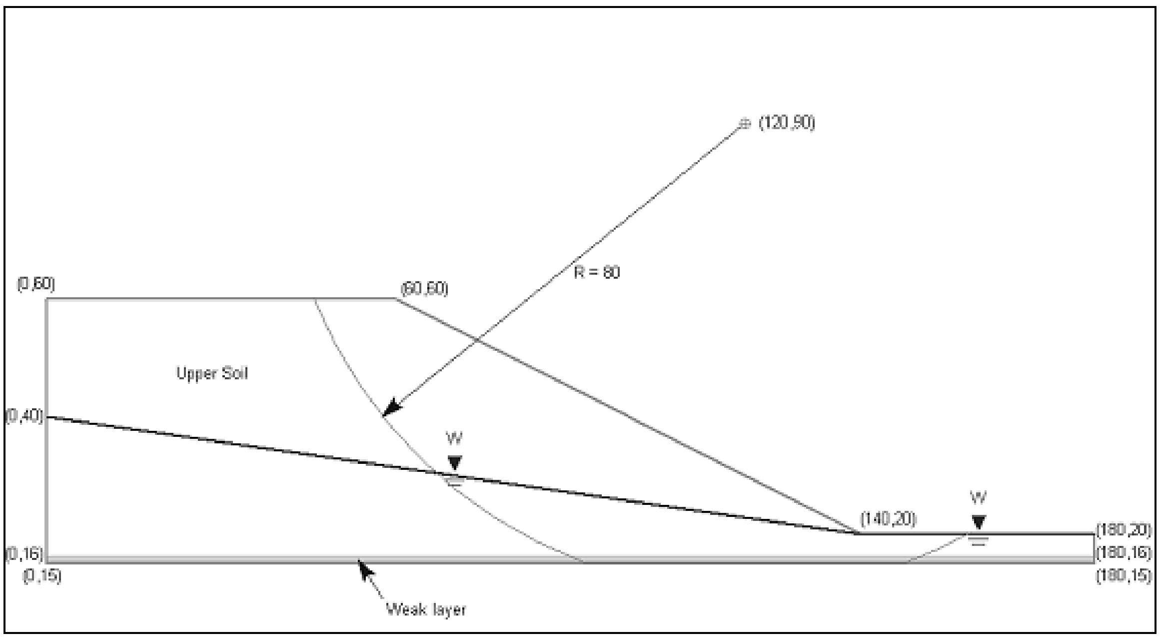

Figure 1 – Geometry

Results (Slide2 limit-equilibrium results are for a Composite Circular)

Case 1: Dry Slope

Method	Slide2	Fredlund & Krahn	Zhu, Lee, and Jiang	SSR
Ordinary	1.300	1.288	1.300	1.34
Bishop Simplified	1.382	1.377	1.380	
Spencer	1.382	1.373	1.381	
GLE/Morgenstern-Price	1.372	1.370	1.371	

Case 2: Ru

Method	Slide2	Fredlund & Krahn	Zhu, Lee, and Jiang	SSR
Ordinary	1.039	1.029	1.038	1.05
Bishop Simplified	1.124	1.124	1.118	
Spencer	1.124	1.118	1.119	
GLE/Morgenstern-Price	1.114	1.118	1.109	

Case 3: Water Table

Method	Slide2	Fredlund & Krahn	Zhu, Lee, and Jiang	SSR
Ordinary	1.174	1.171	1.192	1.13
Bishop Simplified	1.243	1.248	1.260	
Spencer	1.244	1.245	1.261	
GLE/Morgenstern-Price	1.237	1.245	1.254	

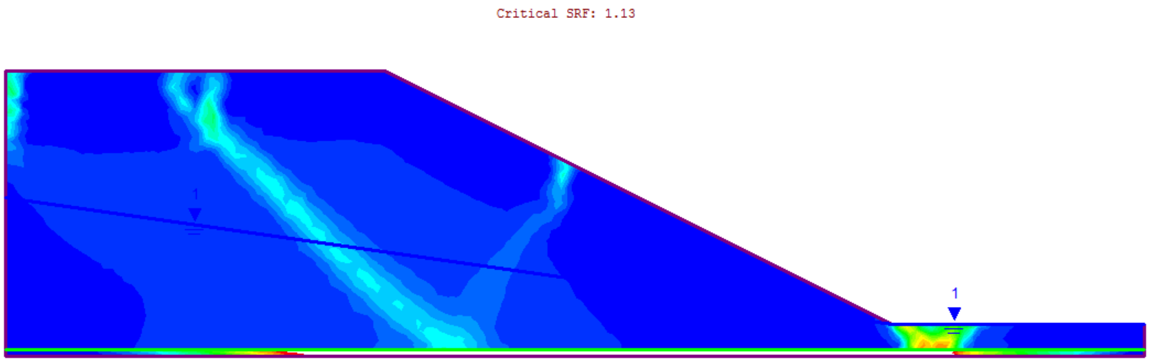

Figure 2 Solution Using SSR – Case 3 with water table (contour range: 0 – 0.02)

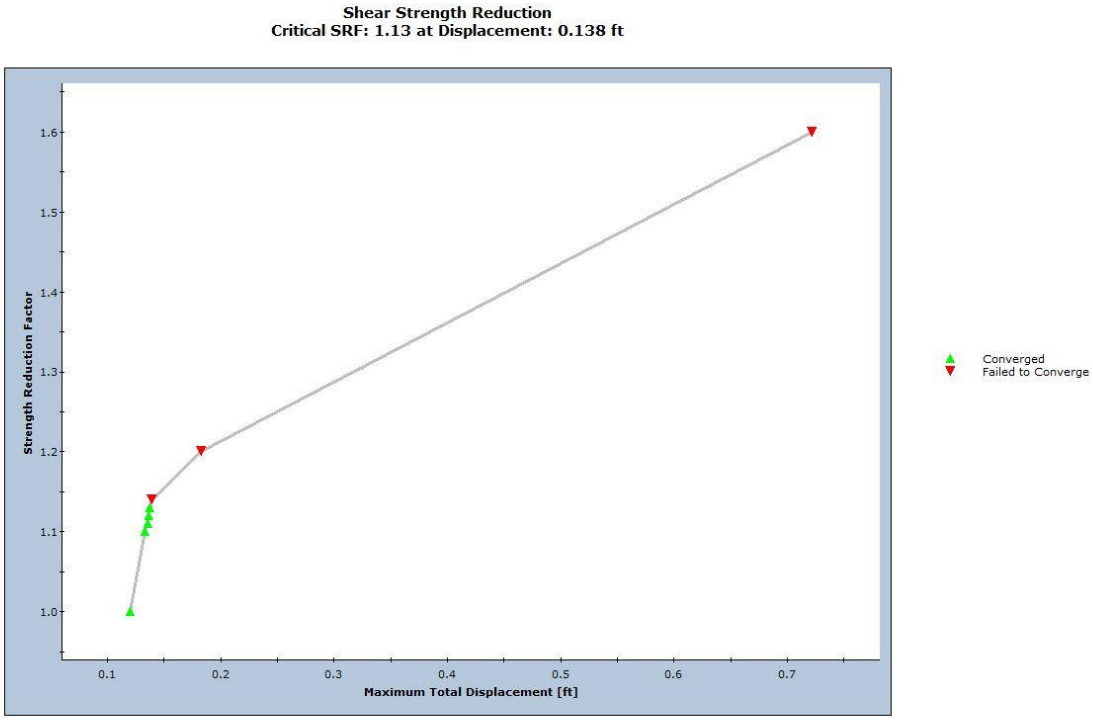

Figure 3 –SSR Convergence Graph – Case 3 with water table

19 Undrained Layered Slope

Introduction

This model is taken from Low (1989). It consists of a slope with three layers with different undrained shear strengths.

Problem description

Verification Problem #24 for Slide2 - Geometry is shown in Figure 1. The material properties are given in Table 1.

Table 1: Material Properties

	Cu (KN/m2)	γ (KN/m3)
Upper Layer	30	18
Middle Layer	20	18
Bottom Layer	150	18

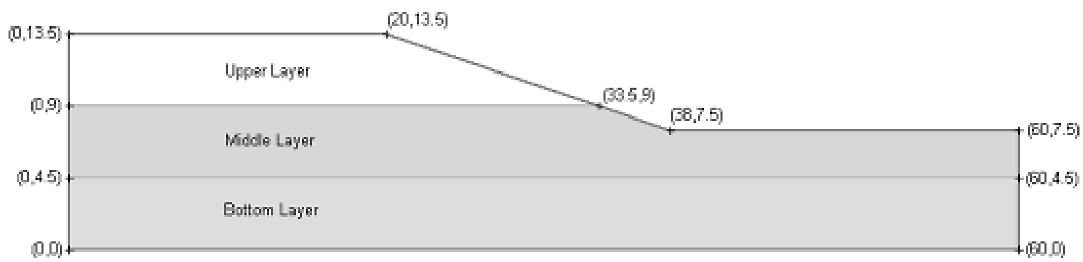

Figure 1 – Geometry

Results – (Slide2 limit-equilibrium results are for circular auto refine search)

Method	Factor of Safety
SSR (RS2)	1.41
Ordinary (Slide2)	1.439
Bishop (Slide2)	1.439

Low (1989) Ordinary Factor of Safety=1.44

Low (1989) Bishop Factor of Safety=1.44

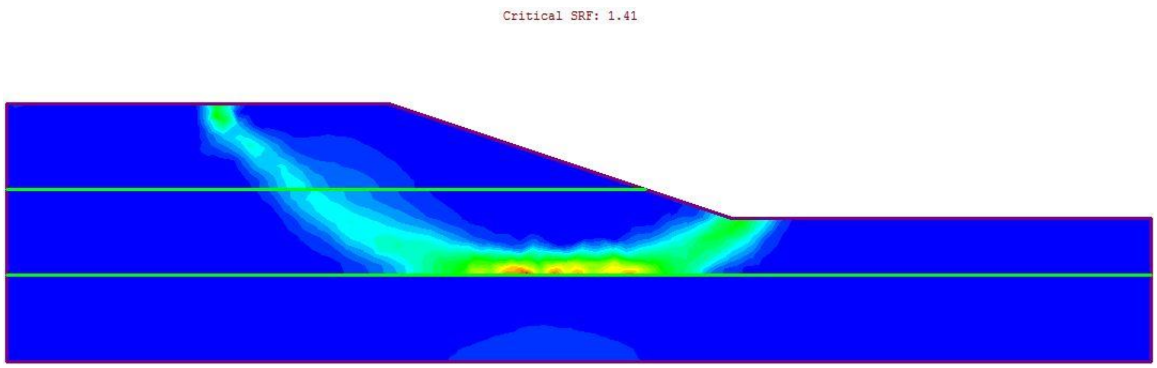

Figure 2 Solution Using SSR

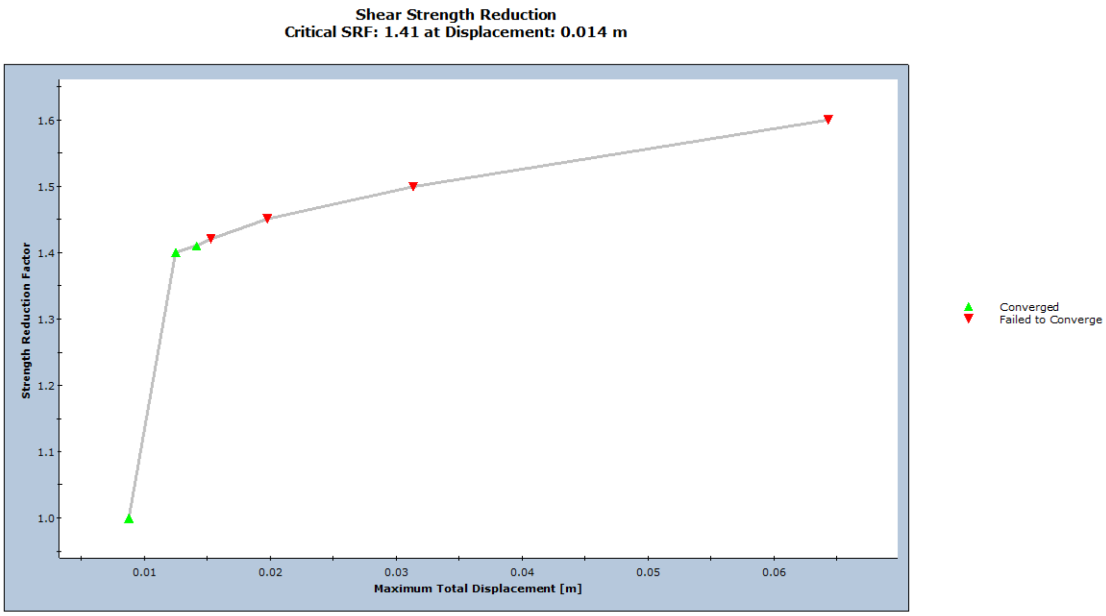

Figure 3 –SSR Convergence Graph

Introduction

This model is taken from Chen and Shao (1988). It analyses the classical problem in the theory of plasticity of a weightless, frictionless slope subjected to a vertical load. This problem was first solved by Prandtl (1921)

Problem description

Verification Problem #25 for Slide2 - Geometry is shown in Figure 1. The slope geometry, equation for the critical load, and position of the critical slip surface is defined by Prandtl and shown in Figure 1. The critical failure surface has a theoretical factor of safety of 1.0. The analysis uses the input data of Chen and Shao and is shown in Table 1. The geometry, shown in Figure 2, is generated assuming a 10m high slope with a slope angle of 60 degrees. The critical uniformly distributed load for failure is calculated to be 149.31 kN/m, with a length equal to the slope height, 10m.

Geometry and Properties

Table 1: Material Properties

	c (kN/m^2)	ϕ (deg.)	γ (kN/m^3)
soil	49	0	1e-6

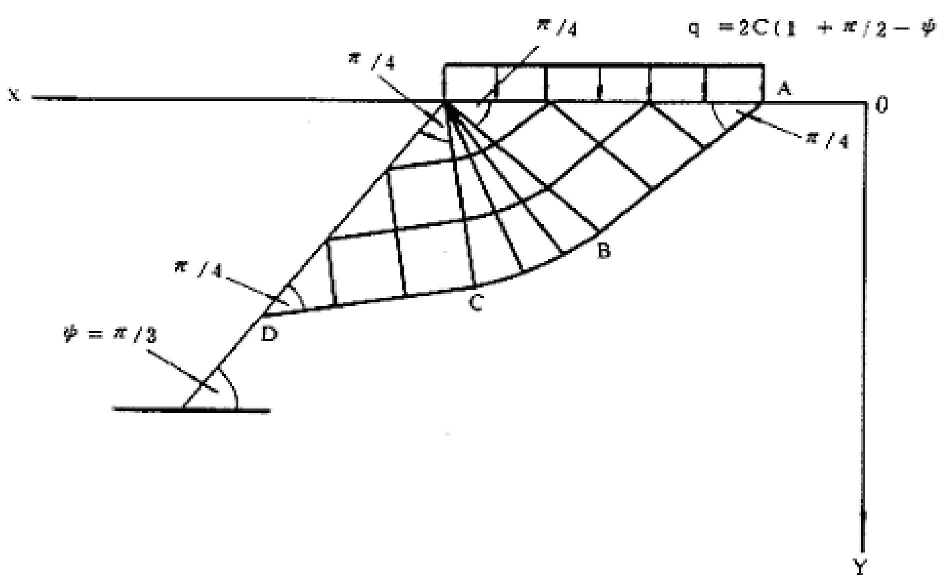

Figure 1 – Closed-form solution (Chen and Shao, 1988)

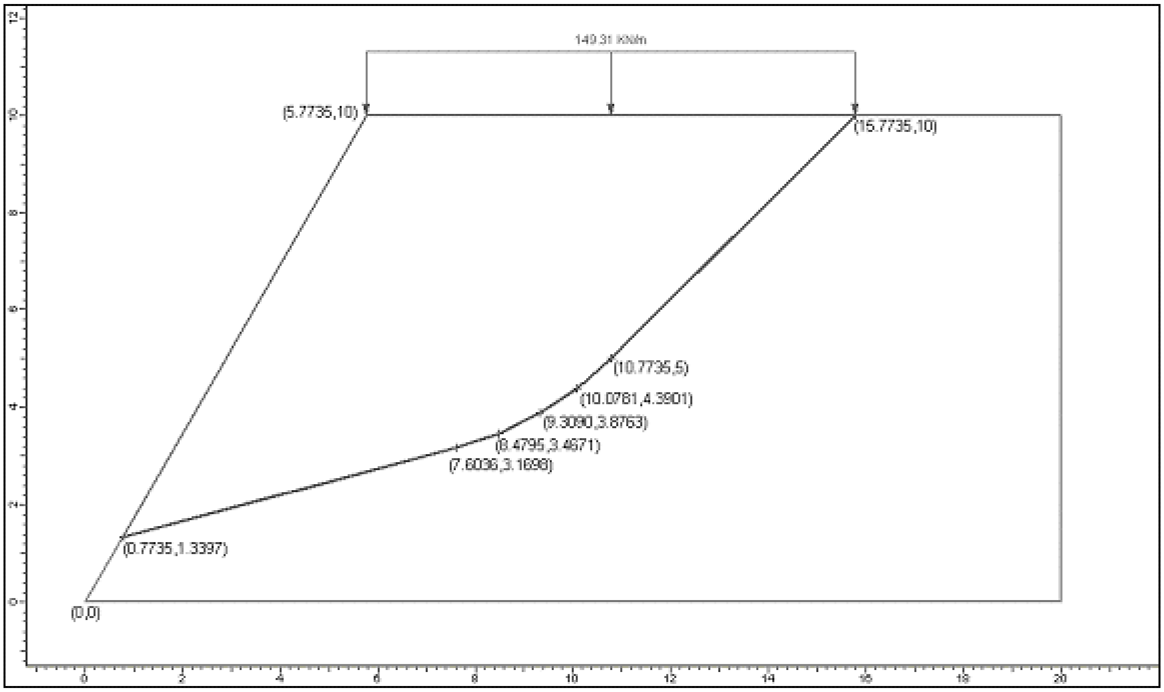

Figure 2 Geometry

Results

Method	Factor of Safety
SSR (RS2)	1.0
Spencer (Slide2)	1. 051
GLE/M-P (Slide2)	1. 009

Chen and Shao (1988) Spencer Factor of Safety = 1.05

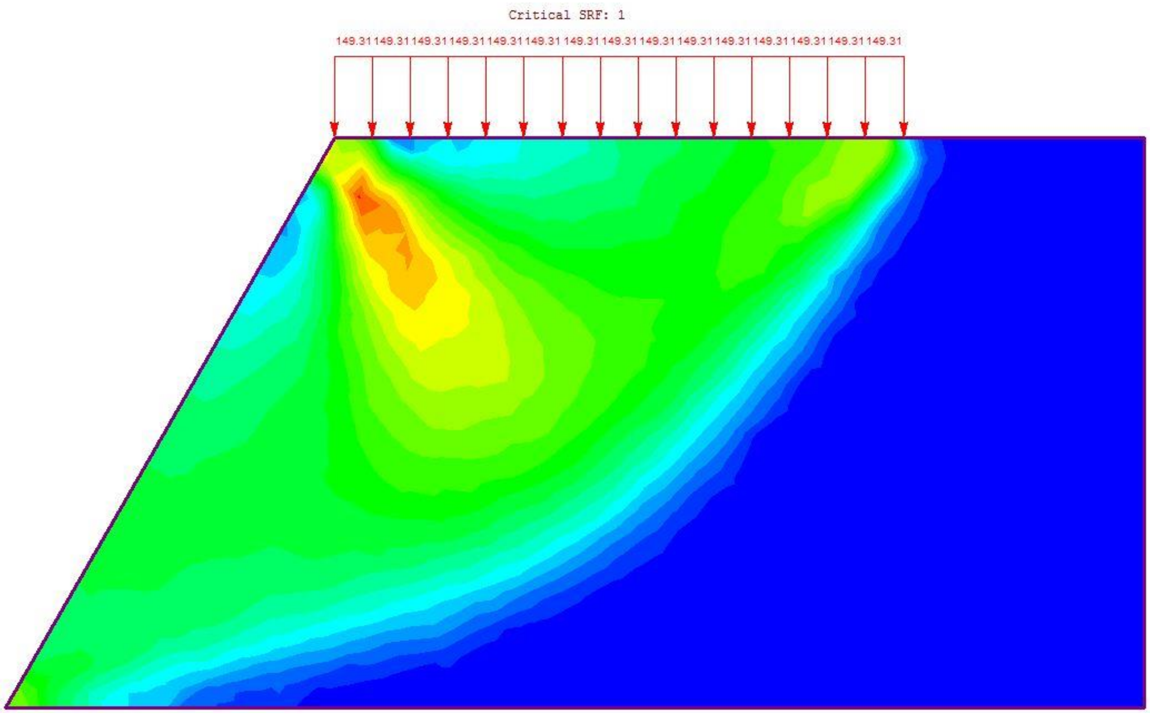

Figure 3 – Solution Using SSR

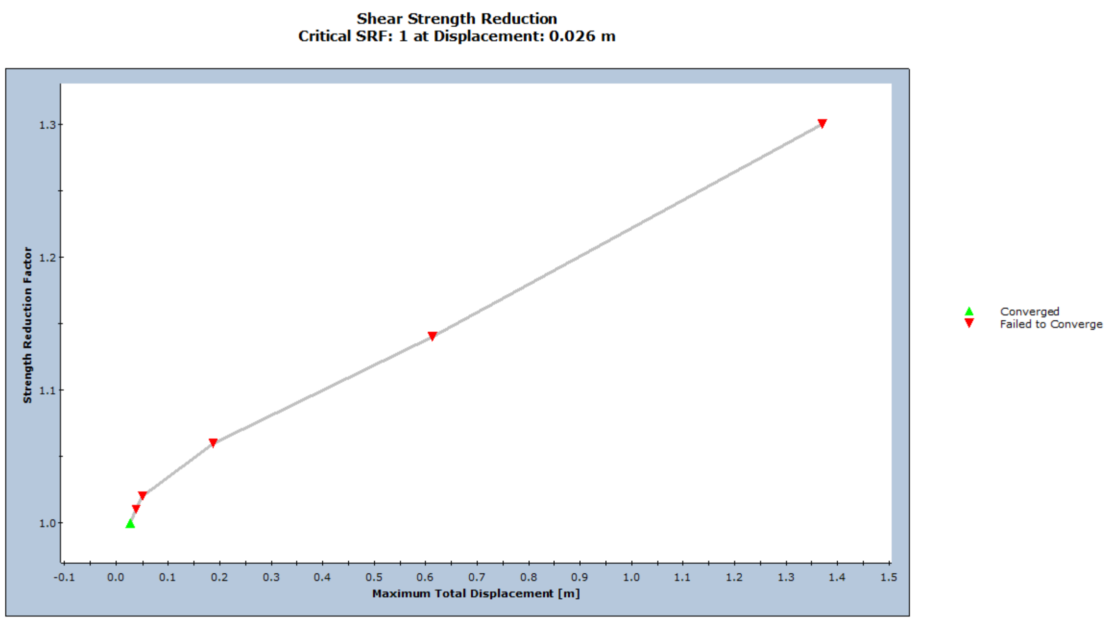

Figure 4 – SSR Convergence Graph

21 Slope with Vertical Load (Prandtl's Wedge Bearing Capacity)

Introduction

This verification test models the well-known Prandtl solution of bearing capacity:

$$q_c = 2C(1+\pi/2)$$

Problem description

Verification problem #26 for Slide2 - Geometry is shown in Figure 1. The material properties are given in Table 1. With cohesion of 20kN/m2, q_c is calculated to be 102.83 kN/m. A uniformly distributed load of 102.83kN/m was applied over a width of 10m as shown in the below figure. The theoretical noncircular critical failure surface was used.

Geometry and Properties

Table 1: Material Properties

	c (kN/m^2)	ϕ (deg.)	γ (kN/m^3)
soil	20	0	1e-6

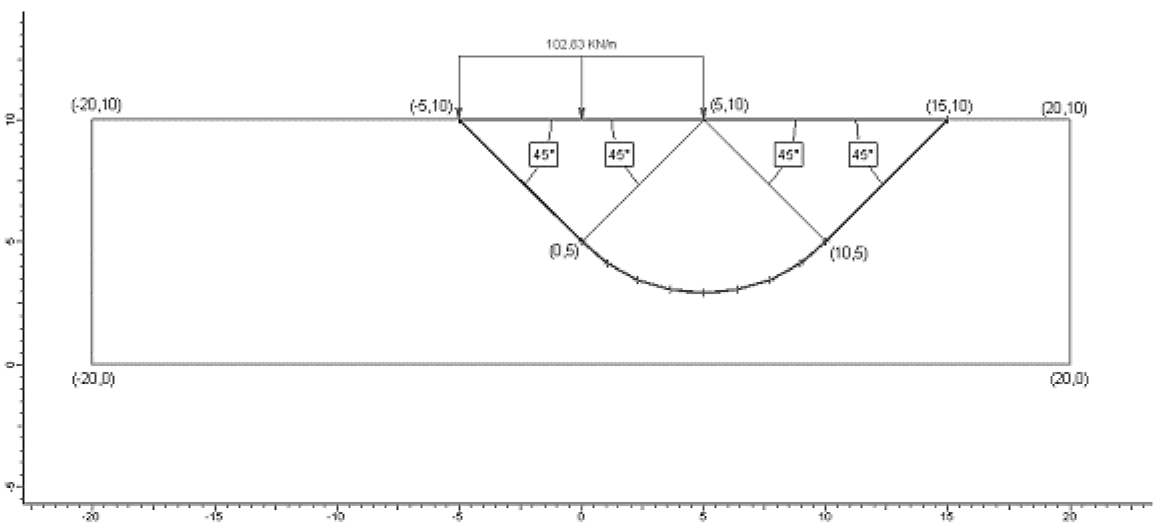

Figure 1 Geometry

Results

Method	Factor of Safety
SSR (RS2)	1.01
Spencer (Slide2)	0.941

Theoretical factor of safety=1.0

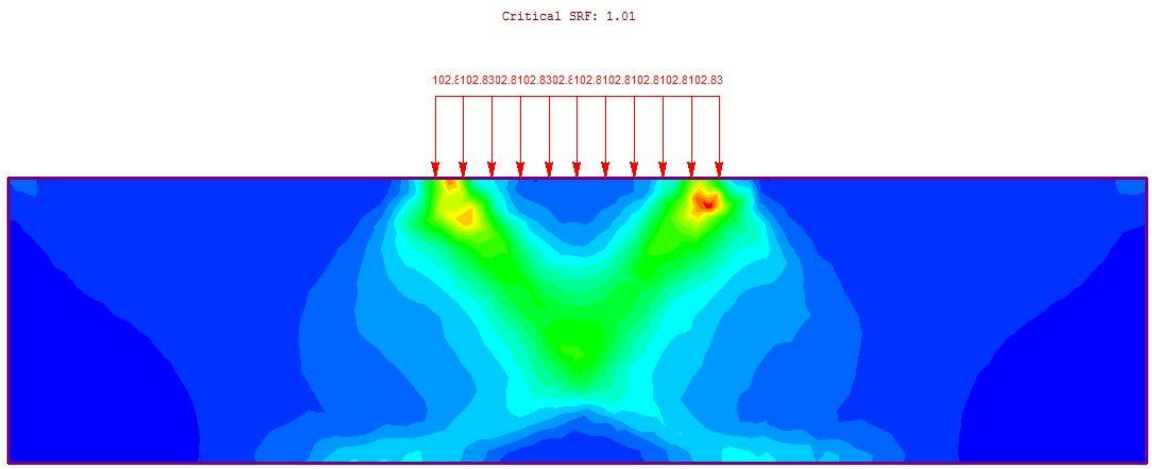

Figure 3 Solution Using SSR

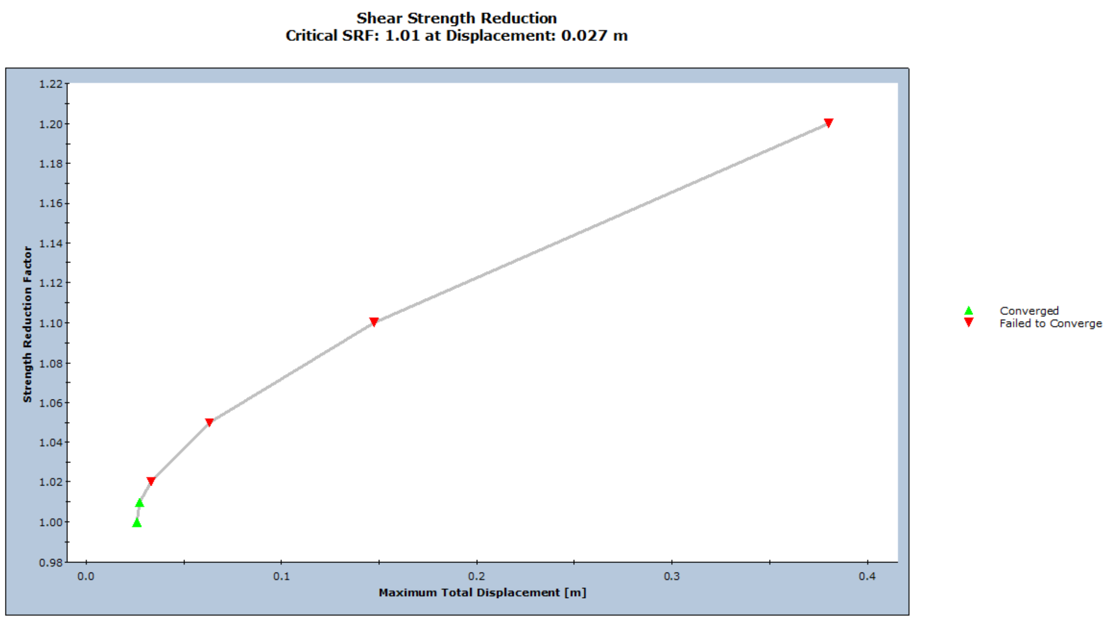

Figure 4 – SSR Convergence Graph

22 Layered Slope with Undulating Bedrock

Introduction

This model was taken from Malkawi, Hassan and Sarma (2001) who took it from the XSTABL version 5 reference manual (Sharma 1996). It consists of a 2 material slope overlaying undulating bedrock. There is a water table and moist and saturated unit weights for one of the materials. The other material has zero strength. The model is done with imperial units (feet,psf,pcf) to be consistent with the original XSTABL analysis.

Problem description

Verification problem #27 for Slide2 is shown in Figure 1. The material properties are given in Table 1. One of the interesting features of this model is the different unit weights of soil 1 below and above the water table. Another factor is the method of pore-pressure calculation. The pore pressures are calculated using a correction for the inclination of the phreatic surface and steady state seepage. RS2, Slide2 and XSTABL allow you to apply this correction. The pore pressures tend to be smaller than if a static head of water is assumed (measured straight up to the phreatic surface from the center of the base of a slice). Since RS2 does not allow for a saturated and moist unit weight, the more conservative saturated unit weight is used. RS2 does not allow for zero strength materials, this plays havoc with the plasticity calculations in a finite-element analysis. To solve this problem, a distributed load is used to replace the influence of soil 2 as shown in Figure 2.

Geometry and Properties

Table 1: Material Properties

	c (psf)	ϕ (deg.)	γ moist (pcf)	γ saturated (pcf)
Soil 1	500	14	116.4	124.2
Soil 2	0	0	116.4	116.4

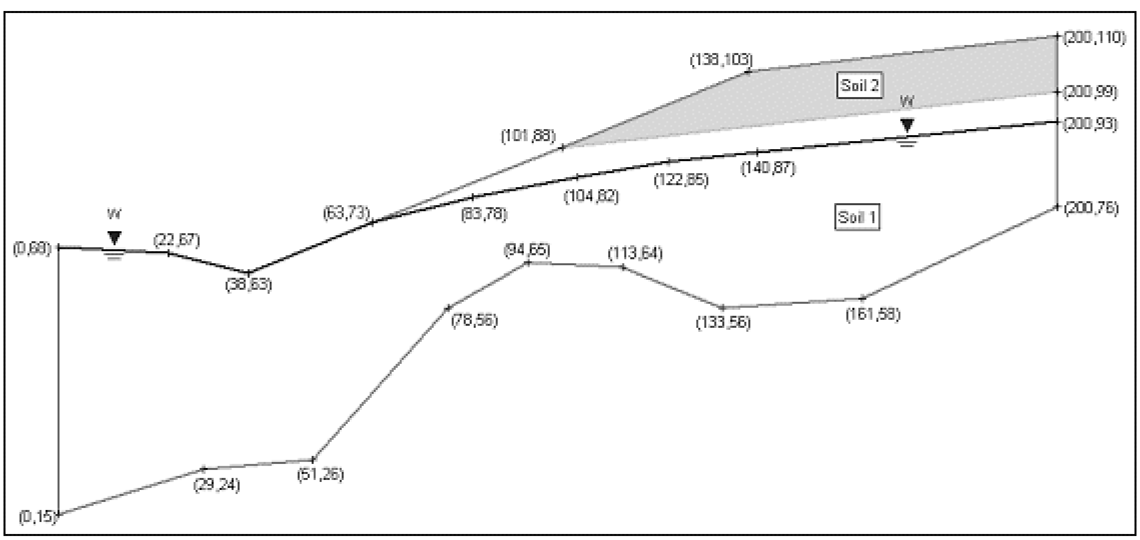

Figure 1 – Geometry

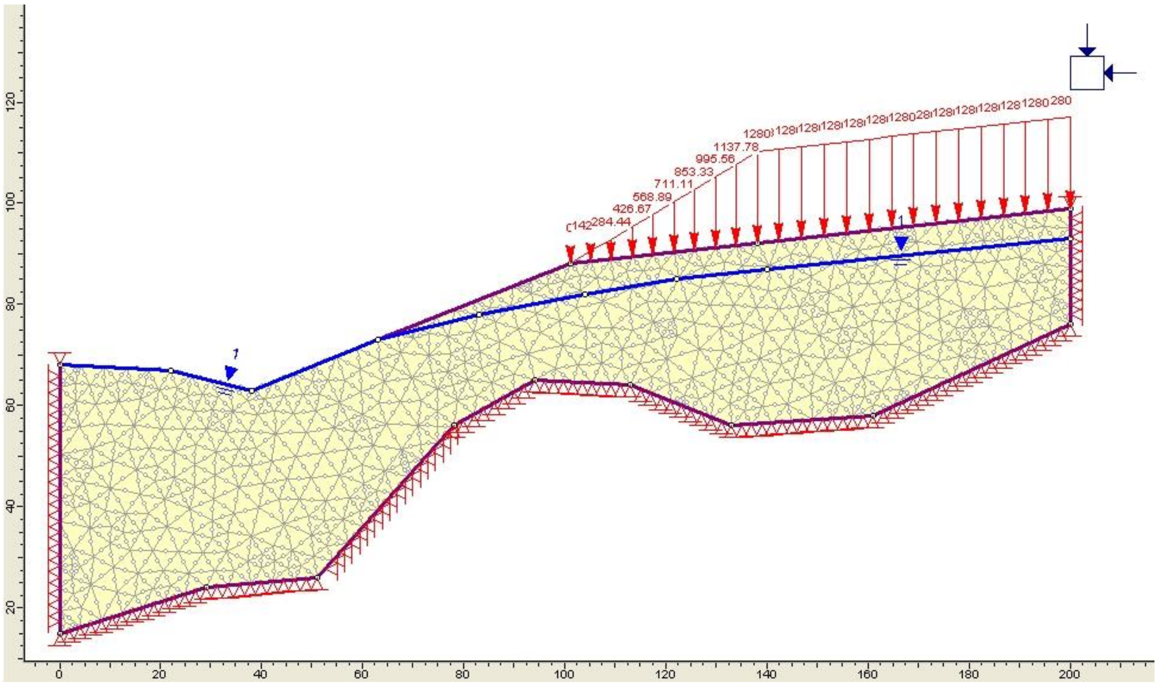

Figure 2 – RS2 Model

Results (Circular analysis in Slide2)

Method	Factor of Safety
SSR	1.52
Bishop	1.51
Spencer	1.51
GLE/M-P (half-sine)	1.51

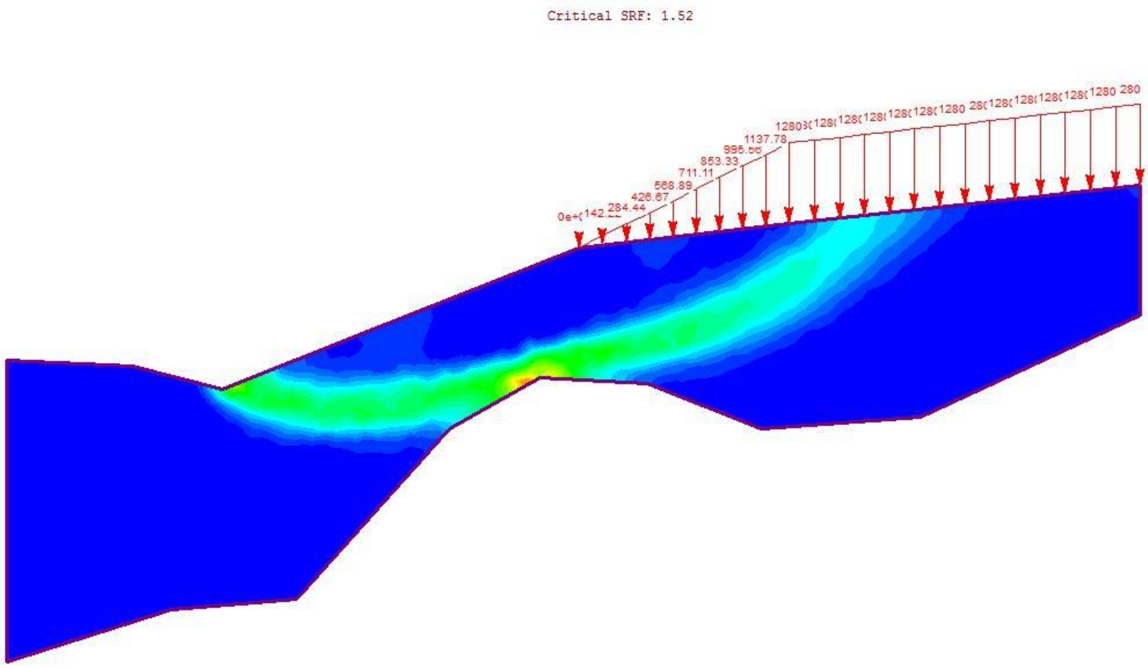

Figure 3 – RS2 SSR Maximum Shear Strain Plot

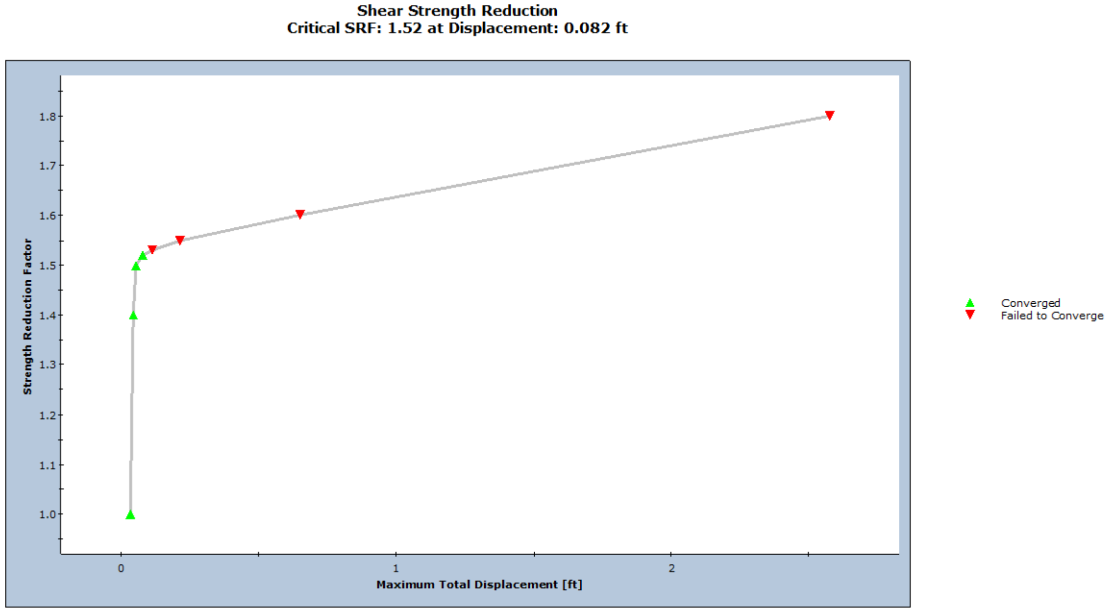

Figure 4 – SSR Convergence Graph

Introduction

This model is taken from Duncan (2000). It looks at the failure of the 100 ft high underwater slope at the Lighter Aboard Ship (LASH) terminal at the Port of San Francisco.

Problem description

Verification #29 for Slide2 - Geometry is shown in Figure 1. All geoemetry and property values are determined using the figures and published data in Duncan (2000). The cohesion is taken to be 100 psf at an elevation of -20 ft and increase linearly with depth at a rate of 9.8 psf/ft. The stability of the bench is of interest, thus the material above elevation -20 and to the right of the bench (x>350) is given elastic properties (can't fail).

Geometry and Properties

Table 1: Material Properties

	cohesion (datum) (psf)	Datum (ft)	Rate of change (psf/ft)	Unit Weight (pcf)
San Francisco Bay Mud	100	-20	9.8	100

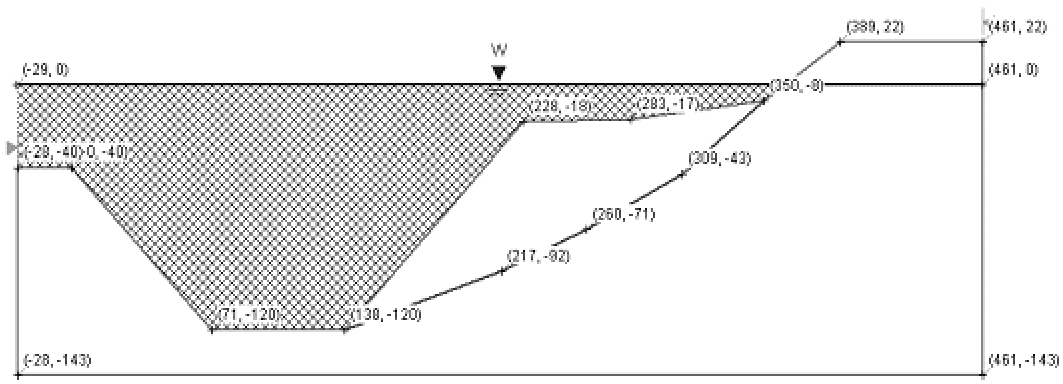

Figure 1 - Geometry

Results

Method	Deterministic Factor of Safety
SSR (RS2)	1.12
Janbu Simplified	1.13
Janbu Corrected	1.17
Spencer	1.15
GLE	1.16

Duncan (2000) quotes a factor of safety of 1.17.

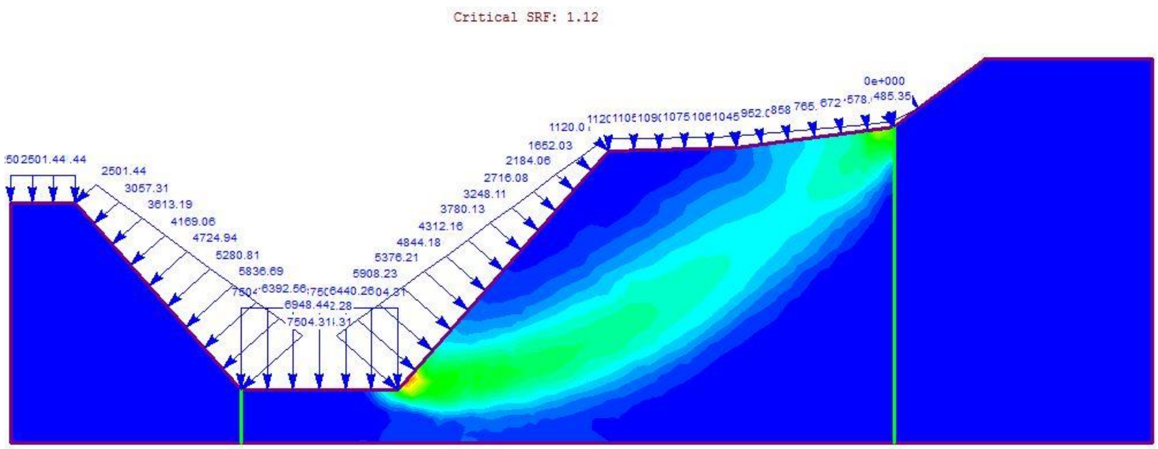

Figure 2 – RS2 SSR Maximum Shear Strain Plot

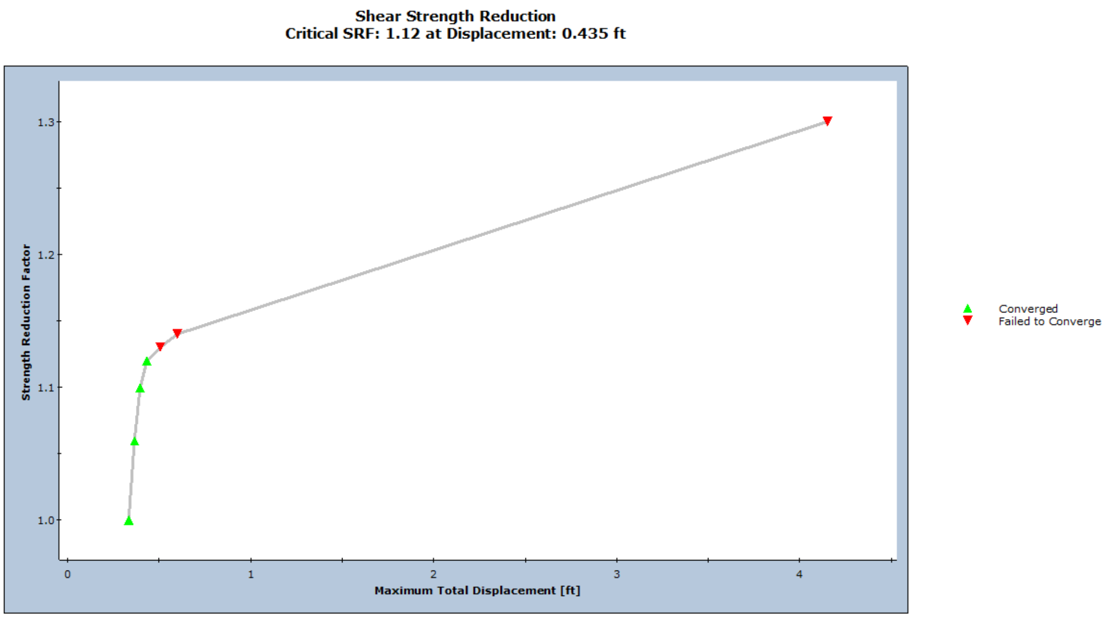

Figure 4 –SSR Convergence Graph

24 Layered Slope with Geosynthetic Reinforcement

Introduction

This model is taken from Borges and Cardoso (2002), their case 3 example. It looks at the stability of a geosynthetic-reinforced embankment on soft soil.

Problem description

Verification problem #32 for Slide2 - Geometry is shown in Figures 1 and 2. The sand embankment is modeled as a Mohr-Coulomb material while the foundation material is a soft clay with varying undrained shear strength. The geosynthetic has a tensile strength of 200 KN/m, and frictional resistance against slip of 30.96 degrees. The reinforcement force is assumed to be parallel with the reinforcement. There are two embankment materials, the lower embankment material is from elevation 0 to 1 while the upper embankment material is from elevation 1 to either 7 (Case 1) or 8.75m (Case 2). The geosynthetic is at elevation 0.9, just inside the lower embankment material.

Geometry and Properties

Table 1: Material Properties

	c′ (kN/m^2)	ϕ′ (deg.)	γ (kN/m^3)
Upper Embankment	0	35	21.9
Lower Embankment	0	33	17.2

	Cu (kN/m^2)	γ (kN/m^3)
Clay1	43	18
Clay2	31	16.6
Clay3	30	13.5
Clay4	32	17
Clay5	32	17.5

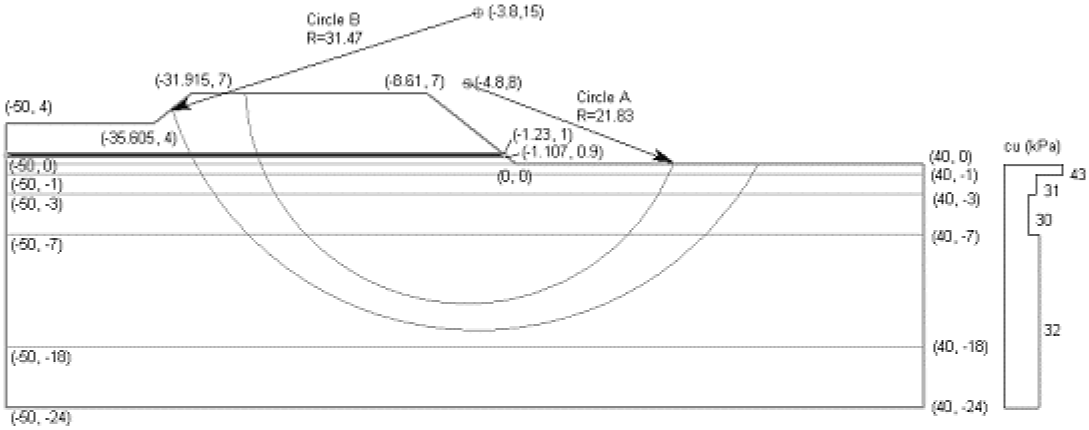

Figure 1 – Case 1 – Embankment height = 7m

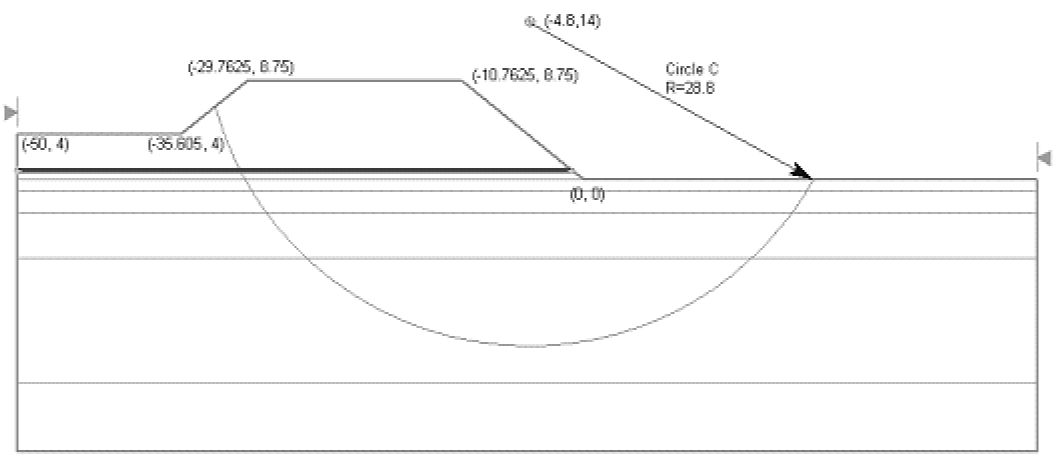

Figure 2 – Case 2 – Embankment height = 8.75m

Results – Case 1 – Embankment height = 7m

	Factor of Safety
SSR	1.15
Circle A (Slide2)	1.23
Circle A (Borges)	1.25
Circle B (Slide2)	1.22
Circle B (Borges)	1.19

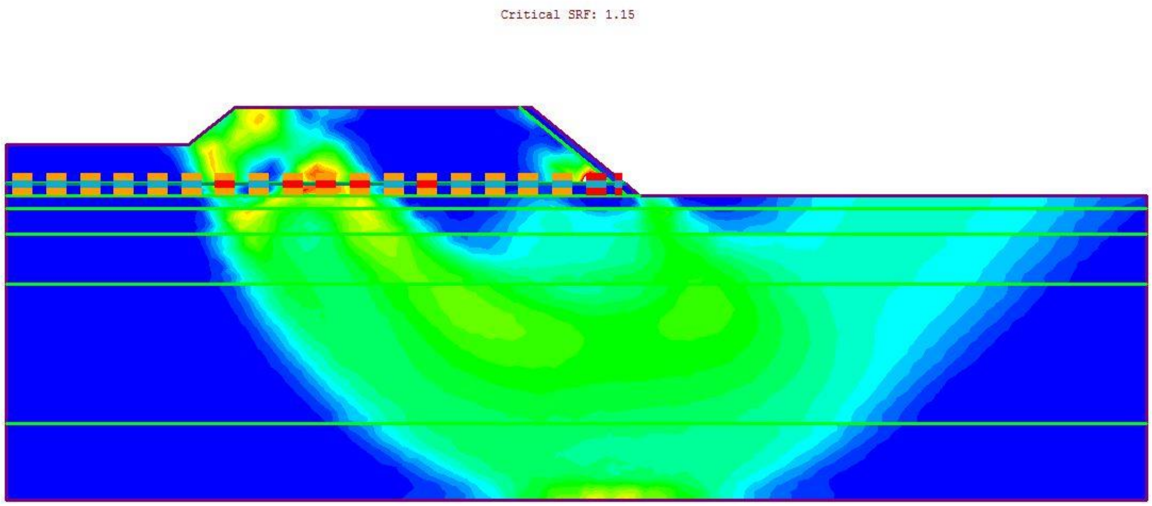

Figure 3 – Case 1 – Shear Strain plot, failed geotextile shown in red

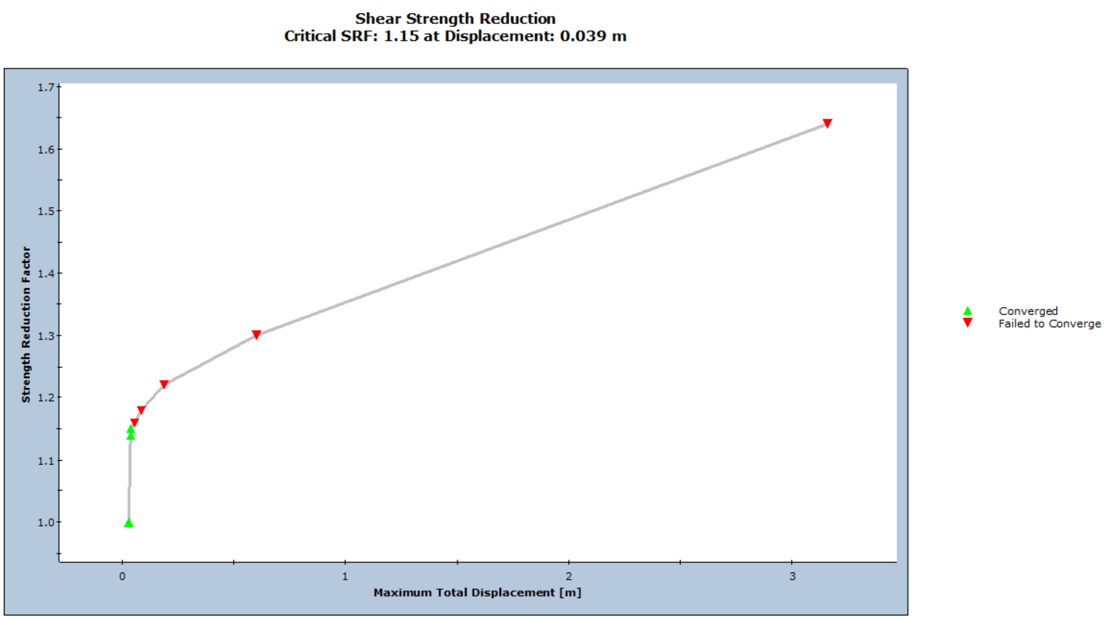

Figure 4 – Case 1 – SSR Convergence Graph

Results – Case 2 – Embankment height = 8.75m

	Factor of Safety
SSR	0.95
Circle C (Slide2)	0.98
Circle C (Borges)	0.99

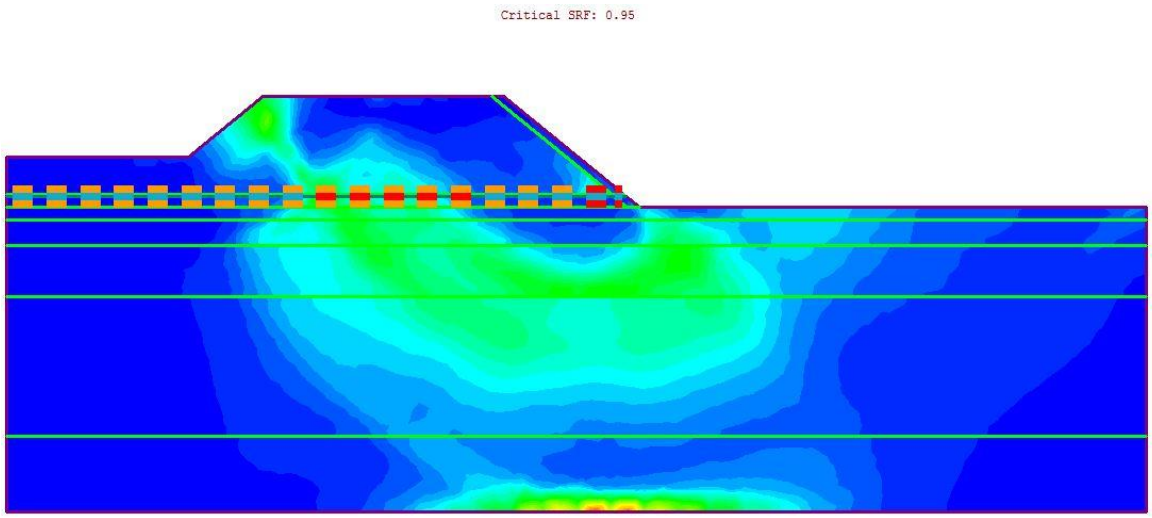

Figure 5 – Case 2 – Shear Strain plot, failed geotextile shown in red

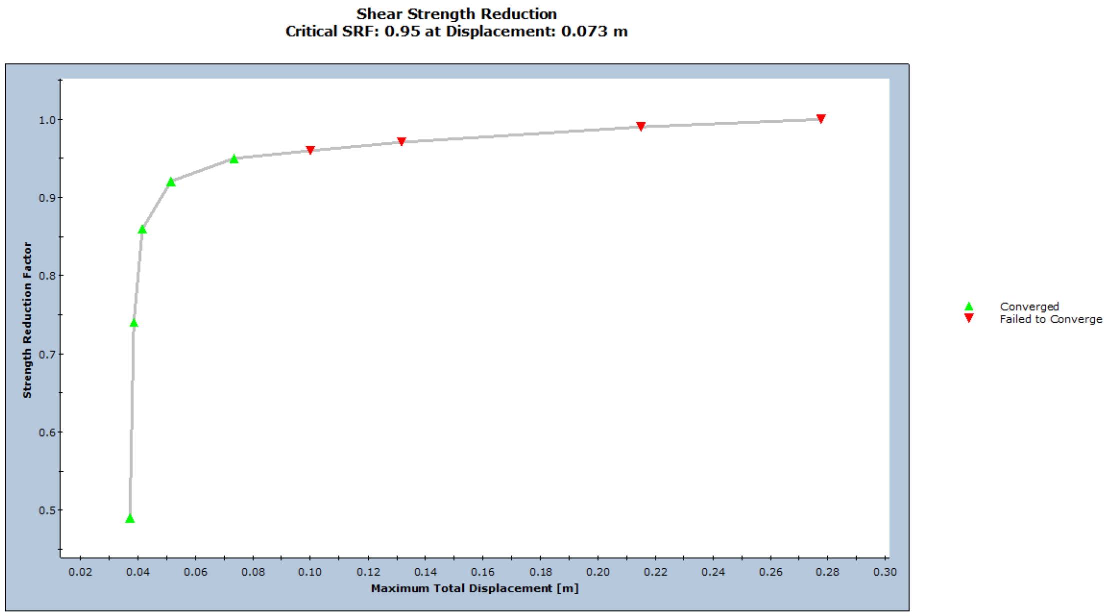

Figure 6 – Case 2 – SSR Convergence Graph

Introduction

Verification #25 comes from El-Ramly et al (2003). It looks at the assessment of the factor of safety of a Syncrude tailings dyke in Canada.

Problem description

Verification problem #33 for Slide2 - The original model from the El-Ramly et al paper is shown in Figure 1. The input parameters for the RS2 model are provided in Table 1. The RS2 model is shown on Figure 2.

As in the El-Ramly et al paper, the Bishop simplified analysis method is used for the *Slide2* analysis.

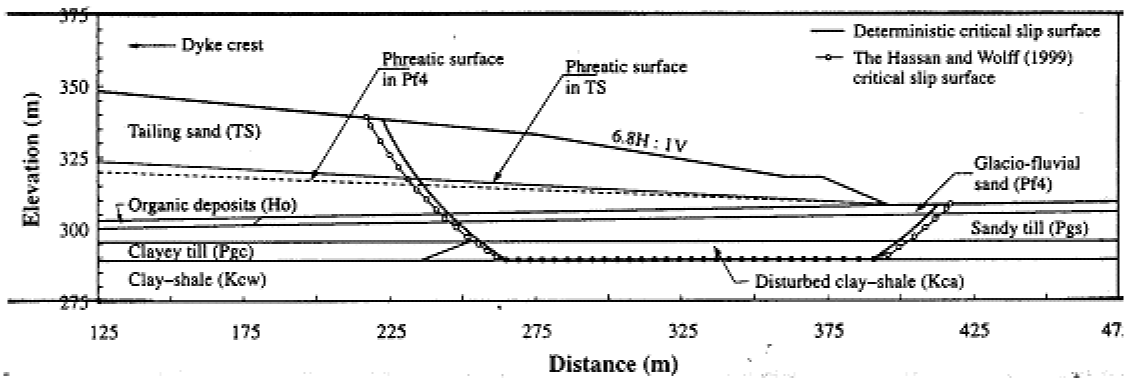

Figure 1

Table 1: Material Properties

Material	c´ (kN/m^2)	ϕ´ (deg.)	γ (kN/m^3)
Tailing sand (TS)	0	34	20
Glacio-fluvial sand (Pf4)	0	34	17
Sandy till (Pgs)	0	34	17
Disturbed clay-shale (Kca)	0	7.5	17

Geometry and Properties

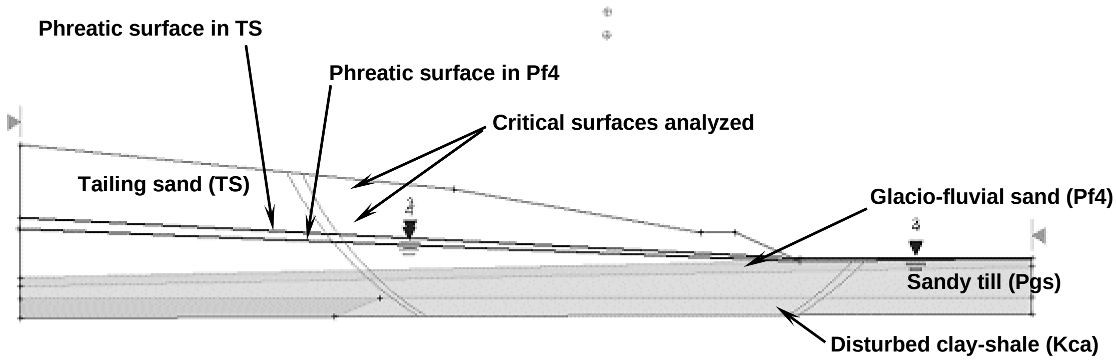

Figure 2a

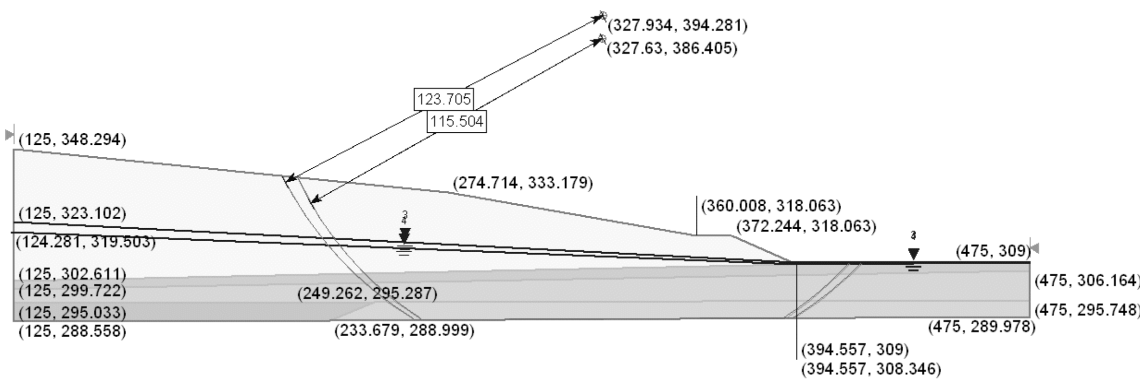

Figure 2b

Note: Phreatic Surfaces do not intersect at toe

Results

	Factor of Safety
SSR	1.29
Slide2 (Bishop)	1.305
El-Ramly et al	1.31

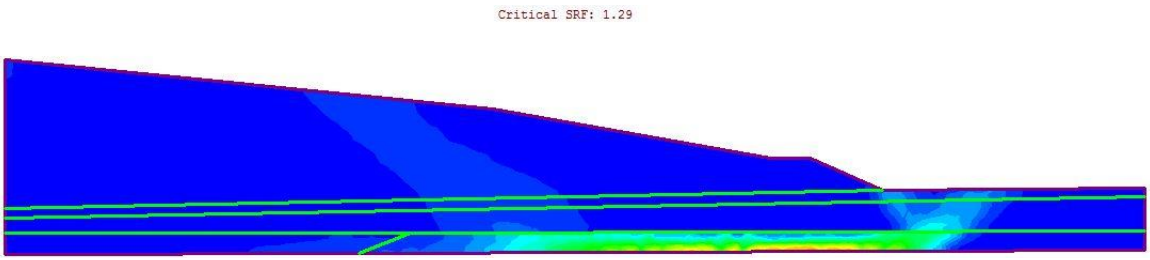

Figure 3 – Shear Strain plot

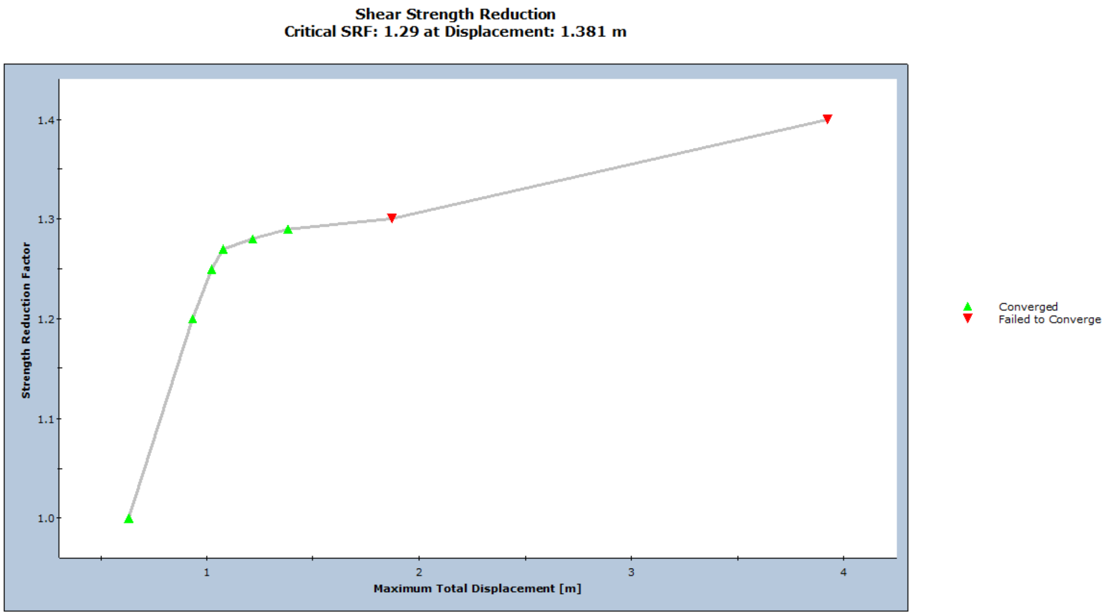

Figure 4 – SSR Convergence Graph

Introduction

This model is taken from Wolff and Harr (1987). It is a model of the Clarence Cannon Dam in north eastern Missouri, USA. This verification compares factor of safety results from RS2, Slide2 and those determined by Wolff and Harr for a non-circular critical surface.

Problem description

Verification problem #34 for Slide2 - Wolff and Harr evaluate the factor of safety against failure of the Cannon Dam along the specified non-circular critical surface shown on Figure 1 (taken from their paper). Properties are given in Table 1. The RS2 model is shown on Figure 2.

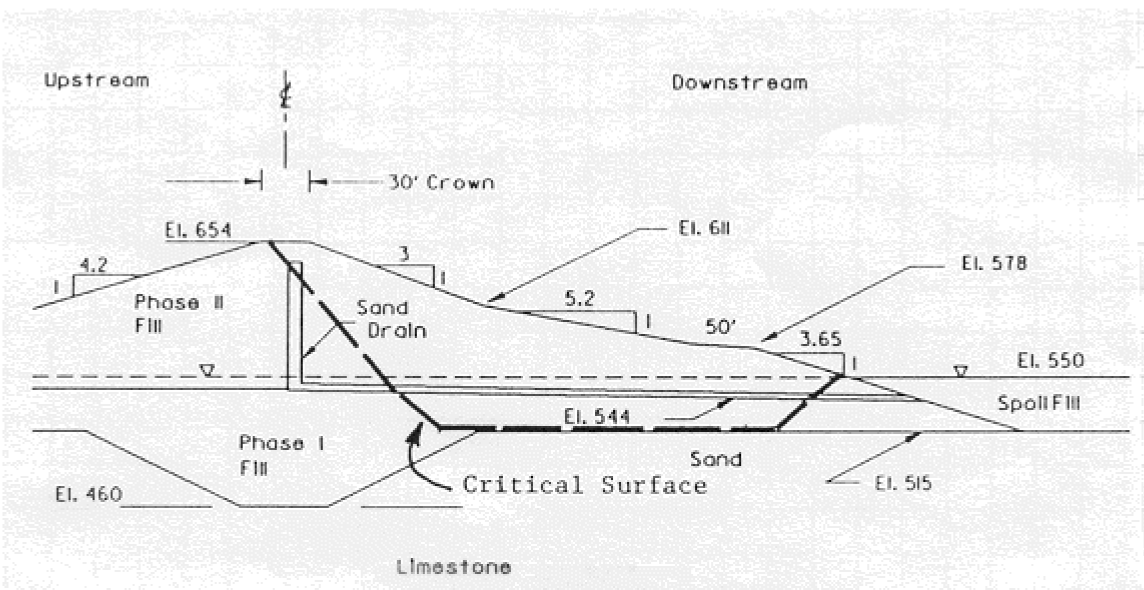

Figure 1

Geometry and Properties

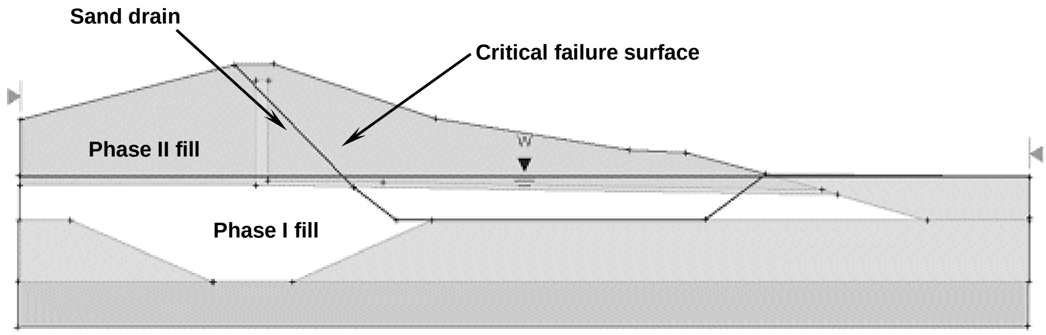

Figure 2

Table 1: Material Properties*

Material	c′ (lb/ft^2)	ϕ′ (deg.)	γ (lb/ft^3)
Phase I fill	2,230	6.34	150
Phase II fill	2,901.6	14.8	150
Sand drain	0	30	120

*Information on the non-labeled soil layers in the model shown on Figure 2 is omitted because it has no influence on the factor of safety of the given critical surface.

Results

	Deterministic Factor of Safety
SSR	2.29
Slide2 (GLE method)	2.333
Slide2 (Spencer method)	2.383
Wolff and Harr	2.36

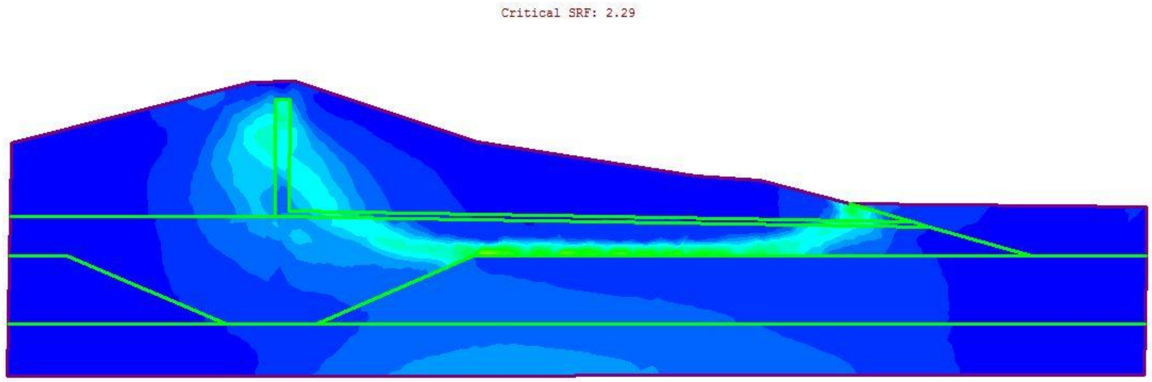

Figure 3 – Shear Strain plot

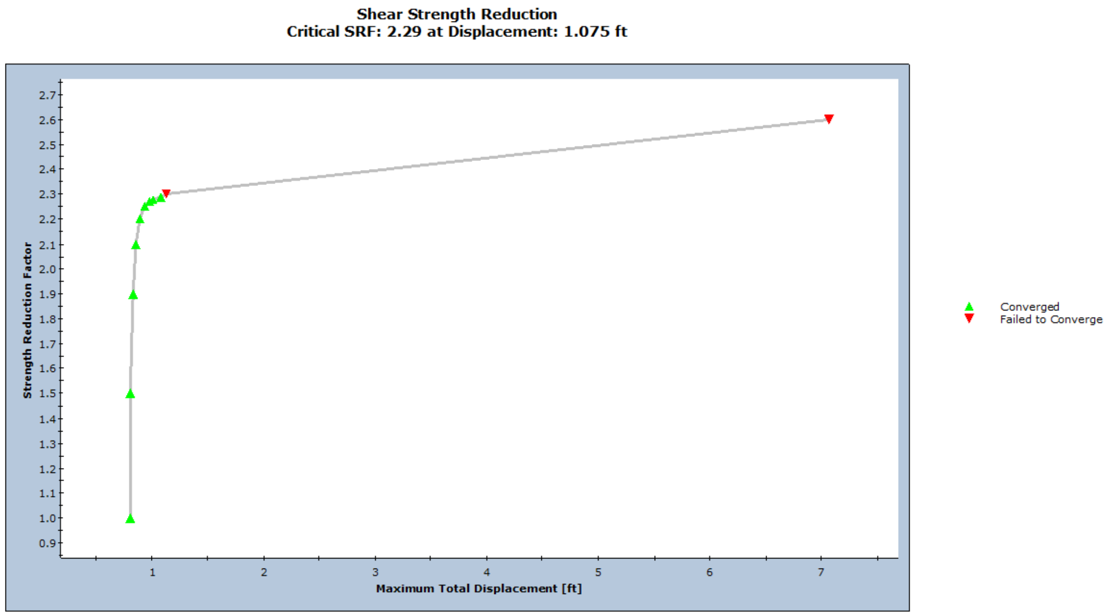

Figure 4 – SSR Convergence Graph

Introduction

This model is taken from Li and Lumb (1987) and Hassan and Wolff (1999). It analyzes a simple homogeneous slope with pore pressure defined using Ru.

Problem description

Verification problem # 36 for Slide2 - The geometry of the homogeneous slope is shown in Figure 1 and material parameters are provided in Table 1.

Geometry and Properties

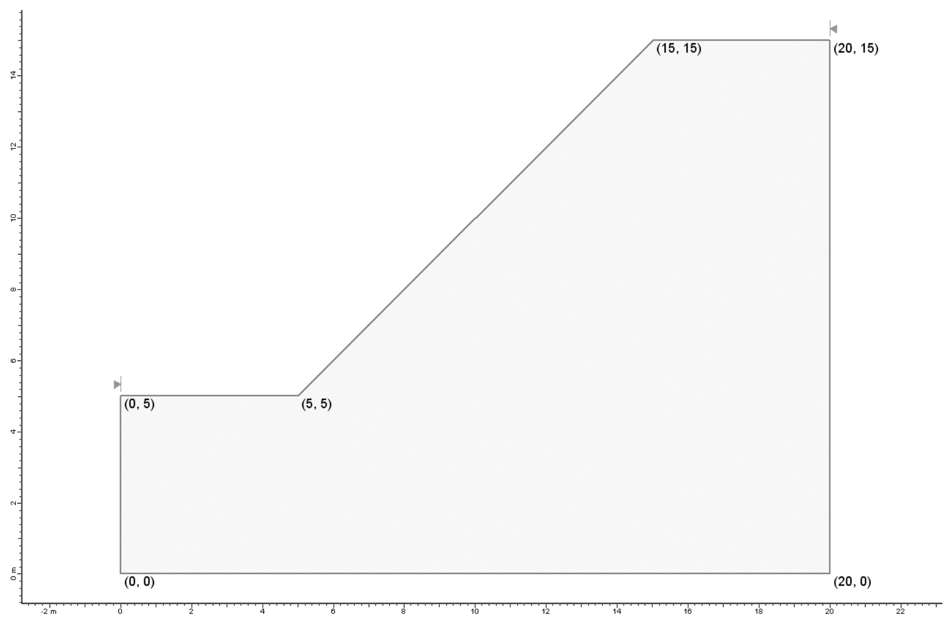

Figure 1

Table 1: Material Properties

Property	Mean value
c' (kN/m^2)	18
ϕ' (deg.)	30
γ (kN/m^3)	18
r_u	0.2

Results

	Deterministic Factor of Safety
SSR	1.31
Slide2 (Bishop method)	1.339
Hasssan and Wolf	1.334

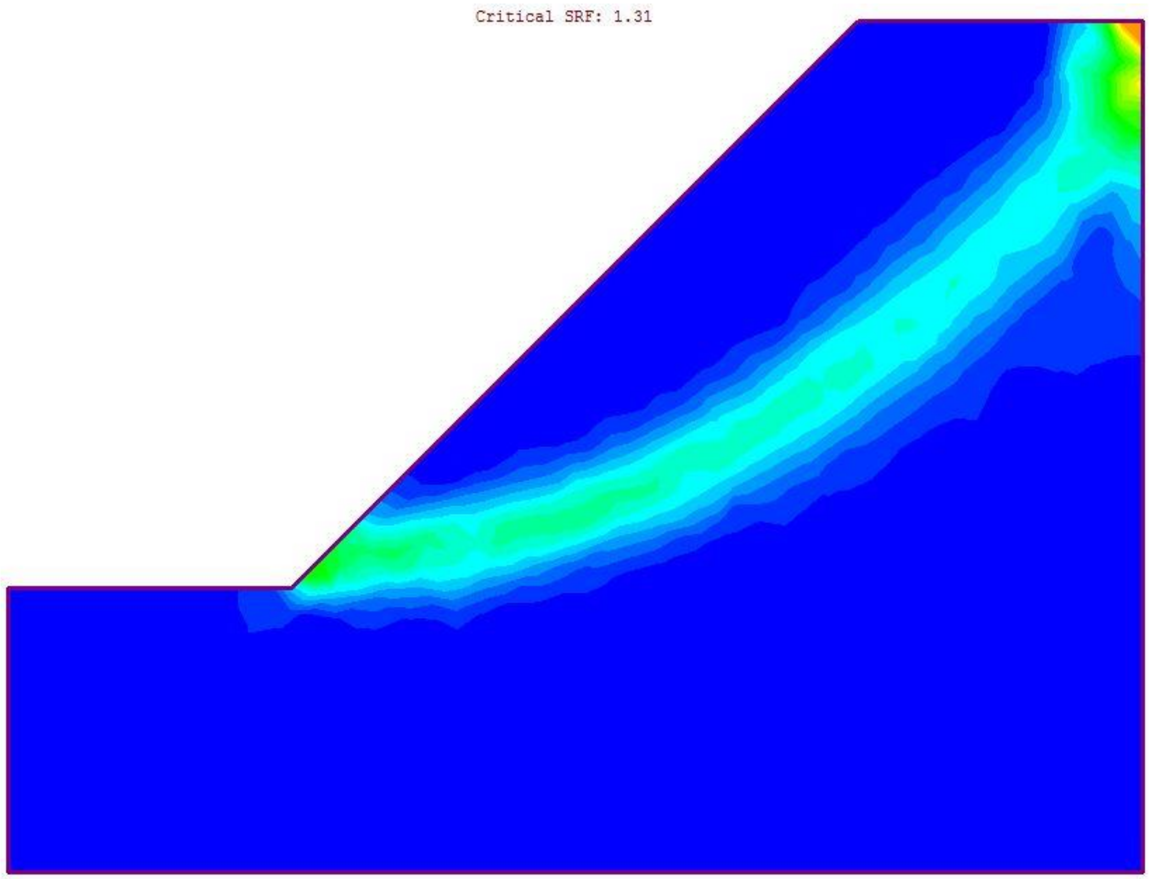

Figure 2 – Shear Strain plot

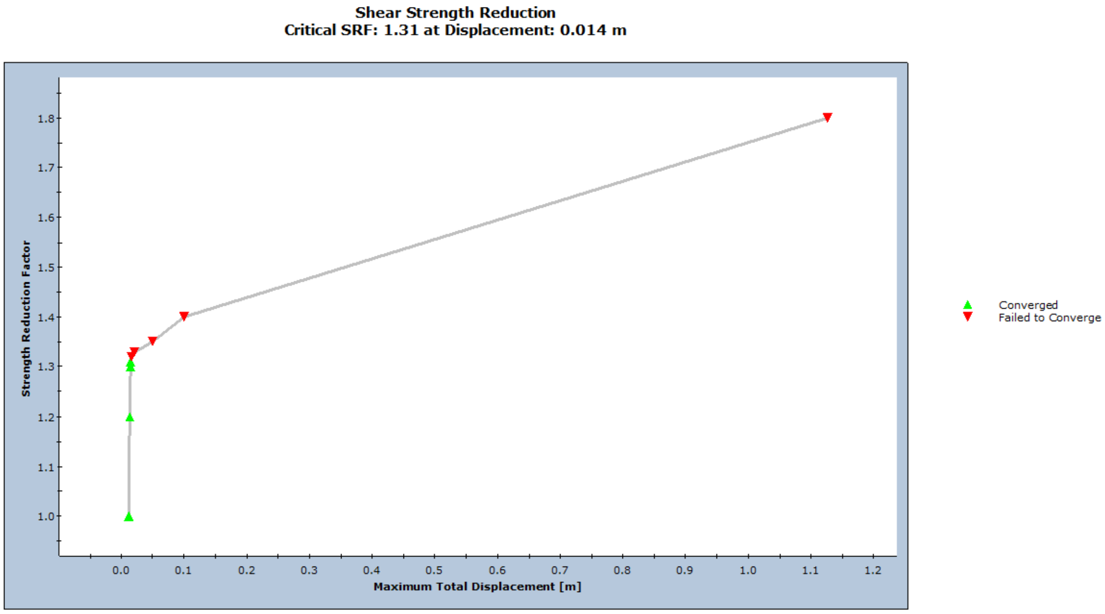

Figure 3 – SSR Convergence Graph

Introduction

Verification #28 models a typical steep cut slope in Hong Kong. The example is taken from Ng and Shi (1998). It illustrates the use of finite element groundwater and stress analysis in the assessment of the stability of the cut.

Problem description

Verification problem #38 for Slide2 - The cut has a slope face angle of 28^{o} and consists of a 24m thick soil layer, underlain by a 6m thick bedrock layer. Figure 1 describes the slope model.

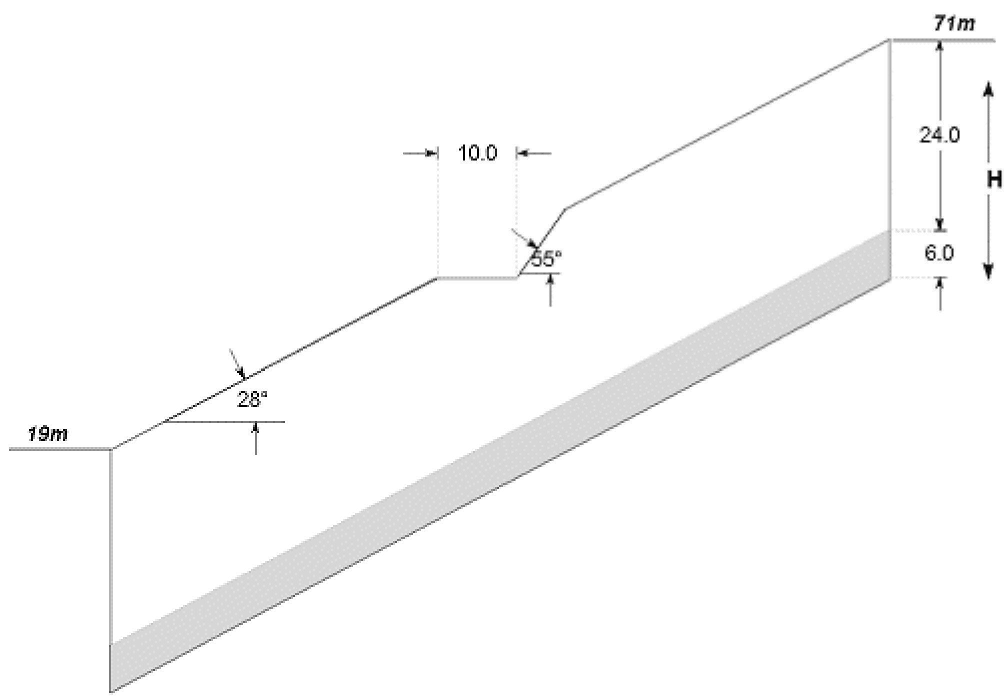

Figure 1 Model geometry

Steady-state groundwater analysis is conducted using the finite element module in RS2. Initial conditions of constant total head are applied to both sides of the slope. Three different initial hydraulic boundary conditions (H=61m, H=62m, H=63m) for the right side of the slope are considered for the analyses in this section, Figure 1. Constant hydraulic boundary head of 6m is applied on the left side of the slope. Figure 2 shows the soil permeability function used to model the hydraulic conductivity of the soil, Ng (1998).

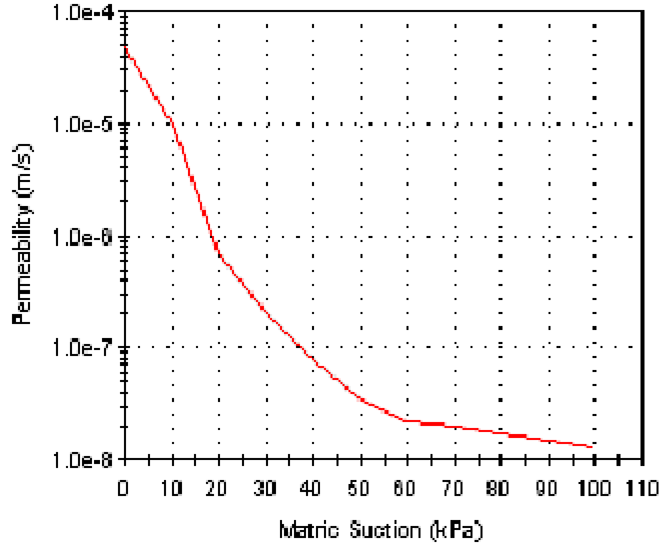

Figure 2 – Hydraulic conductivity function*

The negative pore water pressure, which is commonly refereed to as the matrix suction of soil, above the water table influences the soil shear strength and hence the factor of safety. Ng and Shi used the modified Mohr-Coulomb failure criterion for the unsaturated soils, which can be written as:

$$\tau = c' + (\sigma_n - u_a)\tan\varphi' + (u_a - u_w)\tan\varphi_b$$

where σ_n is the normal stress, φ_b is an angle defining the increase in shear strength for an increase in matrix suction of the soil. Table 1 shows the material properties for the soil.

* The raw data for Figure 2 can be found in the verification data file.

Table 1 Material properties

c' (kPa)	φ' (deg.)	φ_b (deg.)	γ (kN/m^3)
10	38	15	16

Both positive and negative pore water pressures predicted from groundwater analysis engine were used in the stability analysis. To match the results, the extent of the failure is limited to a region close to the cut. The region is limited by using an elastic (infinite strength) material outside this region.

Results

H **(total head at right side of slope)**	RS2***(SSR)***	***Slide2***	**Ng. & Shi (1998)**
61m	1.64	1.616	1.636
62m	1.55	1.535	1.527
63m	1.41	1.399	1.436

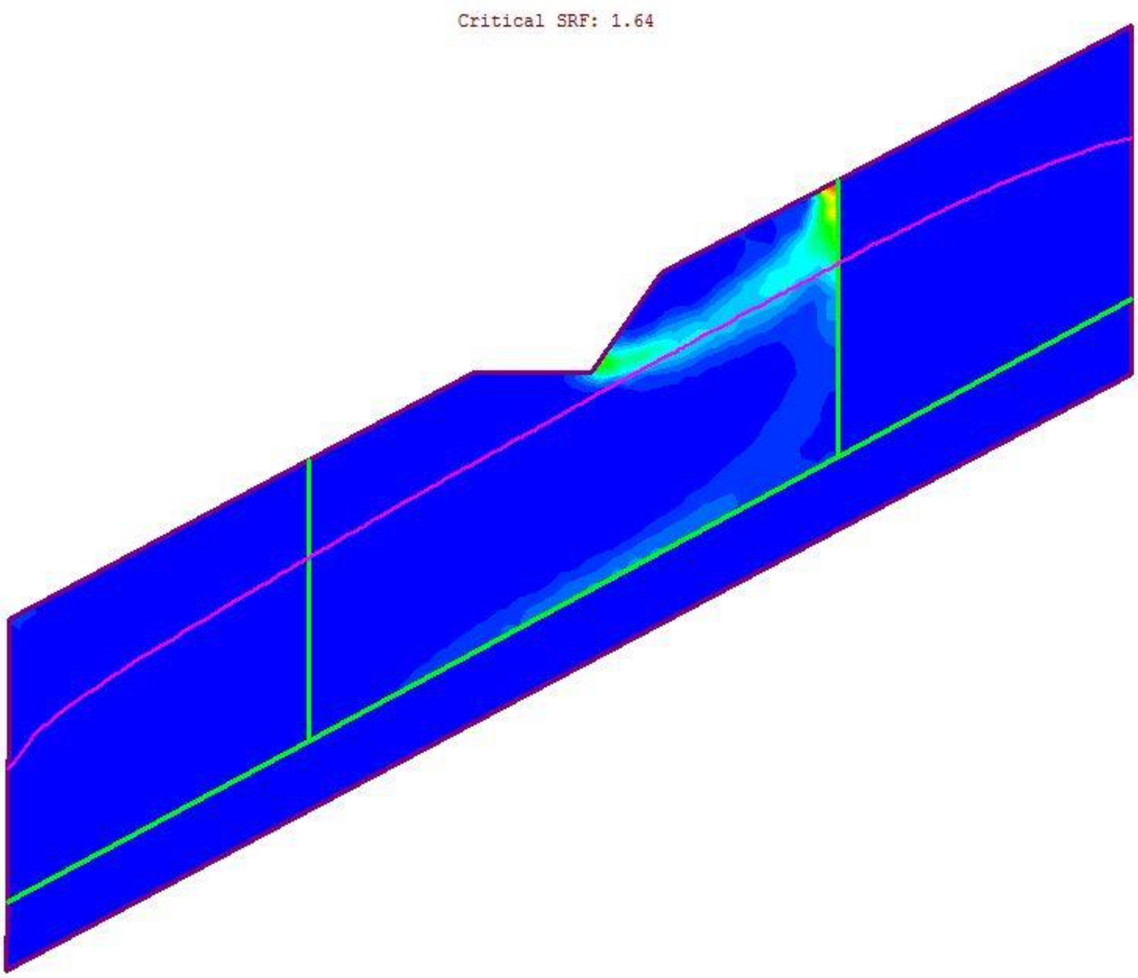

Figure 3 –Shear Strain plot (H=61m)

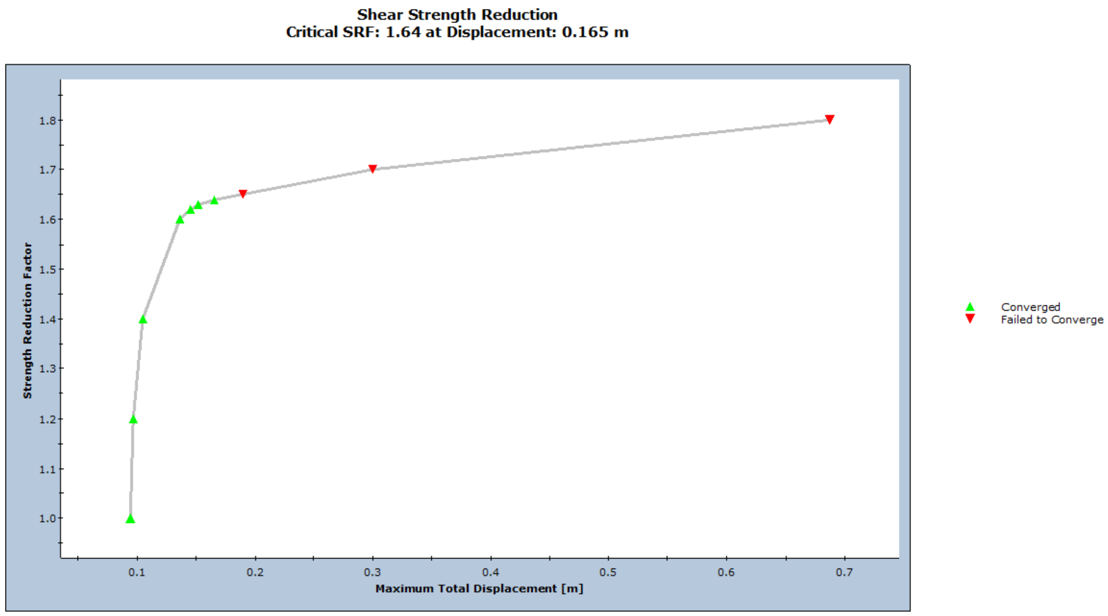

Figure 4 – SSR Convergence Graph (H=61m)

Introduction

This model is taken from Tandjiria (2002), their problem 1 example. It looks at the stability of a geosynthetic-reinforced embankment on soft soil. The problem looks at the stability of the embankment if it consists of either a sand fill or an undrained clayey fill. Both are analyzed.

Problem description

Verification problem #29 is shown in Figures 1 and 2. The purpose of this example is to compute the required reinforcement force to yield a factor of safety of 1.35. Both circular and non-circular surfaces are looked at. In each case, the embankment is modeled without the reinforcement; the critical slip surface is located, and then used in the reinforced model to determine the reinforcement force to achieve a factor of safety of 1.35. This is done for a sand or clay embankment, circular and non-circular critical slip surfaces. Both cases incorporate a tension crack in the embankment. In the case of the clay embankment, a water-filled tension crack is incorporated into the analysis. The reinforcement is located at the base of the embankment. The model was analyzed with both Spencer and GLE (half-sine interslice function) but Spencer was used for the force computation. The reinforcement is modeled as an **active** force since this is how Tandjiria et.al. modelled the force.

Geometry and Properties

Table 1: Material Properties

	Cu/c´ (kN/m^2)	ϕ´ (deg.)	γ (kN/m^3)
Clay Fill Embankment	20	0	19.4
Sand Fill Embankment	0	37	17
Soft Clay Foundation	20	0	19.4

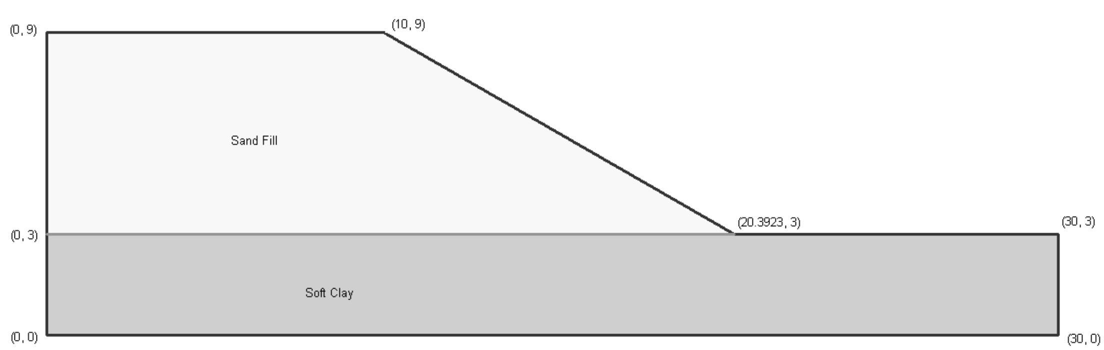

Figure 1 - Sand Fill Embankment

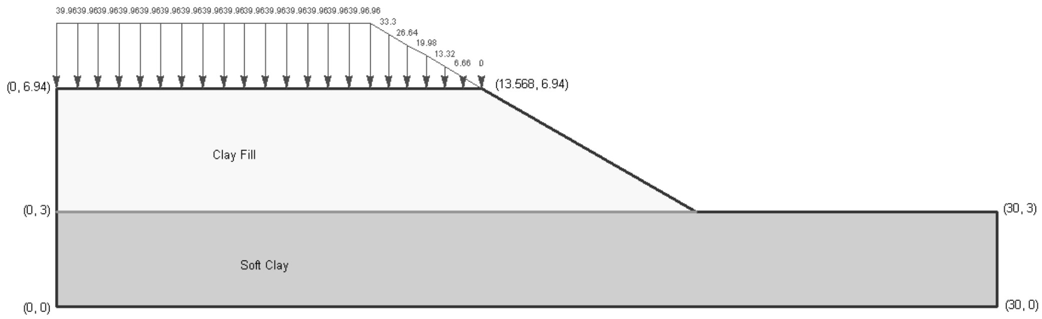

Figure 2 - Clay Fill Embankment

Results – Sand embankment with no reinforcement

Method	Factor of Safety
SRF	1.25
Circular Limit-Equilibrium	
Spencer	1.209
GLE/M-P	1.218
Tandjiria (2002) Spencer	1.219
Non-circular Limit-Equilibrium	
Spencer	1.189
GLE/M-P	1.196
Tandjiria (2002) Spencer	1.192

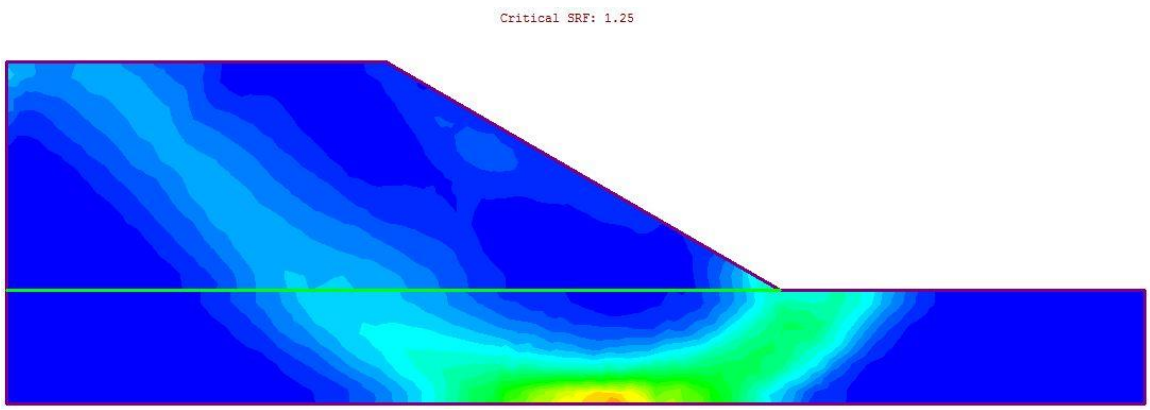

Figure 3 – Shear Strain Plot for Sand Fill Embankment

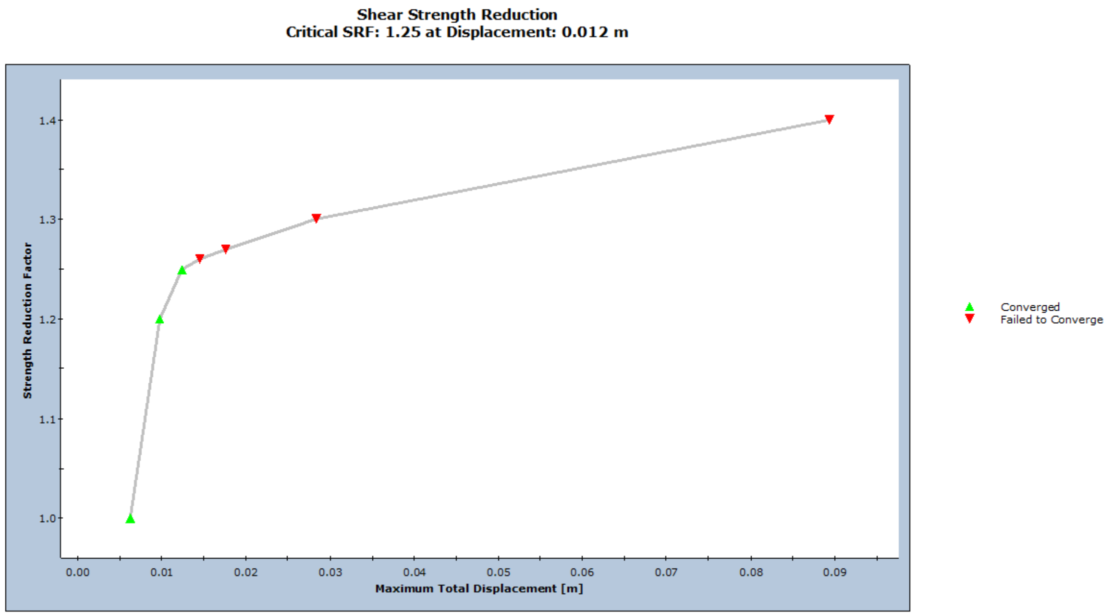

Figure 4 – SSR Convergence Graph for Sand Fill Embankment

Results – Clay embankment with no reinforcement

Method	Factor of Safety
SRF	0.99
Circular Limit-Equilibrium	
Spencer	0.975
GLE/M-P	0.975
Tandjiria (2002) Spencer	0.981
Non-circular Limit-Equilibrium	
Spencer	0.932
GLE/M-P	0.941
Tandjiria (2002) Spencer	0.941

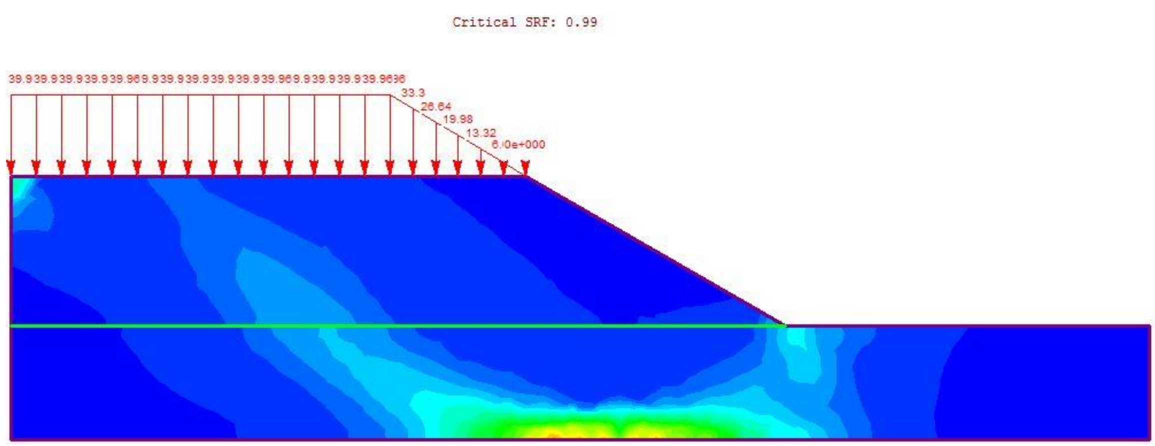

Figure 5 – Shear Strength Plot for Clay Fill Embankment

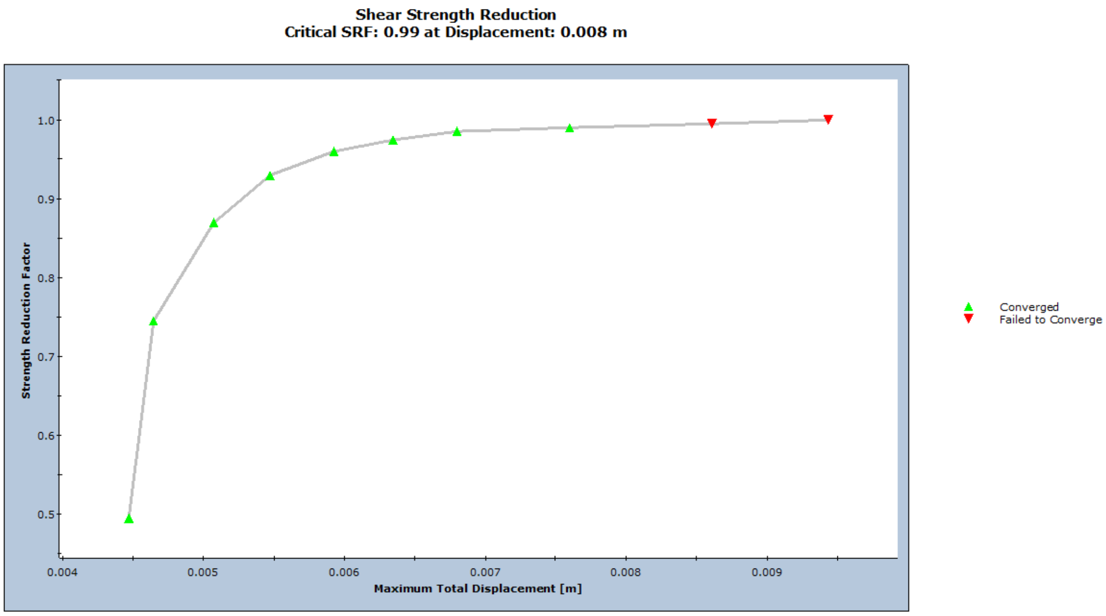

Figure 6 – SSR Convergence Graph for Clay Fill Embankment

Introduction

This problem was taken from J. Perry (1993), Fig. 10. It involves material for which the relationship between effective normal stress and shear stress is described by the non-linear power curve.

Problem Description

This problem analyzes a simple homogeneous slope (Fig. 1). The dry soil is assumed to have non-linear power curve strength parameters. The computed factor of safety and failure surface obtained from the SRF method are compared to those given by Janbu limit-equilibrium analysis of the non-linear surface shown in Fig. 2.

Geometry and Properties

Table 1: Material Properties

Parameter	Value
A	2
b	0.7
γ (kN/m^3)	20.0

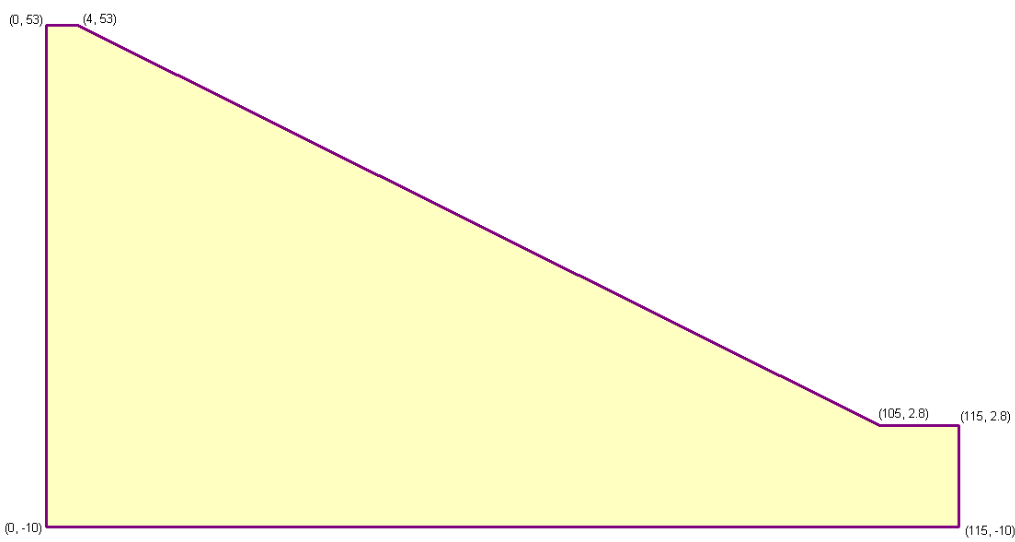

Figure 1

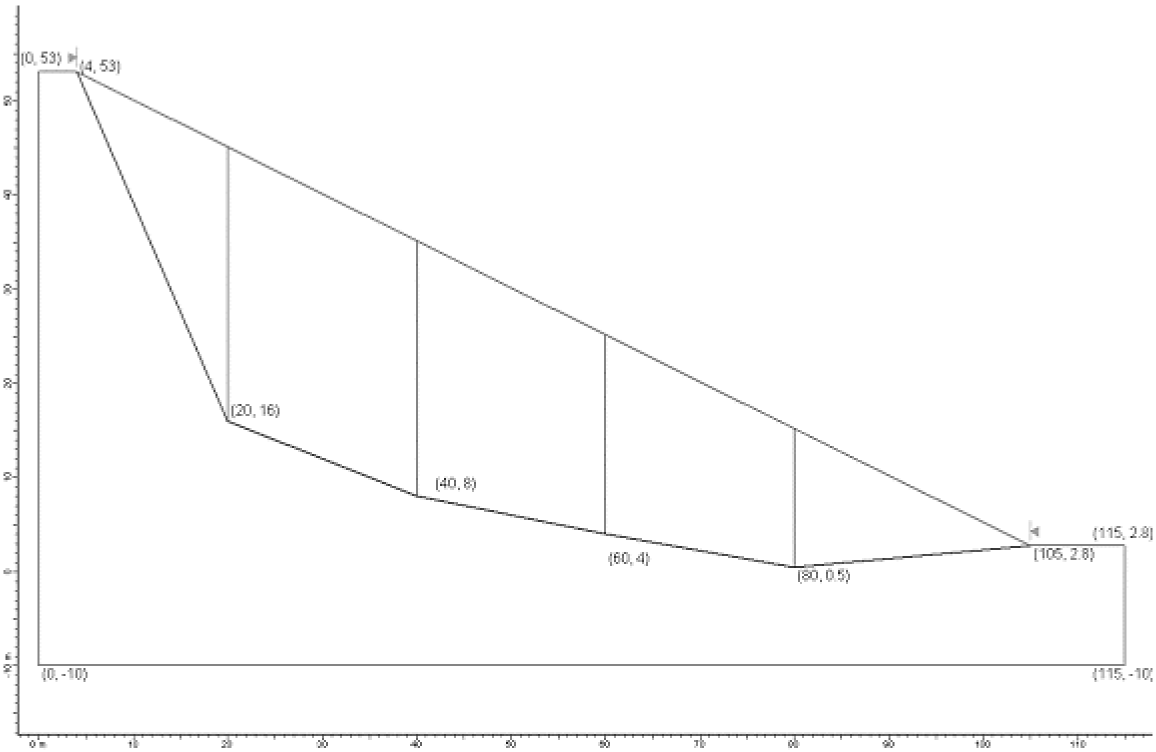

Figure 2

Results

Method	Factor of Safety
SRF	0.91
SLIDE2 Janbu Simplified	0.944

Note: Referee Factor of Safety = 0.98 [Perry]

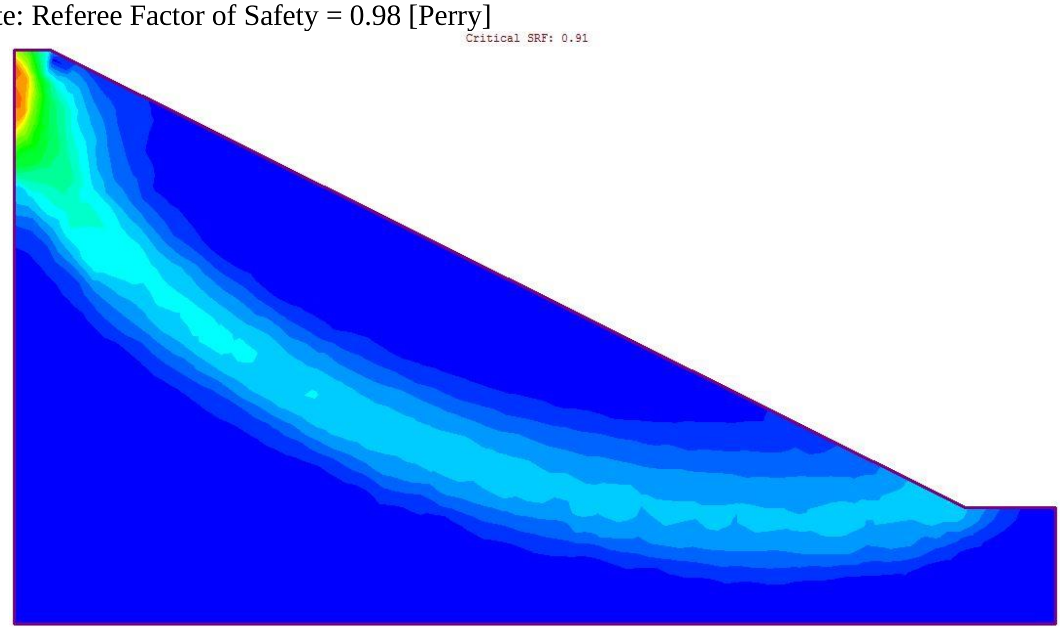

Figure 3 – Shear Strain Plot

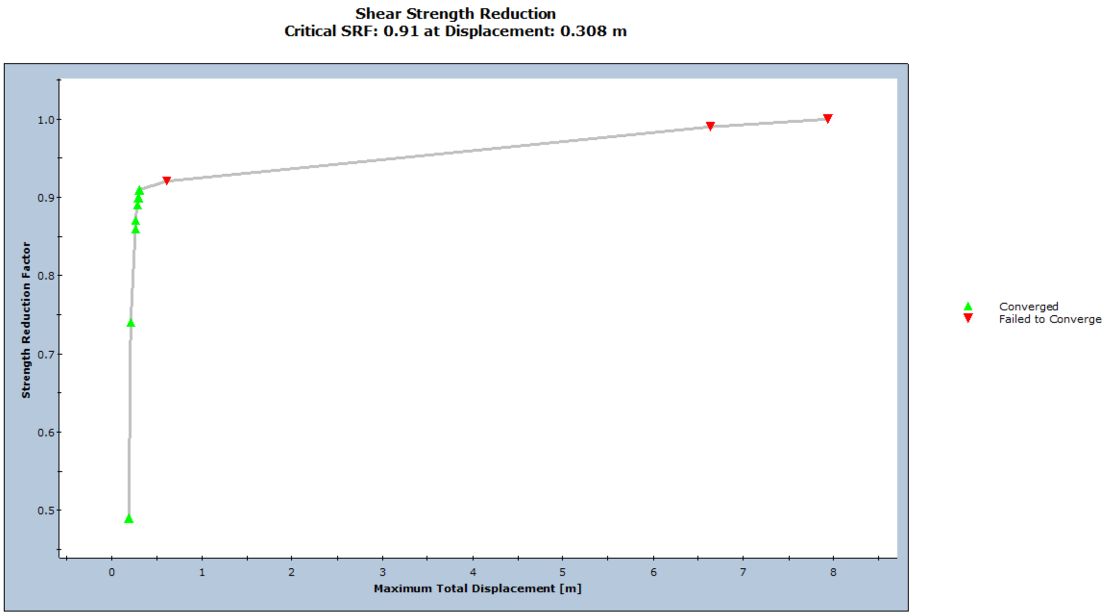

Figure 4 – SSR Convergence Graph

31 Homogeneous Slope Analysis Comparing Mohr-Coulomb and Power Curve Strength Criteria

Introduction

This problem was taken from Baker (2003). It is his first example problem comparing linear and non-linear Mohr envelopes.

Problem Description

Verification problem #31 compares two homogeneous slopes of congruent geometry (Figure 1) under different strength functions (Table 1). The factor of safety is determined for the Mohr-Coulomb and Power Curve strength criteria. The power curve criterion used by Baker has the non-linear form:

$$\tau = P_a A\left(\frac{\sigma}{P_a} + T\right)^n \ \ldots \ P_a = 101.325 \text{ kPa}$$

The factor of safety was determined using the material properties that Baker derives from his iterative process; these values should be compared to the accepted values.

Geometry and Properties

Table 1: Material Properties

Material	c′ (kN/m^2)	ϕ′ (deg.)	γ (kN/m^3)	A	n	T
Clay	11.64	24.7	18	0.58	0.86	0
Clay, iterative results	0.39	38.6	18	--	--	--

Figure 1 - Geometry

Results

Strength Type	Method	Factor of Safety
Power Curve	SRF (Generalized Hoek-Brown)	1.11
	Janbu Simplified	0.92
	Spencer	0.96
Mohr-Coulomb	SRF	1.53
	Janbu Simplified	1.47
	Spencer	1.54
Mohr-Coulomb with iteration results (c′ = 0.39 kPa, ϕ′ = 38.6 °)	SRF	0.98
	Janbu simplified	0.96
	Spencer	0.98

Baker (2003) non-linear results: FS = 0.97
Baker (2003) M-C results: FS = 1.50

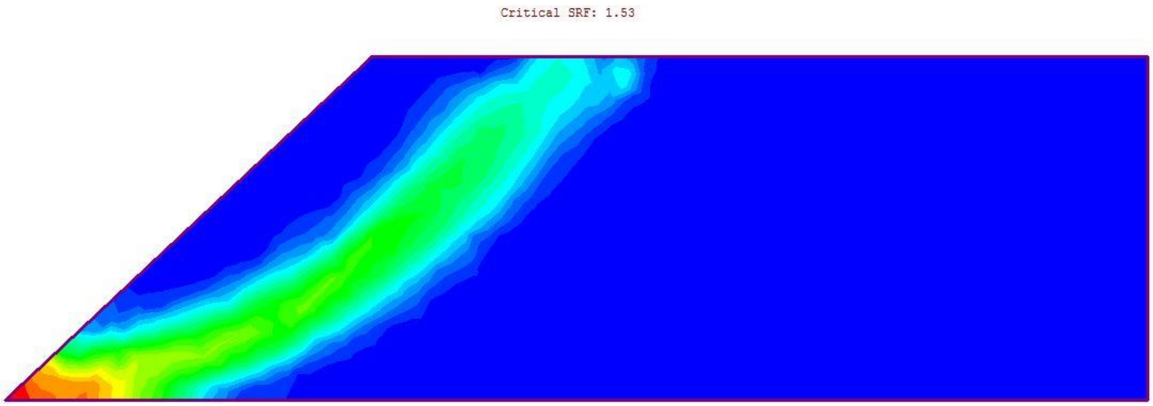

Figure 2 – Shear Strain Plot for Mohr-Coulomb criterion

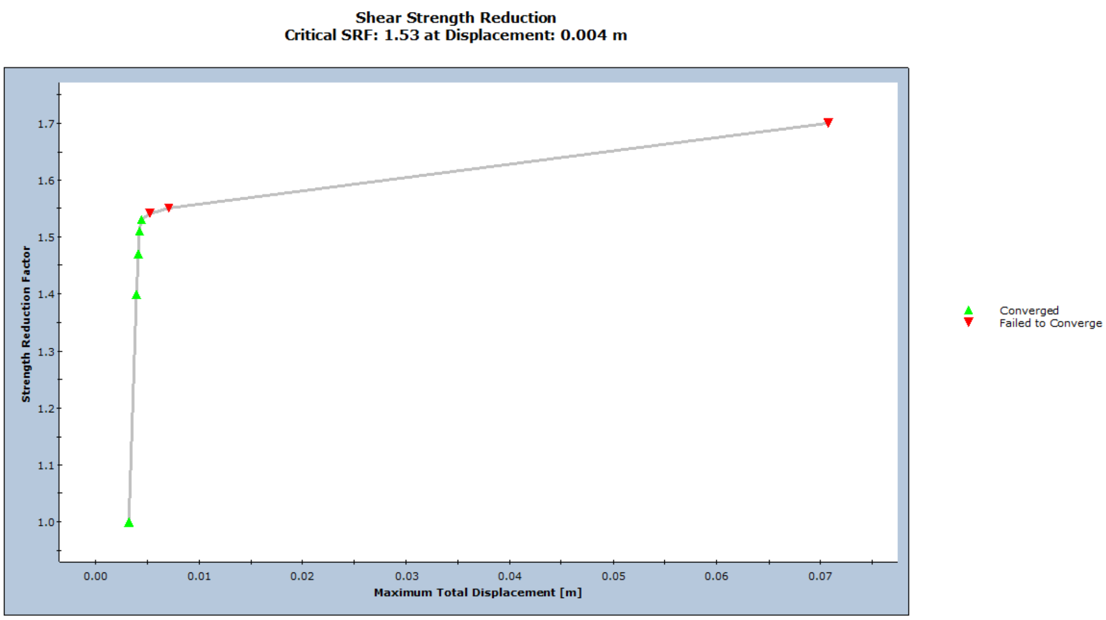

Figure 3 – SSR Convergence Graph for Mohr-Coulomb Criterion

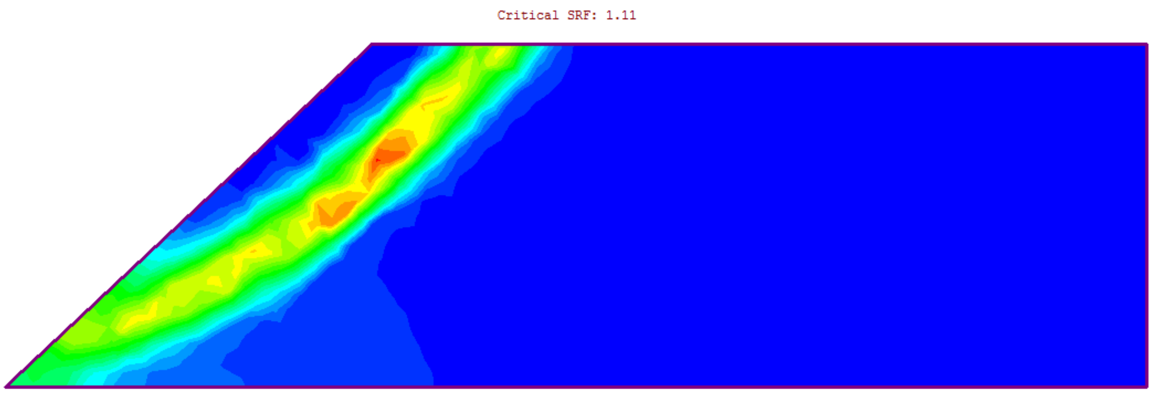

Figure 4 – Shear Strain Plot for Power Curve Criterion

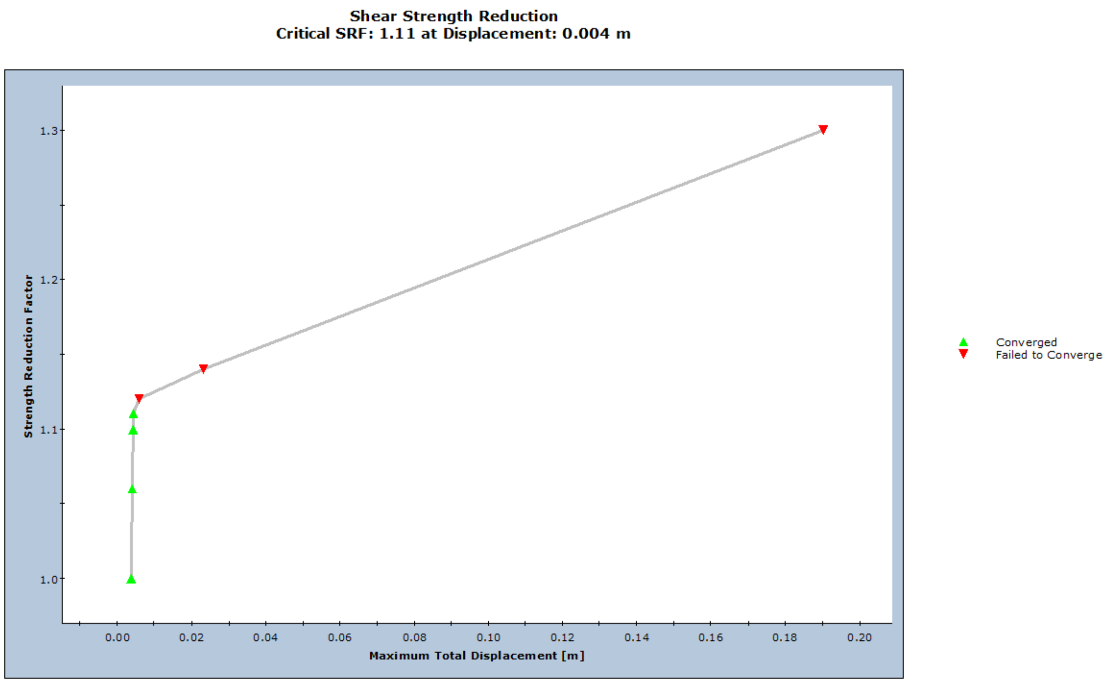

Figure 5 – SSR Convergence Graph for Power Curve Criterion

Introduction

This problem was taken from Baker (2003). It is his second example problem comparing linear and non-linear Mohr envelopes.

Problem Description

Verification problem #45, (#56 for Slide2) compares two homogeneous slopes of congruent geometry (Figure 1) under different strength functions (Table 1). The critical circular surface factor of safety and maximum effective normal stress must be determined for both Mohr-Coulomb strength criterion and Power Curve criterion. The power curve criterion was derived from Baker's own non-linear function:

$$\tau = P_a A\left(\frac{\sigma}{P_a} + T\right)^n \ \ldots\ P_a = 101.325 \text{ kPa}$$

The power curve variables are in the form:

$$\tau = a(\sigma_n + d)^b + c$$

Finally, the critical circular surface factor of safety and maximum effective normal stress must be determined using the material properties that Baker derives from his iterative process; these values should be compared to the accepted values.

Geometry and Properties

Table 1: Material Properties

Material	c´ (kN/m^2)	ϕ´ (deg.)	γ (kN/m^3)	A	n	T
Clay	11.64	24.7	18	0.58	0.86	0
Clay, iterative results	0.39	38.6	18	--	--	--

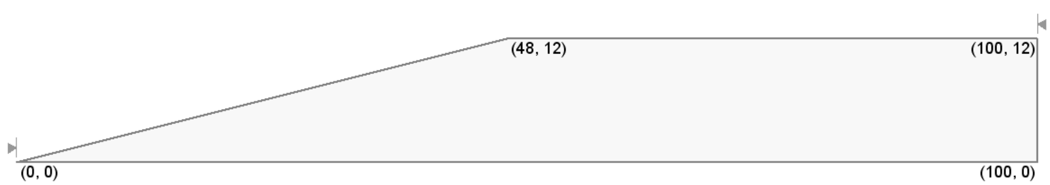

Figure 1 - Geometry

Results

Strength Type	Method	Factor of Safety
Power Curve	SRF	2.74
	Janbu Simplified (Circular)	2.56
	Spencer (Circular)	2.66
Mohr-Coulomb	SRF	2.83
	Janbu Simplified (Circular)	2.66
	Spencer (Circular)	2.76

Baker (2003) non-linear results: FS = 2.64
Baker (2003) M-C results: FS = 2.66

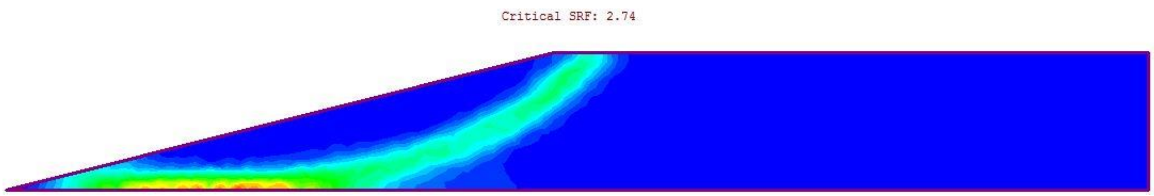

Figure 2 – Shear Strain Plot for Power Curve Criterion.

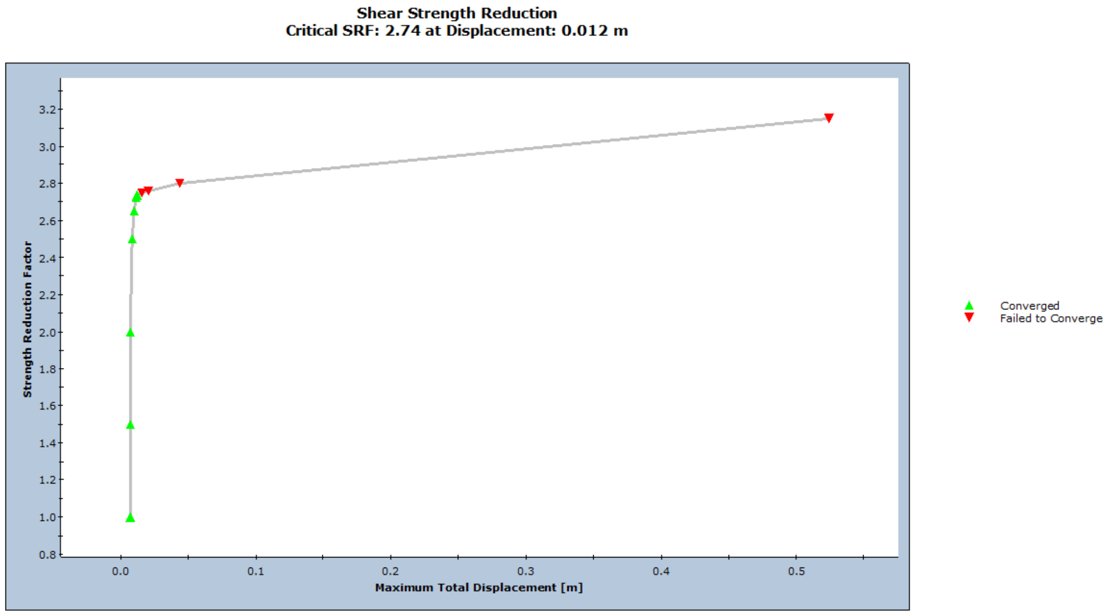

Figure 3 – SSR Convergence Graph for Power Curve Criterion

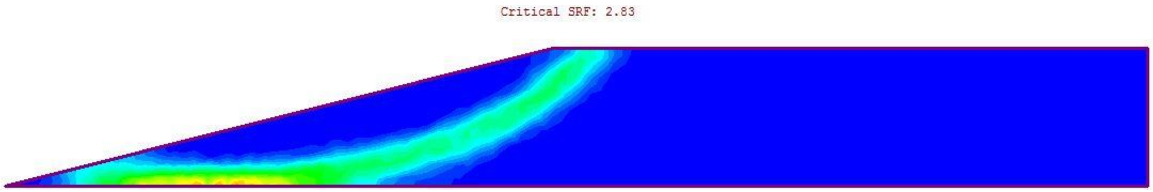

Figure 4 – Shear Strain Plot for Mohr-Coulomb Criterion.

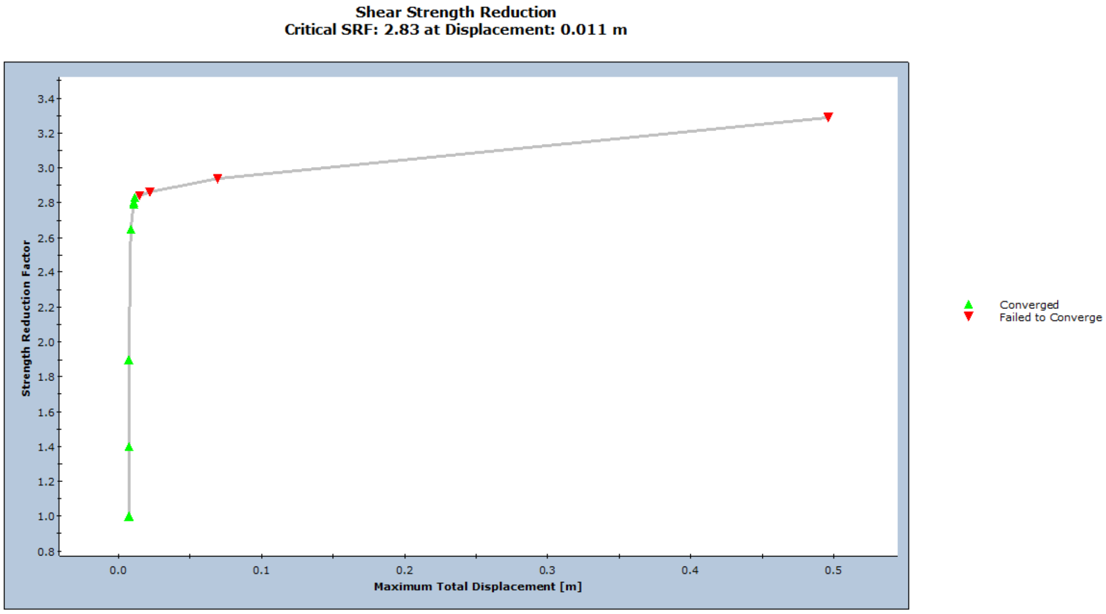

Figure 5 – SSR Convergence Graph for Mohr-Coulomb Criterion

33 Homogeneous Slope Analysis Comparing Mohr-Coulomb and Power Curve Strength Criteria II

Introduction

In December 2000, Pockoski and Duncan released a paper comparing eight different computer programs for analysis of reinforced slopes. This is their second test slope.

Description

Verification Problem #33 analyses an unreinforced homogeneous slope. A water table is present, as is a dry tension crack (Figure 1). The circular critical failure surface and factor of safety for this slope are required (40x40 grid).

Geometry and Properties

Table 1: Material Properties

Material	c′ (psf)	ϕ′ (deg.)	γ (pcf)
Sandy clay	300	30	120

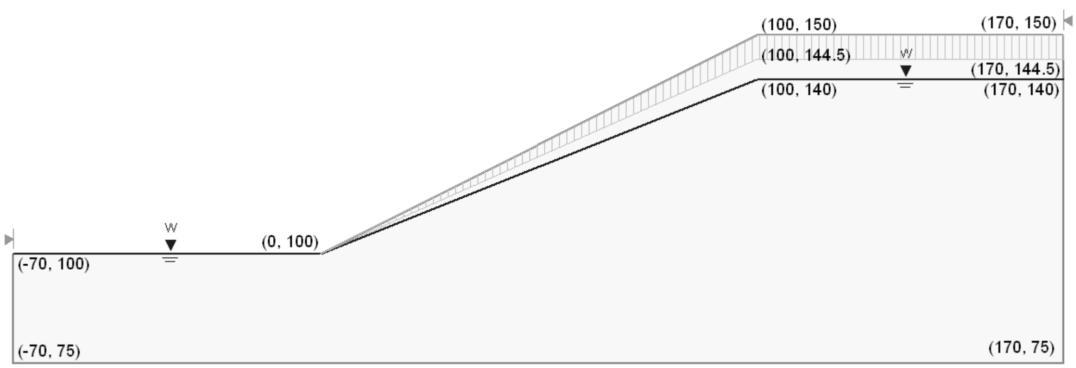

Figure 1 - Geometry

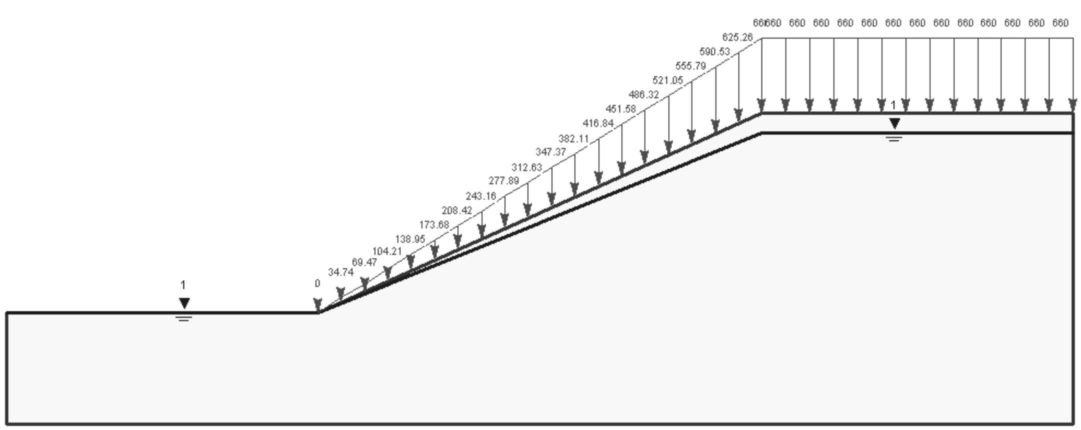

Figure 2 - Geometry

Results

Method	SRF	SLIDE2	UTEXAS4	SLOPE/W	WINSTABL	XSTABL	RSS
SRF	1.28	--	--	--	--	--	--
Spencer	--	1.30	1.29	1.29	1.32	--	--
Bishop simplified	--	1.29	1.28	1.28	1.31	1.28	1.28
Janbu simplified	--	1.14	1.14	1.14	1.18	1.23	1.13
Lowe-Karafiath	--	1.31	1.31	--	--	--	--
Ordinary	--	1.03	--	1.02	--	--	--

SNAIL FS = 1.18 (Wedge method)
GOLD-NAIL FS = 1.30 (Circular method)

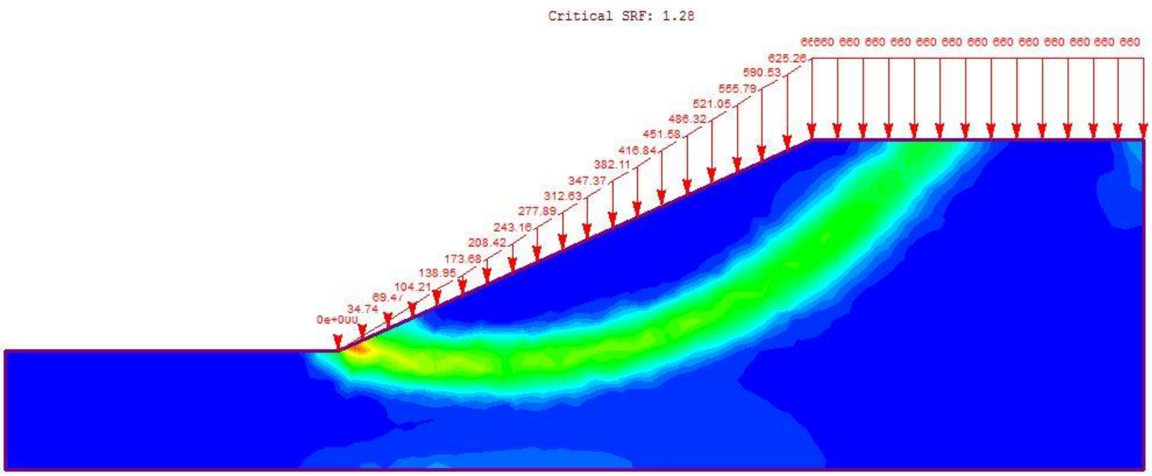

Figure 3 – Shear Strain Plot

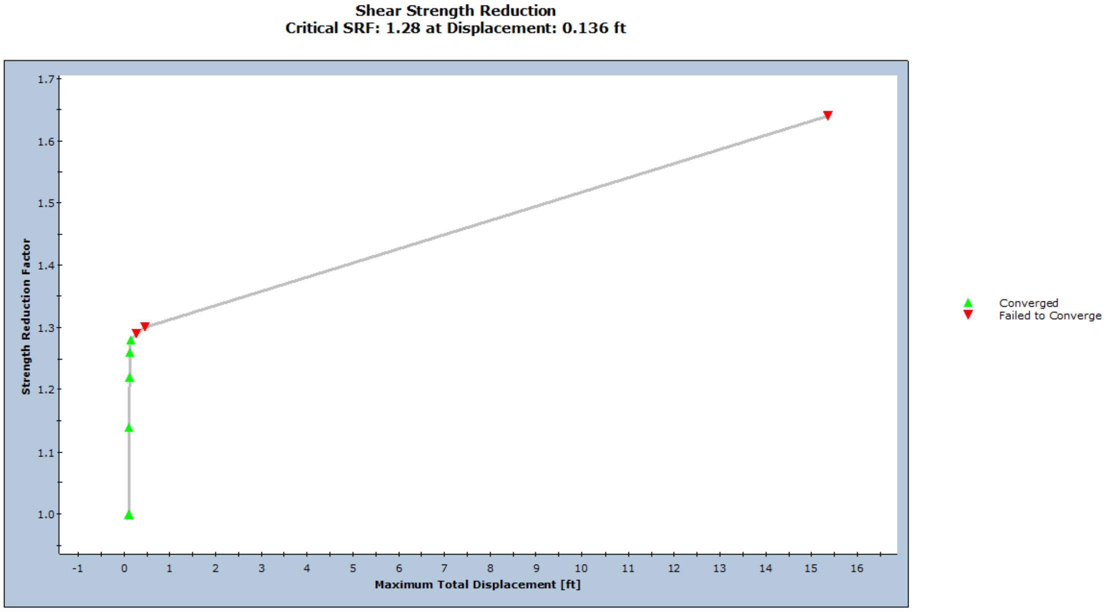

Figure 4 – SSR Convergence Graph

34 Homogeneous Slope Analysis Comparing Mohr-Coulomb and Power Curve Strength Criteria III

Introduction

This problem was taken from Baker (2003). It is his third example problem comparing linear and non-linear Mohr envelopes.

Description

Verification problem #34 compares two homogeneous slopes of congruent geometry (Figure 1) under different strength functions (Table 1 and 2). The critical circular surface factor of safety and maximum effective normal stress must be determined for both Mohr-Coulomb strength criterion and Power Curve criterion. The power curve criterion was derived from Baker's own non-linear function:

$$\tau = P_a A\left(\frac{\sigma}{P_a} + T\right)^n \text{ … } P_a = 101.325 \text{ kPa}$$

The power curve variables are in the form:

$$\tau = a(\sigma_n + d)^b + c$$

Finally, the critical circular surface factor of safety and maximum effective normal stress must be determined using the material properties that Baker derives from his iterative process; these values should be compared to the accepted values.

Geometry and Properties

Table 1: Material Properties – Power Curve criterion

	Baker's Parameters			SLIDE2 Parameters			
Material	A	n	T	a	b	c	d
Clay	0.535	0.6	0.0015	3.39344	0.6	0	0.1520

Table 2: Material Properties – Mohr-Coulomb criterion

Material	c′ (kN/m^2)	ϕ′ (deg.)	γ (kN/m^3)
Clay	6.0	32	18

Figure 1 - Geometry

Results

Strength Type	Method	Factor of Safety
Power Curve	SRF	1.47
	Janbu Simplified	1.35
	Spencer	1.47
Mohr-Coulomb	SRF	1.38
	Janbu Simplifed	1.29
	Spencer	1.37

Baker (2003) non-linear results: FS = 1.48
Baker (2003) M-C results: FS = 1.35

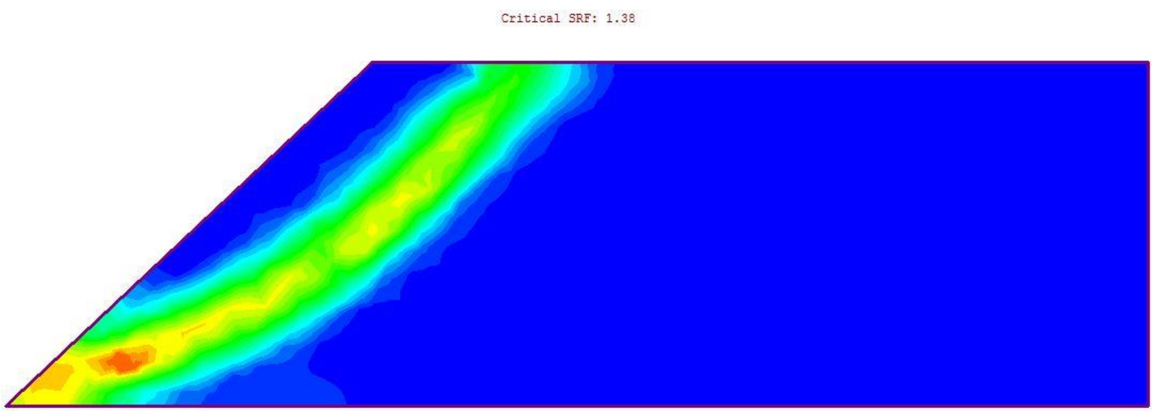

Figure 2 – Shear Strain Plot for Mohr-Coulomb Criterion

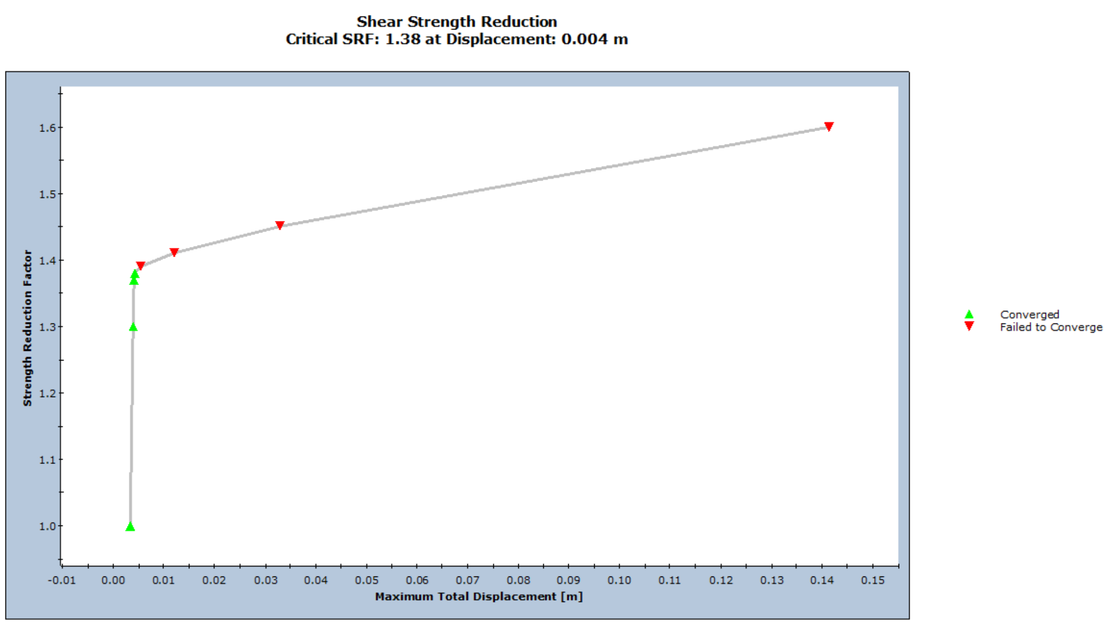

Figure 3 – SSR Convergence Graph for Mohr-Coulomb Criterion

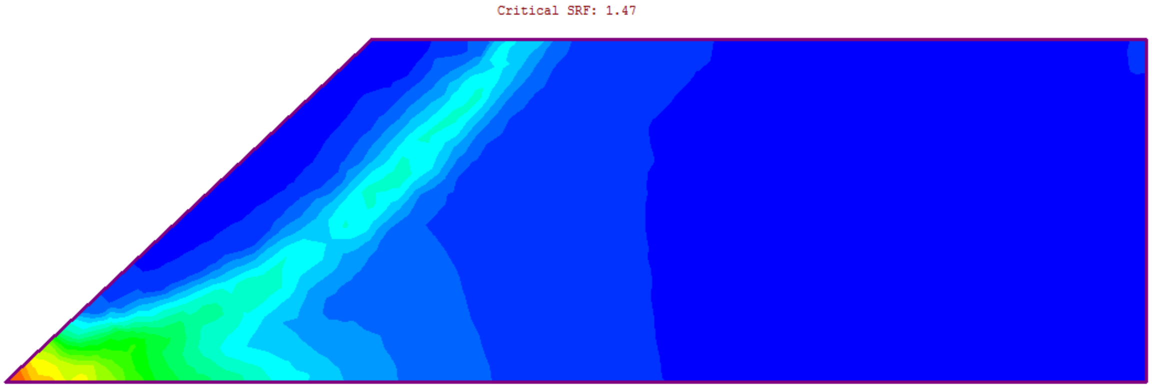

Figure 4 – Shear Strain Plot for Power Curve Criterion

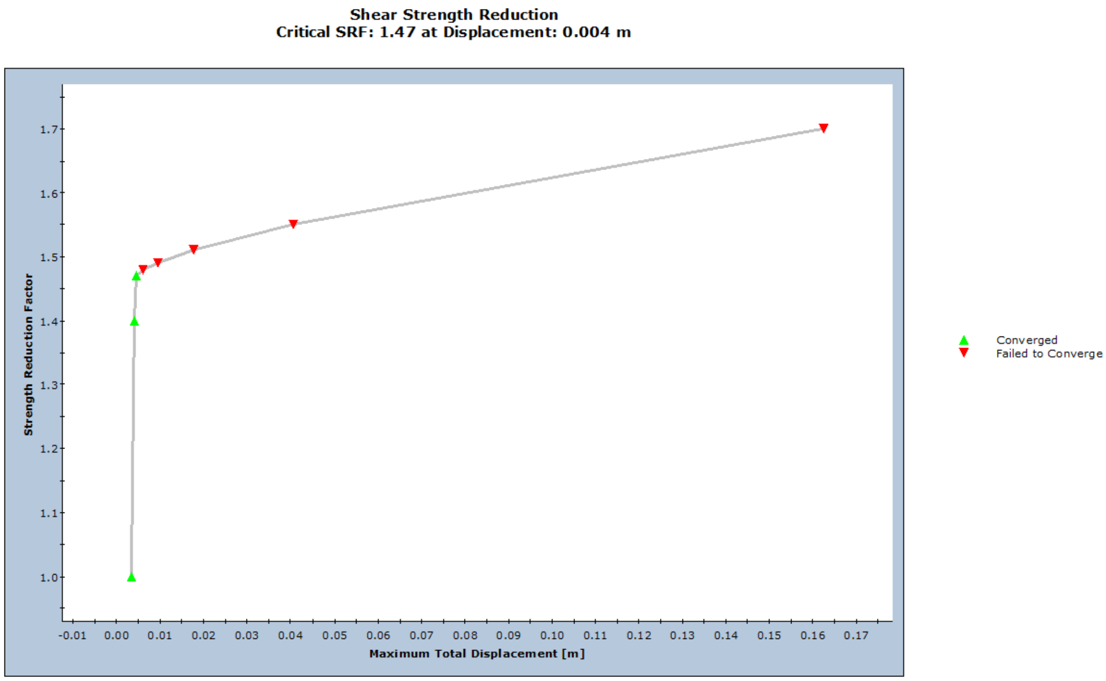

Figure 5 – SSR Convergence Graph for Power Curve Criterion

References

1. Arai, K., and Tagyo, K. (1985), “Determination of noncircular slip surface giving the minimum factor of safety in slope stability analysis.” Soils and Foundations. Vol.25, No.1, pp.43-51.

2. Baker, R. (1980), “Determination of the critical slip surface in slope stability computations.” International Journal for Numerical and Analytical Methods in Geomechanics, Vol.4, pp.333-359.

3. Borges, J.L. and Cardoso, A.S. (2002), “Overall stability of geosynthetic-reinforced embankments on soft soils.” Geotextiles and Geomembranes, Vol. 20, pp. 395-421.

4. Chen, Z. and Shao, C. (1988), “Evaluation of minimum factor of safety in slope stability analysis” Canadian Geotechnical Journal, Vol. 25, pp.735-748.

5. Chowdhury, R.N. and Xu, D.W. (1995), “Geotechnical system reliability of slopes.” Reliability Engineering and System Safety. Vol. 47, pp. 141-151.

6. Craig, R.F., (1997). Soil Mechanics, 6th Edition.

7. Duncan, M.J., (2000), “Factors of Safety and Reliability in Geotechnical Engineering.” Journal of Geotechnical and Geoenvironmental Engineering. April, pp. 307-316.

8. El-Ramly, H., Morgenstern, N.R. and Cruden, D.M. (2003), “Probabilistic stability analysis of a tailings dyke on presheared clay-shale.” Canadian Geotechnical Journal, Vol. 40, pp. 192-208.

9. Fredlund, D.G. & Krahn, J. (1977), “Comparison of slope stability methods of analysis.” Canadian Geotechnical Journal Vol. 14, No. 3, pp 429-439.

10. Giam, P.S.K. & I.B. Donald (1989), “Example problems for testing soil slope stability programs.” Civil Engineering Research Report No. 8/1989, Monash University, ISBN 0867469218, ISSN 01556282.

11. Giam, P.S.K. (1989), “Improved methods and computational approaches to geotechnical stability analysis.” Ph.D. Thesis, Dept. of Civil Engineering, Monash University.

12. Greco, V.R. (1996), “Efficient Monte Carlo technique for locating critical slip surface.” Journal of Geotechnical Engineering. Vol.122, No.7, July, pp. 517-525.

13. Hassan, A.M. and Wolff, T.E. (1999), “Search algorithm for minimum reliability index of earth slopes.” Journal of Geotechnical and Geoenvironmental Engineering, Vol. 125, No. 4, April, 1999, pp. 301-308.

14. Ireland, H.O. (1954), “Stability analysis of the Congress Street open cut in Chicago.” Geotechnique. Vol. 4, pp. 163-168.

15. Kim, J., Salgado, R., Lee, J. (2002), “Stability analysis of complex soil slopes using limit analysis.” Journal of Geotechnical and Geoenvironmental Engineering. Vol.128, No.7, July, pp. 546-557.

16. Li, S.K. and Lumb, P. (1987), “Probabilistic design of slopes.” Canadian Geotechnical Journal, Vol. 24, No. 4, pp. 520-535.

17. Low, B. (1989), “Stability analysis of embankments on soft ground.” Journal of Geotechnical Engineering, Vol.115, No.2, pp. 211-227.

18. Malkawi, A.I.H.,Hassan, W.F., and Sarma, S.K. (2001), “Global search method for locating general slip surfaces using monte carlo techniques.” Journal of Geotechnical and Geoenvironmental Engineering. Vol.127, No.8, August, pp. 688-698.

19. Ng, C.W.W. and Shi Q. (1998), “A numerical investigation of the stability of unsaturated soil slopes subjected to transient seepage” Computers and Geotechnics, Vol.22, No.1, pp.1-28.

20. Pilot, G., Trak, B. and La Rochelle, P. (1982). “Effective stress analysis of the stability of embankments on soft soils.” Canadian Geotechnical Journal, vol.19, pp. 433-450.

21. Prandtl, L. (1921), “Uber die Eindringungsfestigkeit (Harte) plastischer Baustoffe und die Festigkeit von Schneiben (On the penetrating strength (hardness) of plastic construction materials and the strength of curring edges).” Zeitschrift fur Agnewandte Mathematik und Mechanik, vol.1, pp.15-20.

22. Sharma, S. (1996), “XSTABL, an integrated slope stability analysis program for personal computers”, Reference manual, version 5. Interactive Software Designs Inc., Moscow, ID.

23. Spencer, E. (1969), “A method of analysis of the stability of embankments assuming parallel inter-slice forces.” Geotechnique, Vol.17, pp.11-26.

24. Tandjiria, V., Low, B.K., and Teh, C.I. (2002), “Effect of reinforcement force distribution on stability of embankments.”, Geotextiles and Geomembranes, No. 20, pp. 423-443.

25. Wolff, T.F. and Harr, M.E. (1987), “Slope design for earth dams.” In *Reliability and Risk Analysis in Civil Engineering 2*, Proceedings of the Fifth International Conference on Applications of Statistics and Probability in Soil and Structural Engineering, Vancouver, BC, Canada, May, 1987, pp. 725-732.

26. XSTABL (1999), Reference Manual, Version 5.2, pp. 57-60.

27. Yamagami, T. and Ueta, Y. (1988), “Search noncircular slip surfaces by the Morgenstern-Price method.” Proc. 6th Int. Conf. Numerical Methods in Geomechanics, pp. 1335-1340.

28. Perry, J. (1993), “A technique for defining non-linear shear strength envelopes, and their incorporation in a slope stability method of analysis.” Quarterly Journal of Engineering Geology, No.27, pp. 231-241.

29. Jiang, J-C., Baker, R., and Yamagami, T. (2003), “The effect of strength envelope nonlinearity on slope stability computations.” Canadian Geotechnical Journal, No.40, pp.308-325.

30. Baker, R., and Leshchinsky, D. (2001), “Spatial Distributions of Safety Factors.” Journal of Geotechnical and Geoenvironmental Engineering, February 2001, pp. 135-144.

31. Baker, R. (2003), “Inter-relations between experimental and computational aspects of slope stability analysis.” International Journal for Numerical and Analytical Methods in Geomechanics, No.27, pp. 379-401.

32. Baker, R. (1993), “Slope stability analysis for undrained loading conditions.” International Journal for Numerical and Analytical Methods in Geomechanics, Vol. 17, pp. 15-43.

33. Sheahan, T., and Ho, L. (2003), “Simplified trial wedge method for soil nailed wall analysis.” Journal of Geotechnical and Geoenvironmental Engineering, February 2003, pp. 117-124.

34. SNAILZ (1999), Reference Manual, Version 3.XX, pp. 1-43.

35. Zhu, D., Lee, C.F., and Jiang, H.D. (2003), “Generalised framework of limit equilibrium methods for slope stability analysis.” Géotechnique, No. 4, pp. 377-395.

36. Zhu, D., and Lee, C. (2002), “Explicit limit equilibrium solution for slope stability.” International Journal for Numerical and Analytical Methods in Geomechanics, No. 26, pp. 1573-1590.

37. Priest, S. (1993), “Discontinuity analysis for rock engineering.” Chapman & Hall, London, pp. 219-226.

38. Yamagami, T., Jiang, J.C., and Ueno, K. (2000), “A limit equilibrium stability analysis of slope with stabilizing piles.” Slope Stability 2000, pp. 343-354.

39. Pockoski, M., and Duncan, J.M., “Comparison of Computer Programs for Analysis of Reinforced Slopes.” Virginia Polytechnic Institute and State University, December 2000.

40. Loukidis, D., Bandini, P., and Salgado, R. (2003), “Stability of seismically loaded slopes using limit analysis.” Géotechnique, No. 5, pp. 463-479.

41. US Army Corps of Engineers (2003), “Engineering and Design: Slope Stability.” Engineer Manual 1110-2-1902.